G.YAR-MUKHAMEDOVA
T. NENASTINA
M. VED'
A. KARAKURKCHI
N. SAKHNENKO

NANOCOMPOSITE ELECTROLYTIC COATINGS BASED ON COBALT ALLOYS WITH REFRACTORY METALS: OBTAINING, PROPERTIES, APPLICATION

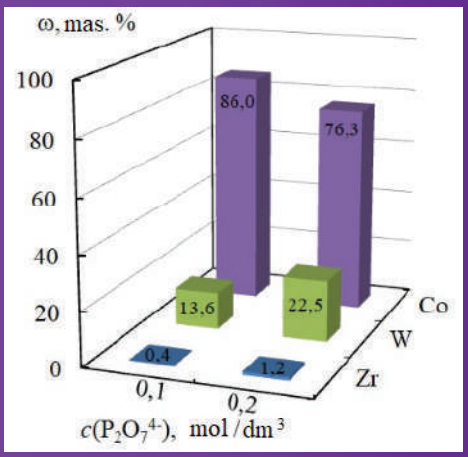

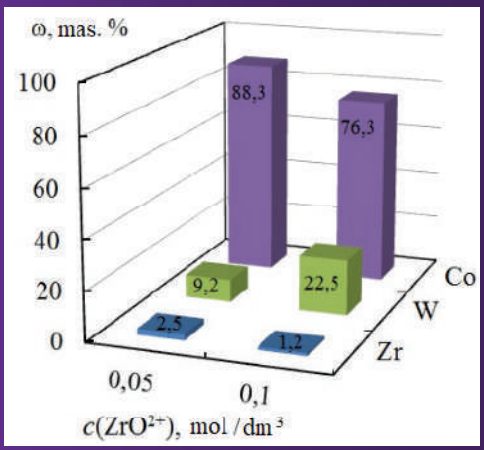

Алматы 2022

AL-FARABI KAZAKH NATIONAL UNIVERSITY

NANOCOMPOSITE ELECTROLYTIC COATINGS BASED ON COBALT ALLOYS WITH REFRACTORY METALS: OBTAINING, PROPERTIES, APPLICATION

Monograph

Almaty
«Kazakh University»
2022

UDC 544.6
LDC 24.57
N 21

Recommended by the Academic Council of Faculty of Physics and Technology and Publishing Board of al-Farabi KazNU (protocol No. 6 dated 07.02.2022) and RISO of Al-Farabi Kazakh National University (protocol No.1 of september 29, 2022)

Reviewers:
doctor of chemical sciences, professor **Z.A. Mansurov**
doctor of physics and mathematical sciences, professor A**.E. Davletov**

N 21 **Nanocomposite** electrolytic coatings based on cobalt alloys with refractory metals: obtaining, properties, application / G.Yar-Mukhamedova, T. Nenastina, M. Ved', N. Sakhnenko, A. Karakurkchi. – Almaty: Kazakh University, 2022 . – 212 p.

ISBN 978-601-04-6049-2

Modern electrochemical technologies for surface treatment of titanium alloys to create protective, antifriction, dielectric, and catalytically active materials are considered. The physicochemical fundamentals of the processes of plasma-electrolytic formation of conversion and composite electrolytic coatings are highlighted. Separate stages of electrode reactions, regularities of the influence of electrolyte components, and electrolysis parameters on the composition, structure, and morphology of synthesized materials are examined in detail. Considerable attention is paid to improving the synthesis of multicomponent alloys and composites based on cobalt from aggregative stable and stable electrolyte solutions, and flexible control of the composition and functional properties of materials is an urgent scientific and technical problem, the solution of which is the presented study. The monograph summarizes the results of the project AP 08855457, "Development of an innovative technology for producing nanocrystalline composite coatings for fuel cell electrodes and hydrogen energy". This research has been funded by the Science Committee of the Ministry of Education and Science of the Republic of Kazakhstan.

The monograph is designed for specialists in the field of chemical technology, as well as teachers, graduate students, and students of higher educational institutions.

UDC 544.6
LDC 24.57

ISBN 978-601-04-6049-2

CONTENT

INTRODUCTION

The creation of compact equipment and devices without the use of the latest materials with a wide range of functional properties is impossible in the period of the rapid development of new directions in various industries and environmental technologies. One of the ways to solve this problem is to form thin electrolytic coatings on the surface of traditional structural materials. Such coatings make it possible to increase the strength characteristics, increase the temperature range of use, and also impart a spectrum of new valuable properties to the materials. To expand the possibilities of using electrolytic coatings, in addition to pure metals, composites and alloys are used, consisting of two or more components.

At the moment, a large number of binary and ternary cobalt-containing alloys are known [1 - 6]. Of particular interest are metal alloys, which are difficult to obtain from aqueous solutions in pure form (W, Mo, Zr, Ni, etc.), but under certain conditions they can be co-precipitated with other metals, including cobalt. The increased interest of researchers and technologists in electrolytic thin-film coatings with metal alloys of the iron triad with d4-elements, in particular molybdenum and tungsten, is due to the possibility of obtaining materials whose functional properties and performance characteristics significantly exceed those of alloy-forming components [7-10].

One of the world trends in functional electroplating is the creation of composite electrochemical coatings (CEC) based on cobalt. The principle of obtaining CEC is based on coprecipitation from electrolyte suspensions together with metals of dispersed particles of various nature and size. Being included in the composition of coatings, the particles of the second phase significantly improve their performance characteristics (hardness, wear resistance, corrosion resistance) and give them new properties (antifriction, magnetic, catalytic). This predetermines the widespread use of composite coatings in various industries. However, an unsolved technology problem remains to ensure the aggregate stability of electrolyte suspensions for the production of CEC.

The above arguments testify to the relevance of the topic under consideration. The use of such coatings will allow solving a number of

practical problems, including the creation of new and improvement of existing electrochemical technologies of hardening [11-13] and protection against corrosion [14, 15].

Among the advantages of using these technological solutions, it should be noted that there is no thermal effect on the material of the products, which can cause undesirable changes in the structure and physical and mechanical properties of the metal; insignificant material costs for work; formation of coatings of a given thickness with a minimum allowance for machining and increased functional properties; the ability to automate the process with the simultaneous processing of a significant number of parts, which generally reduces the cost of the technological process.

An equally important area of application of multicomponent coatings based on cobalt alloys is electrocatalytic materials. They are more accessible in comparison with traditional materials based on platinum group metals [16 - 18] and are no less effective, in particular, in the synthesis of hydrogen. The creation of efficient autonomous energy sources has been and remains one of the most urgent areas that ensure the energy stability of any country. Among a wide range of energy sources, fuel cells are positioned as the most environmentally friendly and promising, since the reactions in them are reduced to the formation of water from fuel - hydrogen and oxygen [19 - 21]. In a number of works [15, 22 - 25], it is proposed to use transition metal alloys to replace precious metals. This is especially promising in the context of the use of new types of fuel (methanol, ethanol, formaldehyde, and hydrocarbons) in fuel cells [26]. Such liquid fuels have significant advantages over pure hydrogen because they are easy to store and transport.

Note that the use of coatings with multicomponent alloys as materials for catalytic converters [27] gave a new impetus to solving the problem of synthesizing non-platinum catalysts for the chemical industry, eco- and energy technologies.

Thus, the development of scientific foundations for the synthesis of multicomponent alloys and composites based on cobalt from aggregatively stable and stable electrolyte solutions, as well as flexible control of the composition and functional properties of materials, is an urgent scientific and technical problem, the solution of which is the presented study.

Chapter 1

FEATURES OF OBTAINING COMPOSITE ELECTROLYTIC COATINGS BASED ON COBALT

1.1 Functional materials based on cobalt

The main part of the obtained cobalt is consumed in the production of various metallurgical alloys [28, 29], since the addition of cobalt makes it possible to increase the heat resistance and wear resistance of steels, and provides an improvement in their mechanical and other operational properties. Magnetic cobalt alloys are especially in demand, in particular, hard magnetic alloys such as $SmCo_5$, $PrCo_5$, which are characterized by significant magnetic energy [30].

Alloys of cobalt with molybdenum have found application as catalysts for organic synthesis processes, and are also classified as efficient electrocatalysts for the hydrogen evolution reaction [31]. It should be noted that the properties of galvanic alloys of cobalt with molybdenum can vary significantly depending on the ratio of the components. Alloys with a high cobalt content exhibit magnetic properties and can be used in devices for recording and storing information. The increased content of molybdenum in the alloy determines the indicators of hardness, chemical and corrosion resistance. Therefore, such materials can be used to increase the wear resistance of machine parts operating at elevated temperatures or in aggressive environments [32, 33].

A fairly large number of electrolytic systems based on cobalt with refractory metals and methods for their preparation are known. For example, to obtain a Co-W alloy with anti-corrosive and catalytic properties in [34], a citrate-pyrophosphate electrolyte was used, with a composition, mol / dm^3: $CoSO_4$ - 0.1; Na_2WO_4 - 0.2; Na_3Cit - 0.2; $K_4P_2O_7$ - 0.2; Na_2SO_4 - 0.5; with the addition of 2 ml/L of water-

soluble resin neonol, the effectiveness of which was shown earlier [35]. The alloy was deposited in the range of current densities 5.0-30.0 mA / cm^2 at a temperature of 50 °C. The resulting coatings contain about 22 at.% W, and the current efficiency is in the range of 40-70%.

A polyligand citrate-pyrophosphate electrolyte was also used in [36] to obtain a Co-Mo alloy. It is shown that an increase in the current density in the range of 1.0-10.0 A / dm^2 leads to a decrease in the content of refractory metal in the alloy from 45.6 to 33.8 wt.%, And an increase in temperature in the range of 25-70 °C promotes an increase in the content of molybdenum from 37.6 to 42.2 wt.%.

A number of works are devoted to the electrodeposition of cobalt-containing coatings with molybdenum [32, 37 - 39], tungsten [41], phosphorus or sulfur [40]. The materials obtained, according to the authors, can be used as electrocatalysts for the evolution of hydrogen, incl. on an industrial scale.

Analysis [42] shows that Co-W alloys obtained from citrate-pyrophosphate electrolyte have high corrosion resistance in chloride solutions, comparable to that of electrolytic chromium. The coatings also demonstrate high electrocatalytic activity in the reaction of hydrogen evolution in an alkaline medium.

In works [14, 43 - 48] it is noted that inductive coprecipitation of molybdenum with cobalt at a low content of a refractory component in the coatings allows preserving the magnetic properties of the obtained functional material.

The main limitation of the widespread introduction of technologies for the electrochemical synthesis of cobalt alloys with d-elements remains the problem of predicting the composition and properties of the obtained coatings associated with rather complex processes occurring both in the electrolyte and at the electrolyte / electrode interface during cathodic polarization.

1.2 Features of coprecipitation of cobalt with refractory metals

Electrochemical deposition of alloys is a very important and promising area of electroplating. At present, several tens of techni-

cally important alloys are obtained by electrolysis on a large scale, most of which are two-component [49].

As is known, the conditions for obtaining an electrolytic alloy of two or more metals on the cathode are close values of their release potentials, due to which the deposition of these metals is joint. The potentials of metal precipitation can be brought closer by varying the activities of ions and overvoltage [50]. The activities of ions can be changed due to complexation [51], as well as by using surfactants.

The study of the regularities of the general discharge of several types of ions is of paramount importance for electrochemistry, since in almost all cases in aqueous solutions of electrolytes there are various ions participating in the reduction reactions at the electrode. In addition to its theoretical value, the study of the mechanism of joint discharge of ions is also of considerable practical interest, since it allows one to control the process of obtaining electrolytic alloys with a set of new properties [52].

Electrochemical deposition of tungsten, molybdenum, and zirconium with cobalt into the alloy is difficult because of the significant difference in the standard electrode potentials of the alloy-forming components. It is impossible to obtain individual coatings with tungsten and molybdenum from aqueous solutions, but with metals of the iron family (Fe, Co, Ni), they can be coprecipitated into an alloy [53–55]. At the same time, the question of the form in which refractory metals are included in the composition of the resulting coatings remains unclear and debatable and is the subject of research.

According to N. Fukushima et al. [56], the role of metals of the iron subgroup as co-precipitants is that they are catalytically active. At the same time, a significant amount of atomic hydrogen is released on their surface, and partially reduced refractory metals form an oxide film, which subsequently contributes to the reduction of oxoanions by atomic hydrogen to the metallic state.

N. Elias and E. Gileadi, using the Ni-W alloy as an example, proposed a model characterizing the process of alloy formation from moderately alkaline citrate electrolytes in the presence and absence of NH_3 [57, 58]. According to the authors, the reduction of alloy-forming components occurs due to the formation of a metal-mixed complex, which is an intermediate citrate complex of a metal ion of

the subgroup of iron and tungsten. According to this mechanism, the deposition of a metal of the iron subgroup can also occur independently from any complex in solution (citrate, ammonia, etc.). The synergistic interaction of Ni and W is shown, as well as the dependence of the content of the refractory component in the alloy on the pH of the electrolyte and the nature of the ligand due to the difference in the stability constants of the complexes. N. Elias and E. Gileadi also found diffuse limitations in tungsten reduction.

A.T. Vasko in his works [59, 60] proposed a radical-film model [61], according to which the electrodeposition of a binary alloy occurs due to the formation of reactive particles of the radical type with the formation of a film of heteropolyanions of refractory metals with subsequent electrochemical reduction of ions of coprecipitated metals at the film boundary / alloy. In this case, the reduction of metals of the iron family occurs through particles (monads) adsorbed at the cathode, which are formed from MOH^+ hydroxocations by a one-electrode reaction with the subsequent formation of a complex intermediate [61].

Partial confirmation of this point of view was obtained in the works of I. Epelboin with R. Wiart [62] and V.S. Rachinskas [63]. This allows us to conclude that the process of alloy formation is preceded by a chemical reaction of the interaction of metal hydroxoforms of the iron triad with oxoanions.

The study by Podlaha and Landolt [64] showed that the Mo content in the alloy does not correlate with the amount of hydrogen released in the side reaction during electrodeposition. It is noted that a high content of Mo in the alloy can be obtained from aqueous electrolytes at different rates of current efficiency (CE).

According to the authors of [65], the most probable mechanism for the coprecipitation of cobalt with molybdenum is the mechanism of reduction of oxoanions to the intermediate oxide MoO_2 in the presence of citrate cobalt complexes in the solution, which act as a catalyst:

$$\begin{matrix} CoCit^- \\ MoO_4^{2-} + 2H_2O + 2e \rightarrow MoO_2 + 4OH^-, \end{matrix} \qquad (1.1)$$

with the subsequent formation of an adsorbed intermediate $M(I)L_{ad}$, (M – Ni, Co, Fe; L – ligand). It is noted that this compound, upon reduction, competes with the refractory component for free active centers on the electrode surface [66-68]:

$$CoCit^{-} + 2e \rightarrow Co + Cit^{3-} \quad (1.2)$$

$$CoCit^{-} + MoO_2 \rightarrow [MoO_2 - CoCit^{-}]_{ad} \quad (1.3)$$

$$[MoO_2 - CoCit^{-}]_{ad} + 2H_2O + 4e \rightarrow Mo + CoCit^{-} + 4OH^{-}. \quad (1.4)$$

The proposed model of the catalytic action of the cathode surface [69, 70] is based on the assumption of the course of the electrodeposition process through the stage of reduction of oxoanions or hydroxide of a refractory metal, followed by its reduction with hydrogen into a metal hydride of the iron subgroup. Taking this into account, it is assumed that the first metal of the iron subgroup is deposited on the cathode, after which the refractory component is deposited.

A. Survila et al. [71] proposed a mechanism for coprecipitation of Co with Mo in the presence of citric acid. Based on the data [72 - 74], it was found that at pH <7, one can limit the consideration of the following reversible reactions:

$$Co^{2+} + pCit^{3-} + qH^{+} \leftrightarrow CoCit_pH_q^{2+q-3p} \quad (1.5)$$

$$MoO_4^{2-} + pCit^{3-} + qH^{+} \leftrightarrow MoO_4Cit_pH_q^{-2+q-3p} \quad (1.6)$$

$$Cit^{3-} + mH^{+} \leftrightarrow CitH_m^{m-3} \quad (1.7)$$

It should be noted that the proposed mechanisms, on the one hand, are to a certain extent a reflection of the scientific views of various electrochemical schools, and on the other, are based on the results of studies of electrochemical systems with specific initial data (concentration of components and their ratio in solution, pH of electrolyte, etc.). therefore, they cannot be sufficiently used to describe all possible reactions during alloy formation.

Special attention should be paid to scientific works devoted to the methods of deposition of electrolytic multicomponent coatings based on cobalt with refractory metals and the study of the factors influencing the alloy formation process.

Electrolytic alloys of cobalt with d^4-metals

For the deposition of binary and ternary alloys of cobalt with tungsten and molybdenum, glycinate, citrate, chloride-citrate, pyrophosphate, and pyrophosphate-citrate electrolytes are most often used [75]. It is noted that the introduction of EDTA (ethylene di-amine tetra acetate) acid into the composition of the electrolytic bath promotes an increase in the content of refractory components in the alloy [76]. In most electrolytes, alloy-forming metals are introduced in the form of cobalt sulfate and sodium tungstate / molybdate, and organic substances are used as ligands.

In [77, 78], the ratio of alloy-forming metals $[Co^{2+}]$: $[MoO_4^{2-}]$ = 8: 1 was used and it was found that the composition of the deposited coatings included from 5 to 25% molybdenum. An increase in the concentration of molybdate ions in the solution contributes to an increase in the content of the refractory component in the alloy composition, but at the same time the quality of the coating deteriorates sharply, the current efficiency and the deposition rate of the alloy decrease. The introduction of ammonium hydroxide into the composition of the citrate electrolyte promotes an increase in the molybdenum content, but the current efficiency of the alloy does not exceed 20% in an acidic medium, and upon alkalinization of the solution's current output, it decreases even more [79, 80].

E. Gomez, E. Pellicer et al. [81], using the example of binary cobalt-molybdenum alloys, note a significant effect on the properties of not only the ratio of alloy-forming metals in the coating, but also the structure of the resulting cathode deposits. Coatings with Co-Mo alloys with a molybdenum content of up to 20 - 23 wt.% Were deposited from sulfate-citrate solutions at a fixed sodium citrate concentration of 0.2 mol / dm3 and varying amounts of cobalt sulfate and sodium molybdate [40]. The content of molybdenum in the alloy increases with increasing cathodic polarization. The structure of the deposits is close-packed hexagonal, but changes to a mixed crystalline-amorphous one with increasing current density [82]. The authors note that the degree of crystallinity depends on the thickness of the deposits: an amorphous structure is characteristic of thin films. The inclusion of molybdenum in cobalt deposits leads to a significant decrease in the coercive force, in particular, coatings with a molybdenum content of 6-10 at.% Are characterized by significantly lower Hc values.

Compact continuous coatings of Co and Co-Mo (ω (Mo) = 1-8 wt.%) Were deposited on copper substrates from ionic liquids of eutectic composition based on choline chloride (ChCl): ChCl - urea and ChCl - ethylene glycol at a current density in within 7–25 mA / cm^2 at temperatures of 90–100 ° C [83].

To obtain amorphous Co-Mo alloys, a unipolar current with a maximum amplitude of 20 A / dm^2 and a pulse duration of 1 ms was used. The content of molybdenum in the alloy depends on the Mo / (Mo + Co) ratio in the solution at constant and pulsed currents. It was found that in the studied modes, the content of molybdenum in the coating does not exceed 40 wt%. the pulse mode provides the highest degree of homogeneity of the amorphous phase. The authors of [84] believe that the deposition of amorphous Co-Mo alloys occurs from the adsorbed intermediate hydrated complex $CoO \cdot xMoO_2 \cdot yH_2O$.

Since the overvoltage of hydrogen evolution on molybdenum and its alloys is low, the deposition rate and the current efficiency of Mo-containing alloys are significantly reduced. In some cases, hydrazine is added to electrolytes to accelerate the process of electrodeposition of molybdenum alloys [85, 86]. An approach is known [87] in which sodium hypophosphite acts as an accelerator, since the introduction of a small amount of phosphorus into the alloy does not change the morphology and functional properties of the material. In this case, the incorporation of phosphorus into the alloy changes the kinetics of coprecipitation of molybdenum with cobalt. A similar effect was obtained in the case of the inclusion of phosphorus in the composition of ternary alloys of tungsten with Co, Ni, and P [84-89]. Investigation of the processes of phosphorus incorporation into the Co-Mo-P alloy is also the subject of papers [90-92].

Known ternary electrolytic alloys of cobalt with molybdenum (tungsten), to which non-metallic impurities - boron, phosphorus, carbon - are incorporated from the electrolyte in small quantities. Amorphous electrolytic alloys Co-Mo-B (51% Co, 47% Mo, and 2% B) with high microhardness, corrosion resistance, wear resistance, and sufficient plasticity were obtained from citrate-phosphate-amiakate electrolyte [93]. The cathode current efficiency is in the range of 29-65%. Citrate-phosphate electrolyte was also used to

obtain coatings with Co-Mo-P alloys containing 8% Mo and 20% P [94-96].

Amorphous Co-Mo-C coatings were obtained by electrodeposi-tion in a magnetic field with the orientation of the field lines parallel to the working electrode [97]. It is noted that the content of molybdenum in the coatings ranges from 27.6 at.% to 34.2 at.%, Which ensures a decrease in the overvoltage of hydrogen evolu-tion on these materials.

The authors of [98] proposed a method for producing a ternary Co-Mo-W alloy from a citrate electrolyte with the ad-dition of Ethylenediaminetetraacetic acid (EDTA). However, such coatings are uneven and have a network of cracks.

In [99], the effect of the current density on the mechanical and tribological properties of coatings with alloys of cobalt with molybdenum and tungsten was established. Experiments have shown that an increase in the current density in the range 2 - 9 A/dm^2 during electrodeposition promotes an increase in the microhardness of the obtained coatings.

In a number of works [100 - 102], the influence of hydrodynamic conditions and temperature on the composition, morphology, and functional characteristics of coatings was investigated. On the basis of the studies carried out, the optimal composition of the electrolyte (mol/dm^3) was proposed: Na_2WO_4 – 0,2; $CoSO_4$ – 0,2; $C_6H_8O_7$ – 0,04; $Na_3C_6H_5O_7$ – 0,25; H_3BO_3 – 0,65, pH 6,8, the deposition temperature is 60 ° C, the average current density is 0.5–3 A / dm^2. At a stirring speed of 400 rpm, the current efficiency was about 90%, and the tungsten content of the alloy was about 40 wt%. With these parameters, the coatings had a maximum microhardness of 570 kg / mm^2.

One of the ways to control the composition and properties of the resulting coatings is the use of various modes of electrolytic alloys.

The Co-W coating deposited at a temperature of 60 ° C in the galvanostatic mode [103] has the appearance of a gray matte layer. An increase in the current density leads to a sharp increase in the current efficiency of the alloy, but has almost no effect on its chemical composition. A decrease in the electrolyte temperature to room temperature causes a drop in the process efficiency to 20%, but

the tungsten content in the alloy remains at the level of 30%. The use of the pulsed mode does not significantly affect the current efficiency, and the dependence of the tungsten content in the alloy on the current amplitude has a maximum at the point 10 A / dm^2 and is ω (W) = 27%.

The authors of [104] carried out a comparative analysis of the effect of stationary and pulsed modes on the content of impurities in the Co – W alloy. Thus, in a stationary mode at a current density of 1 A / dm^2, an alloy was obtained containing 2.4 wt% nonmetallic impurities and 5.3 wt% tungsten, and with an increase in the current density at i = 10 A / dm^2, the impurity content increases to 35 wt.%, and tungsten is reduced to 1.1 wt.%. At the same time, for coatings obtained in a pulsed mode, the content of impurities significantly decreases to 0.33 wt.%, And tungsten increases to 28.2 wt.% With an almost unchanged current efficiency at the level of 80%. Thus, the use of a pulsed current in comparison with a constant one contributes to a noticeable decrease in the content of non-metallic impurities in the Co-W coatings and an increase in the percentage of tungsten with a constant process efficiency, current output (CO).

Binary Co-W coatings obtained in the galvanostatic mode from a gluconate-chloride electrolyte at a temperature of 80 ° C [105] have rather high indicators of wear and corrosion resistance, comparable to electrolytic chromium.

In [106], Co – W coatings were obtained from a complex electrolyte based on regenerated tungsten salts using citric acid as a ligand. According to the research results, the authors conclude that dense amorphous Co-W coatings with a maximum tungsten content of 44.2 wt. % and hardness (Hv) 550 kg / mm2 can be obtained from the proposed electrolyte with pH 7 at a temperature of 60 °C in galvanostatic mode at a current density of 0.5 A / dm^2. The authors note a rather high speed and efficiency of the process - 3.487 g / ($m^2 \cdot h$) and current output 65%.

The authors of [107] developed a peroxide electrolyte from which a cobalt-tungsten alloy with a refractory metal content of up to 30 wt.% And VT up to 70% can be deposited. But the main disadvantage of the proposed electrolyte is its instability, which makes it impossible to use it in industry.

In [108], it was concluded that the efficiency of the process of deposition of a Co – W alloy with a high tungsten content at room temperature in both stationary and pulsed modes was concluded. An increase in the electrolyte temperature to 60 °C, a decrease in the frequency of unipolar pulses (duty cycle q = 11) and a simultaneous increase in the amplitude allows increasing the current efficiency. With a decrease in the pause duration, the current efficiency of the alloy at high values of the current amplitude decreases, while at low values, it increases. In addition, an increase in the pause duration leads to an increase in the tungsten content in a wide range of current densities, which is probably due to the equalization of the concentration of hydrogen ions in the near-cathode layer, as a necessary prerequisite for the implementation of a multistage process of reduction of tungsten (VI) ions.

Since it is known that molybdenum and, especially, tungsten are effective amorphizers of the structure of alloys, this aspect also causes considerable attention to them, since in such systems one can expect a significant increase in the consumer properties of thin-film materials and coatings. The authors of [107] showed that with an increase in the tungsten content to 45 wt.%, The microhardness (Hv) of Co-W deposits increases to 500-600 kg / mm^2, which is comparable to electrolytic chromium. At the same time, the corrosion resistance of coatings in corrosive media also increases, however, only when the concentration of tungsten in the alloy does not exceed 40 wt%. This is explained by the appearance of a network of cracks on the surface of the samples with an increased content of the refractory component.

A group of scientists [109] proposed to obtain Co-W coatings from citrate-chloride electrolytes with polarization by a unipolar pulse current. It is proved that with the same composition of precipitates, the use of non-stationary electrolysis makes it possible to increase the microhardness of the coatings by an average of 15% in comparison with the stationary one. Along with the increased microhardness (400–700 kg / mm2), there is a superadditive increase in the catalytic activity of the obtained coatings in comparison with alloy-forming metals in model reactions of electrolytic hydrogen evolution and catalytic oxidation of benzene [110].

The maximum catalytic effect, according to the data presented, is achieved when the tungsten content in the alloys is 25-35 wt%. The authors draw attention to the fact that in the specified range of the content of the refractory component in the Co-W coating, not only the maximum values of the hydrogen exchange current density are recorded, but also the lowest ignition temperature of the flameless oxidation of benzene [111].

It should be noted that not only their qualitative and quantitative composition, but also their microstructure plays a significant role in ensuring the increased functional properties of coatings. The listed parameters together provide high consumer properties of the obtained materials [112].

The study of the properties of nanocrystalline Co-W coatings deposited from an electrolyte containing cobalt sulfate, sodium tungstate, sodium gluconate, sodium chloride, and borate acid is the subject of the work of the authors [113]. It is shown that varying the current density in the range of 1 - 5 A/dm^2 makes it possible to deposit coatings of different composition and surface morphology. At low current densities, coatings of the crystal structure are deposited, and when the current density is increased to 5 A/dm^2, they are amorphous. Obviously, this is due to an increase in the content of the refractory component in the alloy with an increase in the current density, which plays the role of an amorphizer.

To reduce the roughness and increase the microhardness of Co-W coatings, the authors of [114] proposed an electrolyte composition, g / l: cobalt sulfate $CoSO_4 \cdot 7H_2O$ – 56,2, citric acid $C_6H_8O_7$ – 7,68, sodium citrate $Na_3C_6H_5O_7 \cdot 2H_2O$ – 73,5, boric acid H_3BO_3 – 40, sodium tungstate $Na_2WO_4 \cdot 2H_2O$ – 66,0 with additions of sodium oleate and butynediol. The electrolysis was carried out at a current density of 1 A/dm^2 and a temperature of 60 °C. The authors note the formation of a spheroidal structure of the coating and a decrease in its roughness when these additives are introduced into the working electrolyte. However, an increase in the concentration of additives in the electrolyte leads to an underestimation of the current efficiency, and when the concentration of surfactants in the solution increases by a factor of 2 - 2.5, the microhardness of the coatings decreases threefold.

The authors of [115] investigated the effect of leveling additives (water-soluble neonol resin and OP-10) on the composition and morphology of Co-W coatings deposited from a citrate-pyrophosphate electrolyte. It was found that the introduction of a surfactant does not affect the content of the refractory component in the coating, ω (W) is at a level of 22 at.%. In this case, the introduction of neonol into the electrolyte allows, at i = 5 mA/cm^2, to deposit compact shiny coatings and to increase the current efficiency to 68%, and OP-10 promotes the formation of spherulites and the development of the surface. It is noted that the deposited alloys are characterized by high corrosion resistance in chloride solutions, which correlates with the stability of electrolytic chromium. The authors emphasize a significant decrease in the overvoltage of hydrogen evolution in an alkaline medium on Co-W alloys (by 360 mV at i = 30 mA/cm^2) in comparison with electrolytic cobalt. At the same time, attention is drawn to the undesirable effect of additives in electrolytes on the electrocatalytic properties of the formed precipitates through the leveling effect of surfactants. They improve the mechanical and anti-corrosion properties of coatings, but reduce their true surface area.

In [116], the corrosion and catalytic properties of Co-W coatings with ω (W) = 20-22 at.%, Obtained from citrate-diphosphate electrolytes, were investigated. It has been established that Co-W alloys have high corrosion resistance in chloride solutions, comparable to that of electrolytic chromium. The coatings have a fine-crystalline and spheroidal structure and demonstrate electrocatalytic activity in the reaction of hydrogen evolution in an alkaline medium. Nanocrystalline coatings with a Co – W alloy with a tungsten content of 35 wt% and a grain size of 15 nm were also obtained by N. Fathollahzade and K. Raeissi [117]. The microhardness of these coatings was up to 360 Hv.

N. Tsyntsaru et al. [118] deposited coatings with a Co-W alloy in a galvanostatic mode from a citrate-borate electrolyte with discrete variation of its acidity pH from 5 to 8 at a temperature of 60 ° C and current densities of 3-10 mA / cm^2. According to the data presented, at a cobalt / tungsten ratio in the electrolyte of 1: 1, the tungsten content in the coating increases from 3 at.% To 36 at.% With increasing current

density and increasing pH. Researchers pay attention to the transition from the crystalline to the globular structure of the coatings with an increase in the acidity of the solution from 5 to 8 and a significant decrease in the crystallite size due to an increase in the tungsten content in the coating. An extreme dependence of the microhardness of the Co-W alloy on the amount of the refractory component was found, the maximum of which is observed at a tungsten content of 25 at.% And is 13 GPa. The researchers also note an increase in the coercive force from 170 Oe for pure Co films to 470 Oe for films with 2-3 at.% Tungsten, which is attributed to the formation of solid magnetic Co3W clusters, which can partially be responsible for the semi-solid ferromagnetic behavior. The NS coercive force decreases with an increase in the tungsten content, which, according to the authors, may be due to a gradual decrease in magnetocrystalline anisotropy during the transition of coatings to a nanocrystalline or amorphous structure.

According to the data presented [120 - 122], uniform Co – W coatings with a tungsten content of 30–40 wt% were obtained from citrate electrolytes. The authors note that the composition of the coatings is practically independent of the current density; however, with an increase in iк, the microstructure of the deposited films becomes more perfect. During the electrocrystallization of Co_3W, the formation of a bcc structure was observed, which creates conditions for a solid ferromagnetic behavior of the alloy, and amorphous Co – W alloys with a fcc texture are characterized by soft magnetic behavior.

The authors of [121] presented the results of the deposition of binary Cu-W, Co-W and ternary Co-W-Cu coatings from a citrate-borate electrolyte in a potentiostatic mode at a temperature of 20 ° C and 60 ° C. The authors argue that the efficiency of the deposition process for both binary and ternary Co-Cu-W alloys is more influenced by the tungsten content than by the temperature rise. When the tungsten content in the Co-W coating is 14 - 20 at.%, The process efficiency is close to 50% in comparison with BT = 27.5% at a tungsten content of 20 at.%. At the same time, the authors note that with an increase in the tungsten content to 30 at. % current efficiency does not exceed 20%.

The prospects for using electrolytic alloys of cobalt with molybdenum and tungsten, obtained from citrate-pyrophosphate electrolytes, in the reaction of electrochemical hydrogen evolution are shown in [122]. Z. Ghaferi, S. Sharafi, report that, despite the higher surface defects during the deposition of the Co-W-Fe alloy at lower electrolyte pH values, it is these coatings that have the maximum microhardness at the level of 260 Hv, which is due to the rather high tungsten content in alloy [123, 124].

For these reasons, the control of the formation process of electrolytic coatings of a given composition, although based on the general laws of electroplating, is in many respects empirical and requires the refinement of many methodological aspects.

Composite electrolytic coatings

Composite materials (CM) with a metal matrix are used in many industries. Combining metals with substances of a different nature can significantly increase their performance properties. In this regard, the creation and use of CM is a technologically and economically advantageous condition for production. At present, the improvement of technologies for the production of such materials has made it possible to use them in the aerospace, automotive, shipbuilding and other branches of technology, where a combination of high strength, microhardness, as well as an increase in resistance to wear, exposure to high temperatures and corrosive environments is required. Strengthening of composite materials with a metal matrix is carried out with particles of various shapes and sizes, continuous and discontinuous fibers. CMs with reinforcing particles differ from fiber-reinforced CMs in isotropic properties, lower production costs and the possibility of further processing. The use of modern methods for obtaining composite materials with improved physical, mechanical and chemical properties made it possible to increase the functional properties of metals by applying composite coatings with high strength indicators on their surface.

Such processes for obtaining composites based on a metal matrix are known:

- liquid phase - directional crystallization and / or impregnation of prepared filler frameworks;

- solid-phase - powder technology, diffuse splicing and other thermomechanical technologies;

- gas and vapor phase - condensation from the gas (vapor) phase;

- chemical - chemical, electrochemical and thermochemical deposition [125-128].

One of the many methods of forming a matrix material in the production of metal composites is its precipitation from electrolytes containing a strengthening phase. In industrial electroplating, the technology of deposition of composite electrochemical coatings (ECC) is used by obtaining a metal layer on the cathode, in the volume of which solid dispersed particles are incorporated. In such dispersion-hardened composite materials, dispersed particles are distributed in the volume of the metal matrix. A necessary condition for the formation of a CEC is the presence of a nano- or micro-fine dispersed phase in the electrolyte solution, from which the metal is electrodeposited. In this case, electrolytes are suspensions.

Composite coatings can be obtained from foamy media or emulsions formed when hydrophobic liquids are introduced into electrolytes. When an electric current is applied to the surface of the substrate to be coated, the metal is deposited - the first phase or matrix, as well as powder particles - the second phase, which is cemented by the matrix. The deposition of composite electrolytic coatings is usually carried out with continuous stirring of the suspension, while the particles of the second phase are in suspension and deposition is faster. The choice of the mixing method is determined by the shape of the particles, electrolysis conditions and economic feasibility. In small baths, mechanical stirring is used, in large ones, bubbling with air or inert gas is used. In addition, it is possible to obtain uniform stirring of the suspension by rotating the cathode or circulating the electrolyte [129, 130].

The efficiency of using composite coatings is largely determined by the nature of the dispersed phase, which can be oxides, carbides, borides, nitrides, silicides, the particle size of which does not exceed 3-5 microns. The second phase of composite coatings can also be metal

In [131], the electrodeposition of composite electrochemical coatings from a colloidal nickel-plating electrolyte containing ultra-

fine zirconium diboride powder was studied. Composite coatings Ni-ZrB_2 have a high microhardness of about 10-11 hPa, which exceeds the microhardness of pure nickel by 1.5-2 times. With an increase in microhardness, the internal stresses of the Ni-ZrB_2 CEC decrease. The wear resistance of this CEC is 2-5 times higher than that of chrome coatings, which makes it possible to use the proposed composition for surface hardening of parts of special equipment and industrial equipment.

In [132], a chloride electrolyte was proposed for applying a composite electrolytic coating of nickel-cobalt-aluminum oxide. The paper investigates the effect of electrolysis modes and electrolyte composition on the physical and mechanical properties of ECCs and shows the possibility of replacing wear-resistant chromium coatings with them.

The authors of [133, 134] studied the patterns of incorporation of zirconium dioxide nanoparticles into a nickel matrix during electrodeposition of Ni-ZrO_2 composite coatings from methanesulfonate and sulfate electrolytes. It was shown that nanocomposites with a large amount of zirconium dioxide (up to 5 - 15 wt%) were obtained from methanesulfonate electrolyte, which is explained by a higher partial concentration of ZrO_2 with an increase in the aggregate stability of the dispersed phase in an electrolyte of this type.

A known method [135] for obtaining a composite coating of nickel-zirconium dioxide at a cathode current density of 1 A/dm^2, a temperature of 50 ° C and pH = 4.5 from an electrolyte, which includes (g / dm3): $NiSO_4 \cdot 7H_2O$ - 240; $NiCl_2$ - 45; H_3BO_3 - 40; ZrO_2 (40 nm) - 4-30. The content of ZrO_2 in the resulting sediments is 22 - 42 wt.%. However, as a disadvantage, it should be noted a narrow range of electrodeposition current densities and low aggregate stability of a suspension electrolyte containing zirconium dioxide nanopowder.

In [136], nanocomposite coatings Ni-Mo and Ni-W were obtained by electrochemical deposition in a galvanostatic mode from a nickel plating bath containing nanopowders of molybdenum (<100 nm) or tungsten (<150 nm). The study of the kinetics of the hydrogen evolution reaction showed a high electrochemical activity of the Ni-Mo electrode in comparison with Ni-W.

In [137], the authors investigated a chemical method for the formation of composite electrochemical coatings and foils based on nickel, reinforced with nanosized aluminum oxide. A mechanism for the formation of composites and a mathematical model reflecting the relationship between the content of the strengthening phase in the CEC and the concentration of the Al_2O_3 hydrosol in the electrolyte were proposed. The incorporation of Al_2O_3 nanoparticles into the base metal matrix contributes to a decrease in the grain size and an improvement in the mechanical properties of composites: the microhardness and ultimate strength of composites increase by 1.5 - 2 times, a significant increase in the yield strength is observed in comparison with a nickel coating.

Known composite coatings of the Co-W alloy, reinforced with nanoparticles of aluminum oxide [138], which can be used to replace coatings with hard chromium. This method provides obtaining a Co-W alloy with nanoparticles of aluminum oxide with high wear resistance. But the insufficiently high sedimentation stability of the electrolyte-suspension makes it necessary to maintain the particles in suspension by special operations, for example, ultrasonic or magnetic field treatment.

The authors of [139] developed an electrolyte for the deposition of Co-Mo-TiO2 coatings. The deposition of cobalt on a substrate of copper, chromium-nickel alloys and stainless steels is ensured by the formation of an ammonia-trilonate complex. The ammonium ion catalyzes the electrochemical reaction of the reduction of molybdates to the metal; therefore, the addition of ammonium sulfate to the electrolyte provides an increase in the percentage of molybdenum in the Co-Mo-TiO_2 alloy. The resulting coatings have high adhesion to the carrier and are uniform.

In [140], the principles of the formation of oxide composite nanostructured materials by the electrochemical method are considered, methods are considered, and the advantages of transient electrolysis in the production of such materials are shown. Thus, a review of literary sources does not allow one to determine the ways of forming composite coatings of cobalt with refractory metals directly from aggregatively stable electrolyte solutions with varying parameters and modes of electrolysis.

Thus, from the analysis of the literature it follows that recently

there has been an increase in the interest of researchers in the electrochemical synthesis of both multicomponent alloys based on cobalt and composite coatings with metals of the iron subgroup with refractory components. This is due to the possibility of combining in such coatings a whole range of unique properties inherent in alloy-forming components, and in some cases - superadditive enhancement of operational characteristics. However, the variety of ionic forms of electrolyte components, the presence of a number of competing reactions during the establishment of ionic equilibria, as well as the multistage nature of the electrode process, complicate the interpretation of the results for determining the mechanism of formation and predicting the composition and properties of deposited thin-film materials. At the same time, the results of the analysis of scientific and technical information made it possible to identify the following problem areas in the existing developments, which are the basis for the authors' own research, namely:

- electrolytic systems of cobalt with refractory components have not been sufficiently studied both in Ukraine and abroad. Most of the presented results concern the electrodeposition of binary coatings Co, Ni-W, Mo;

- Electrodeposition of triple coatings based on cobalt with tungsten and molybdenum makes it possible to level the internal stresses inherent in electrolytic thin-film materials, low adhesion, and also to increase the physical and mechanical properties.

- binary systems Co-Mo (W) are aimed at creating mainly catalytic and magnetic materials. In our opinion, Co-Mo-W, Co-Mo-Zr, Co-W-Zr coatings, as well as composites based on them Co-Mo-WOx, Co-Mo-ZrO_2, Co -W-ZrO_2, since the implementation in thin layers of simultaneously increased wear and corrosion resistance, magnetic and catalytic properties makes such coatings universal and allows you to significantly expand the scope of their application.

It should also be noted that to date, systemic studies of the dependence of the elemental composition and morphology of the surface of coatings on electrolysis modes and their correlation with indicators of physicochemical parameters and functional properties have been insufficiently illuminated. The literature completely or partially lacks data on the phase composition of coatings and its

dependence on the nature of polarization (formation by direct or pulsed current).

Thus, taking into account the complexity of the processes of formation of multicomponent coatings and the uncertainty of the conditions for their consumer properties, the solution of such problems has a clearly defined focus on meeting the needs of the industrial complex, in particular, in eco- and energy technologies, in the creation of new materials and coatings with a high level of functional characteristics. Despite a fairly significant amount of research in this direction, the issues of control and management of the quantitative and phase composition, surface morphology, and, accordingly, the properties of coatings remain topical. This determined the goal and objectives of the presented study.

Chapter 2

KINETIC REGULARITIES OF OBTAINING ELECTROLYTIC COATINGS AND COBALT COMPOSITES WITH REFRACTORY METALS

The solution of the tasks requires the study of ionic equilibria in electrolyte solutions and the verification of the working hypothesis about the possibility of cathodic synthesis of multicomponent composites from aggregatively stable and stable electrolyte solutions due to the formation of a strengthening phase of oxides directly in the electrode process. This assumption is based on known information about the stage-by-stage reduction of oxometallates (tungstates and molybdates) during cathodic polarization. This process is also associated with the reduction of cobalt, which makes it possible to flexibly control the electrodeposition process [141] by changing the parameters of the cathode process.

It is known that the features of the co-reduction of cobalt with refractory metals (Mo, W, Zr) directly from the electrolyte solution are due to the mutual influence of thermodynamic and kinetic characteristics of alloy-forming components. The thermodynamic characteristics, first of all, include the equilibrium potentials of metals (Table 2.1), electron and oxygen affinity, ability to complexation and hydrolysis. As can be seen from the above data, the inclusion of zirconium in an alloy with cobalt and molybdenum looks the most problematic due to the potential difference at the level of 1.3-1.7 V.

The crystal chemical parameters reflect the structure and parameters of the crystal lattice of individual metals, the sizes of cations, oxometallates, etc., which significantly affect the mutual arrangement and embedding of atoms in the crystal lattice of the alloy. The ratio of concentrations of salts of alloy-forming metals,

modes and parameters of electrolysis are tools that ensure overcoming the energy and geometric differences of metals, which are restored con-jugately.

Table 2.1

Equilibrium potentials of electrode reactions [177 - 180]

	Reaction	Electrode potential *E*, V
Cobalt		
1	$Co^{2+} + 2e = Co$	$-0{,}277 - 0{,}02951\ \lg c(Co^{2+})$
2	$Co(OH)_2 + 2H^+ + 2e = Co + 2H_2O$	$0{,}095 - 0{,}059$ pH
Molybdenum		
3	$MoO_4^{2-} + 4H^+ + 2e = MoO_2 + 2H_2O$	$0{,}606 - 0{,}1182$pH $+ ,0295\lg c(MoO_4^{2-})$
4	$MoO_4^{2-} + 8H^+ + 3e = Mo^{3+} + 4H_2O$	$0{,}508 - 0{,}1576$pH + $0{,}0197\lg[c(MoO_4^{2-})/c(Mo^{3+})]$
5	$MoO_2 + 4H^+ + 4e = Mo + 2H_2O$	$-0{,}072 - 0{,}059$pH
Tungsten		
6	$WO_4^{2-} + 4H^+ + 2e = WO_2 + 2H_2O$	$0{,}386 - 0{,}1182$ pH $+ ,2951\ \lg c(WO_4^{2-})$
7	$WO_2 + 4H^+ + 4e = W + 2H_2O$	$-0{,}119 - 0{,}0591$ pH
Zirconium		
8	$Zr^{4+} + 4e = Zr$	$-1{,}54 + 0{,}0148\ \lg[Zr^{4+}]$
9	$ZrO^{2+} + H_2O + 4e = Zr + 2OH^-$	$-1{,}570 - 0{,}0295$ pH $+ 0{,}0148\lg[ZrO^{2+}]$
Ionic equilibria		
10	$Zr^{4+} + H_2O = ZrO_2 + 4H^+$	$0{,}91 - 4$pH
11	$ZrO^{2+} + H_2O = ZrO_2 + 4H^+$	$1{,}15 - 2$pH

The competition of metals is also due to their acceptor ability, which is quantitatively characterized by electronegativity and affinity for oxygen (Table 2.2). Sufficiently close values of the relative electronegativity of metals indicate almost identical acceptor properties. However, the strength of bonds with oxygen, which is an electron donor during the formation of heteronuclear complexes with the participation of these metals, will differ, since the binding energy with oxygen is significantly different. So, based on the maximum binding energy of Zr-O among the metals considered, it can be assumed that, other things being equal, zirconium in the electrolyte solution will exist in the form of ZrO_{2+} oxocation, and in coatings there is a high probability of the formation of a phase of ZrO_2 oxides.

Table 2.2

Thermodynamic and crystal chemical characteristics of alloy-forming metals

Parameters	Co	Mo	W	Zr
$E_{M–O}$, kJ/mol	238,5	274,5	223,0	493,0
$E_{M–H}$, kJ/mol	238,5	295,4	305,4	220,0
Electronegativity, X	1,88	2,16	2,36	1,33
Atomic radius, nm	0,125	0,130	0,141	0,160
Ionization energy, eV	7,86	7,10	7,98	6,84
Grid structure	hexagonal	OЦK	OЦK	hexagonal
Grid Parameters, Å	a = 2,505 c = 4,089	3,147	3,160	a = 3,231 c = 5,148

When forming alloys, it is necessary to take into account the difference in the crystal chemical parameters of alloy-forming metals (Table 3.2). The difference in the crystal lattice of cobalt and zirconium from tungsten and molybdenum, as well as the difference in the parameters of the crystal lattices of alloy-forming metals, undoubtedly causes deformation of the alloy lattice and inhibition of linear crystal growth. The atomic radii of molybdenum, tungsten and zirconium exceed the atomic radius of cobalt by 4, 13 and 28%, respectively (Table 2.3), which will cause the displacement of atoms from the equilibrium state during the formation of a monoatomic layer, which increases the probability of the formation of amorphous alloys [142].

From the analysis of E_{M-O} data, it follows that molybdenum, which has a higher energy compared to tungsten, will push it out of the coordination sphere of cobalt. Of particular practical importance is the high thermal solubility of oxygen in zirconium: in β-zirconium it is 2% by weight, whereas in α-zirconium from 5 to 8% by weight of oxygen is dissolved [143]. Thus, according to the strength of the E_{M-O} bond, metals can be arranged in a row [178]: W <Co <Mo <Zr.

2.1 Justification of the choice of ligands for the preparation of composite electrolytic coatings

Considering the value of the standard electrode reduction potentials of cobalt, tungsten, molybdenum and zirconium, the co-deposition of their multicomponent alloys from simple electrolytes is im-

possible [144]. As is known, the convergence of metal potentials is achieved by using ligands forming complex ions with different instability constants [145, 146]. The overwhelming number of ligands are tri- and tetradentant, and, accordingly, have several donor electron pairs. The vast majority of tetradentant ligands can be divided into linear and tetrahedral. When Co(II), having an octahedral acceptor sphere, coordinates the ligand, six nodes are available. And accordingly, ligands of tetrahedral structure will occupy four of the six nodes, leaving two open. These two open nodes can be occupied by two monodentant groups or bidentant ligands. A purposeful combination of ligands can contribute in some cases to the strengthening of all bonds and the formation of mixed complexes superior to monoligand ones in strength, in others - intermediates whose dissociation proceeds with noticeable inhibition. The third group of ligands is characterized by a lack of overall coordination at all. Consequently, the combination of ligands of different nature provides opportunities for conscious control of the electrodeposition process as a whole.

Modern ideas about the mutual influence of ligands in all types of complex compounds, regardless of their geometry [147], suggest that the pyrophosphate ion [148], as a dentate ligand, creates uncompensated induced dipoles, and the resulting dipole strengthens the metal bond with one of the groups, and weakens with the other. Therefore, if neutral substituents or coordination groups are introduced into the solution of an electrolyte containing pyrophosphate complexes as a second ligand, which slightly reduce the effective charge on the central atom, then both ligands can be compatible in the same coordination sphere and can form complex mixed complexes. The citrate ion is considered to be such a ligand.

2.2 Kinetics of cathodic processes of co-deposition of cobalt with refractory metals

To substantiate the rational composition of electrolytes and electrolysis modes, it is necessary to conduct kinetic studies of the regularities of the joint discharge of metals into an alloy or composite coatings.

The study of the mechanism and kinetics of deposition of composite coatings Co-Mo-WOx, Co-Mo-ZrO_2, Co-W-ZrO_2 was carried

out on a specially manufactured electrode, which was a steel wire St3 with a working surface of 0.09 cm^2. A mesh electrode of the Pl 99.9 brand was used as an antielectrode. Before each measurement, the surface of the platinum electrode was treated in a solution of nitrate acid and thoroughly washed with distilled water.

Deposition of composite coatings Co-Mo-WO_x, Co-Mo-ZrO_2 Co-W-ZrO_2 was carried out from citrate-pyrophosphate electrolytes based on cobalt (II) with a varied concentration of components (Table 2.3).

Table 2.3

Compositions of electrolytes for electrolytic deposition of composite coatings based on cobalt alloys

Electrolyte Components	Concentration range, mol/dm^3	pH
Co-Mo-WO_x		
$CoSO_4 \cdot 7\ H_2O$	0,1 – 0,2	8,5–10,5
$Na_2MoO_4 \cdot 2\ H_2O$	0,04 – 0,12	
$Na_2WO_4 \cdot 2\ H_2O$	0,06 – 0,16	
$Na_3C_6H_5O_7 \cdot 2\ H_2O$	0,2 – 0,3	
$K_4P_2O_7$	0,3 – 0,7	
Na_2SO_4	0,3 – 0,5	
Co-Mo-ZrO_2		
$CoSO_4 \cdot 7\ H_2O$	0,1 – 0,3	7,0–10,5
$Na_2MoO_4 \cdot 2\ H_2O$	0,02 – 0,1	
$Zr(SO_4)_2 \cdot 4H_2O$	0,01 – 0,05	
$Na_3C_6H_5O_7 \cdot 2\ H_2O$	0,1 – 0,3	
$K_4P_2O_7$	0,1 – 0,2	
Na_2SO_4	0,3 – 0,5	
Co-W-ZrO_2		
$CoSO_4 \cdot 7\ H_2O$	0,1 – 0,3	6,0 – 10,5
$Na_2WO_4 \cdot 2H_2O$	0,02 – 0,1	
$Zr(SO_4)_2 \cdot 4H_2O$	0,01 – 0,05	
$Na_3C_6H_5O_7 \cdot 2\ H_2O$	0,1 – 0,3	
$K_4P_2O_7$	0,1 – 0,2	
Na_2SO_4	0,3 – 0,5	

Dilute solutions were prepared for kinetic studies of cathode processes, and the concentration of components varied within, mole/dm^3:

$CoSO_4 \cdot 7H_2O$	0,005 – 0,02;
$Na_2MoO_4 \cdot 2H_2O$	0,002 – 0,01;
$Na_2WO_4 \cdot 2H_2O$	0,002 – 0,01;
$Na_3C_6H_5O_7 \cdot 2H_2O$	0,01 – 0,05;
$K_4P_2O_7$	0,01 – 0,03;
$Zr(SO_4)_2 \cdot 4H_2O$	0,001 – 0,005;
Na_2SO_4	1,0.

Let us consider the results of linear voltammetry of cathodic reduction of cobalt with molybdenum, tungsten and zirconium from model solutions of citrate-pyrophosphate electrolytes to establish the mechanism of the cathodic process, kinetic parameters and criteria are calculated, on the basis of which a conclusion is made about the sequence of stages and the nature of the limiting stage in the joint recovery of components.

The application of a systematic approach to the analysis of kinetic patterns in multicomponent systems provides for the analysis of the recovery of individual alloy-forming components with successive complication of the system by adding particles of co-deposited metals and varying ligands. Therefore, it is advisable to establish the mechanism of formation of cobalt composites and alloys according to the following scheme (2.1):

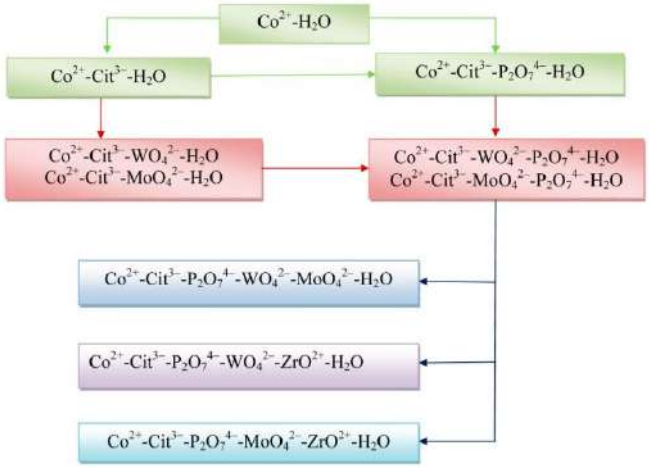

Figure 2.1 - Systems for the study of kinetic patterns of co-reduction of cobalt with molybdenum, tungsten and zirconium

Cathodic reactions in systems:

$$Co^{2+}\text{-}H_2O,\ Co^{2+}\text{-}Cit^{3-}\text{-}H_2O,$$
$$Co^{2+}\text{-}P_2O_7^{4-}\text{-}H_2O,\ Co^{2+}\text{-}Cit^{3-}\text{-}P_2O_7^{4-}\text{-}H_2O.$$

Voltammograms obtained on a steel electrode in solutions with a variable concentration of Co^{2+} ions against a background of 1 mol/dm^3 of sodium sulfate (Fig. 2.2) have a classical form with an adsorption pre–wave in the range of potentials from –(0.4–0.58) of the cobalt reduction current at potentials from –(0.58−0.66) V with a clearly pronounced peak at potentials Ep = −(0.63-0.66) V and a subsequent decrease in current density at potentials from -0.63 to -0.80 V, due to the inhibition of the diffusion of Co^{2+} cations and an increase in the true cathode surface area during the formation of a mono- and poly-layer of cobalt [205]. At potentials more negative than -0.8 V, the reaction of hydrogen release is intensified. It should be noted that peak currents naturally increase with an increase in the concentration of Co^{2+} in solution, and peak potentials become more negative.

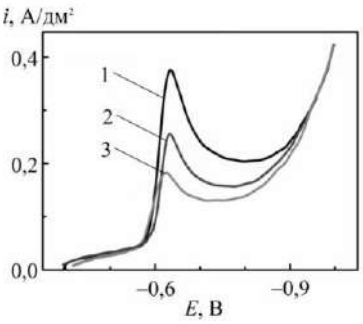

Figure 2.2 - Voltamerograms of a steel electrode on the background 1M Na_2SO_4 when $c(Co^{2+})$, mole/dm^3: 1 – 0,02; 2 – 0,01; 3 – 0,0075; $s = 1 \cdot 10^{-2}$ V/s, $T = 293$ K

Calculated by equation (2.5), the value of the product of the transfer coefficient by the number of electrons az and the Semerano Xs criterion (Table 2.4), the nature of the dependence $i_p / \sqrt{s}$ - s (Fig. 2.3, a), as well as the decrease in αz with concentration indicate the

irreversibility of the cathode process, that is, the deceleration of the charge transfer stage.

Table 2.4

Kinetic parameters of the cathode reaction in the system Co^{2+}-H_2O (background: Na_2SO_4 – 1 mole/dm^3); *s*=0,01 V/s

$c(Co^{2+})$, mole/dm^3	E_c, V	αz	X_s	X_c
0,0075	−0,42	1,2	0,40	0,63
0,01	−0,40	1,0	0,43	
0,02	−0,40	0,85	0,40	

Linear dependences of i_p - s do not originate from the origin in the entire range of cobalt ion concentrations studied (Fig. 2.3), which can be explained by the effect of adsorption of Co^{2+} cations on an electrode made of a foreign metal (steel). A slight decrease in the criterion i_p - √s with the rate of potential sweep, which indicates a subsequent chemical reaction.

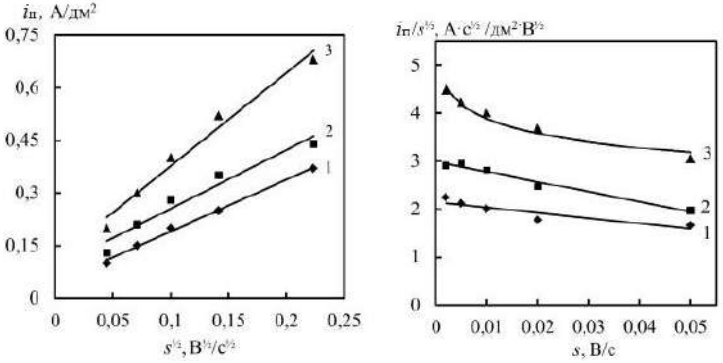

а *б*

Figure 2.3 - Dependence of the characteristic criterion i_p / √s (a) and the current density of the peak i_p (b) of cobalt recovery on the potential sweep rate against the background 1M Na_2SO_4; $c(Co^{2+})$, mole/dm^3: 1 – 0,0075, 2 – 0,01, 3 – 0,02

The value of the concentration criterion X_c (Table 3.6), as well as the nature of the dependencies in the coordinates i_p / c- c and i_p - c (Fig. 2.4) also indicate the presence of the following chemical reaction, the contribution of which to the overall cathode process increases with increasing concentration of cobalt ions in solution.

Taking into account the propensity of cobalt(II) to hydrolysis and an increase in the pH of the near-electrode space due to the parallel reaction of hydrogen evolution, it can be assumed that adsorbed hydroxocations are formed on the cathode surface. $CoON^+$ (K_H = 4.4 · 10-5), the discharge of which will be accompanied by the following reaction of the release of hydroxide ions.

Consequently, the general process of cathodic reduction of cobalt can be represented in the form of successive stages:

$$(Co^{2+})_L + H_2O \leftrightarrow (CoOH^+)_S + H^+ \quad (2.4)$$

$$(CoOH^+)_S + 2e \rightarrow (CoOH^-)_S \quad (2.5)$$

$$(CoOH^-)_S \leftrightarrow Co + OH^-, \quad (2.6)$$

which coincides with the results presented in [202].

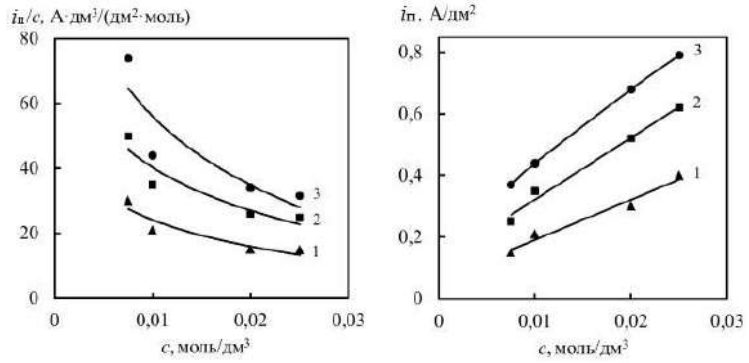

а *б*

Figure 2.4 - Dependence of the characteristic criterion i_p/s (a) and the current density of the peak i_p (b) of cobalt reduction on the background 1M Na_2SO_4 от $c(Co^{2+})$; *s*, B/c: 1 – $5\cdot10^{-3}$, 2 – $2\cdot10^{-2}$, 3 – $5\cdot10^{-2}$

The addition of sodium citrate to solutions with a varied cobalt concentration predictably causes a significant change in pH (pH = 6.3 - 6.8). Taking into account the cobalt hydrolysis constant of the heterogeneous Co^{2+}-H_2O system and the diagram of ionic equilibria in the Cit^{3-} H_2O system in the specified pH range, the formation of citrate complexes is most likely.

The stationary potentials of the steel electrode in Co^{2+} - Cit^{3-} H_2O solutions become more negative compared to the Co^{2+}-H_2O system, the

cathode current density decreases by 1.5 times, and the peaks on the polarization dependences degenerate in the limiting current wave. (fig. 3.20). The slope of the voltammograms becomes more gentle, which indicates a slowdown in the discharge stage and adsorption complications of the process; the potential interval corresponding to the reduction of cobalt becomes twice as large (from -0.60 to -0.70 V), and in the range from -0.70 to -0.90 V, a plateau of limiting current occurs.

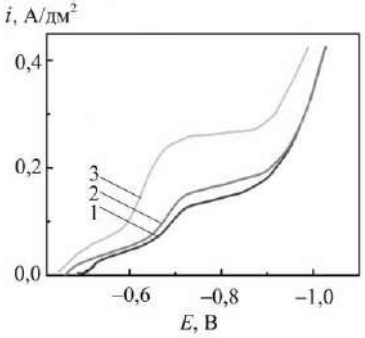

Figure 3.20 - Cathode voltammograms of a steel electrode against a background of 1M Na_2SO_4 in solutions of the composition, mole/dm^3: Cit^{3-} – 0,03; Co^{2+} – 0,0075 (1), 0,01 (2), 0,02 (3); $s = 1 \cdot 10^{-2}$ V/s, $T = 293$ K

The linear nature of the dependence in the coordinates i_p - $\sqrt{s}$, the Semerano X_s criterion and the calculated values of the product of the transfer coefficient by the number of electrons αz, which decrease with the acceleration of the potential sweep, the greater the smaller the ratio $c(Cit^{3-}):c(Co^{2+})$ (Table 3.7), indicate a deceleration of the charge transfer stage.

Table 3.7

Kinetic parameters of cathode reactions in the system Co^{2+}-Cit^{3-}-H_2O (c, mole/dm^3: Cit^{3-} – 0,03; Na_2SO_4 – 1), s=0,01 V/s

$c(Co^{2+})$, mole/dm^3	E_c, V	αz	X_s	X_c
0,0075	−0,48	0,76	0,46	0,95
0,01	−0,46	0,78		
0,02	−0,45	0,85		

The approximation of the concentration criterion X_c to 1 confirms the kinetic control of the cathode process.

The tendency to decrease in $i_p / \sqrt{s}$ with the rate of potential sweep (Fig. 3.21), as well as the decrease in i_p / c with an increase in the concentration of Co^{2+} ions and the nature of the dependence in the coordinates of $i_p - c$ (Fig. 3.22) indicate the contribution of the chemical stage to the overall cathode process.

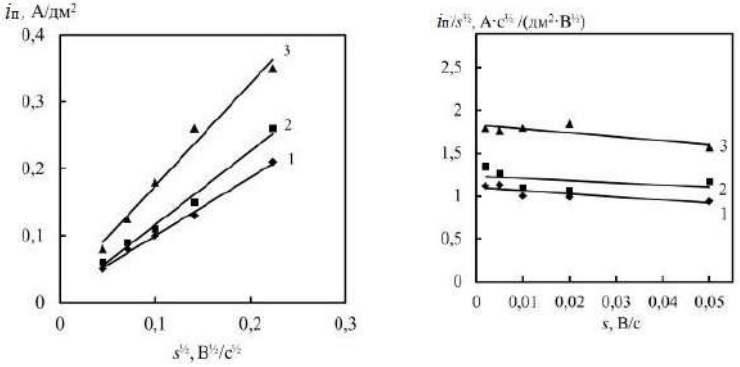

а *б*

Figure 3.21 - Dependence of the characteristic criterion $i_p / \sqrt{s}$ (a) and the current density of the peak i_p (b) cobalt recovery on the potential sweep rate against the background of 1M Na_2SO_4 in solutions of the composition, mole/dm^3: Cit^{3-} – 0,03; $c(Co^{2+})$, mole/dm^3: 1 – 0,0075, 2 – 0,01, 3 – 0,02

The Co^{2+}-Cit^{3-}-H_2O system has been studied [206 - 209], and based on the ionic equilibria and the established kinetic parameters [201, 203, 210 - 212], it can be argued that the dissociation of complex ions occurs reversibly, and the limiting stage of the cobalt reduction process from citrate complexes is the addition of 2 electrons to Co^{2+}.

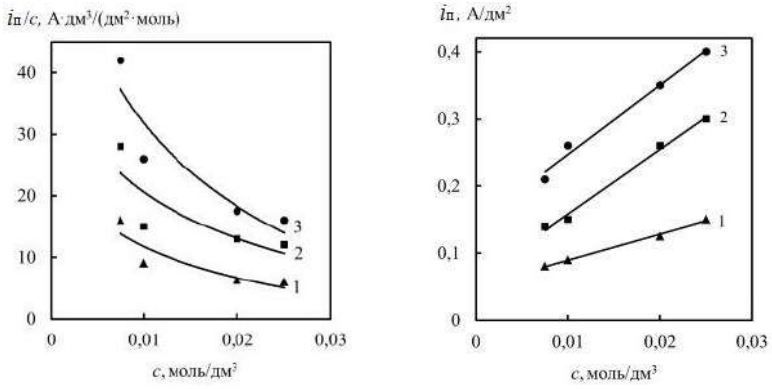

а *б*

Figure 3.22 - Dependence of the characteristic criterion i_p /s (a) and the current density of the peak i_p (b) reduction of cobalt from $c(Co^{2+})$ on the background of 1M Na_2SO_4 from solution, mole/dm³: 0,03 Cit^{3-}; s, mV/s: 1 – 5, 2 – 20, 3 – 50

The reduction of cobalt from a citrate electrolyte can be represented as a complex of sequential reactions:

$$[CoCit]^-_L \leftrightarrow [CoCit]^-_S \quad (3.7)$$

$$[CoCit]^-_S + 2e \rightarrow [CoCit]^{3-}_S \quad (3.8)$$

$$[CoCit]^{3-}_S \leftrightarrow Co + Cit^{3-} \quad (3.9)$$

The form of cathode polarization dependences of cobalt reduction from pyrophosphate electrolyte is similar to the voltammograms obtained for citrate electrolytes, which indicates a similar mechanism. But it is necessary to take into account the stepwise nature of the reduction of particles $[Co(P_2O_7)_2]^{6-}$. Thus, the mechanism of cobalt reduction in the Co^{2+}-$P_2O_7^{4-}$-H_2O system at different concentrations of pyrophosphate will have the following form:

$$[Co(P_2O_7)_2]^{6-}_L \rightarrow [CoP_2O_7]^{2-}_S + P_2O_7^{4-}, \quad (3.10)$$

$$[CoP_2O_7]^{2-}_S + e \rightarrow [CoP_2O_7]^{3-}_S, \quad (3.11)$$

$$[CoP_2O_7]^{3-}_S + e \rightarrow Co + P_2O_7^{4-}. \quad (3.12)$$

When Co^{2+}-Cit^{3-}-H_2O pyrophosphate ion is added to the system, the nature of the polarization dependences changes. The stationary

potentials of the steel electrode in the presence of citrate and pyrophosphate ions in solutions shift towards more negative values compared to Co^{2+}-H_2O and Co^{2+}-Cit^{3-}-H_2O systems, the cathode current density decreases by 2 times compared to Co^{2+}-Cit^{3-}-H_2O (Fig. 3.23).

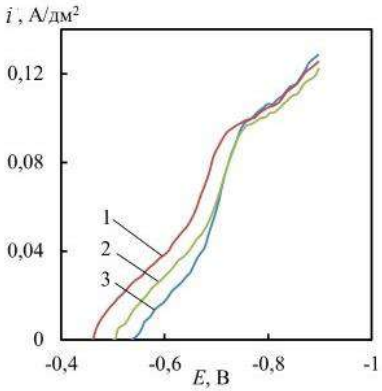

Figure 3.23 - Cathode voltammograms of a steel electrode against a background of 1M Na_2SO_4 in solutions of the composition, mole/dm3: Co^{2+} – 0,01; Cit^{3-} – 0,02; $P_2O_7^{4-}$ – 0,01 (1), 0,02 (2), 0,03 (3); $s = 1 \cdot 10^{-2}$ V/s, $T = 293$ K

The slope of the voltammograms becomes more gentle, which indicates a slowdown in the discharge stage and adsorption complications of the process, the potential interval corresponding to the reduction of cobalt does not change (0.60 -0.70 V), and the limiting current waves are not sufficiently pronounced. Most likely, simultaneously with the reduction of cobalt from mixed complexes, a hydrogen release reaction occurs, as evidenced by oscillations on voltmetograms.

The calculated values of $\alpha z \sim 1{,}1$ indicate a deceleration of the charge transfer stage, which increases with an increase in the concentration of $P_2O_7^{4-}$ relative to Co^{2+} and citrate (Table 3.8). This can be explained by the greater stability of cobalt pyrophosphate complexes compared to citrate ones, and mixed complexes compared to monoligand ones (see Table.3.3). With the ratio of the concentrations of ligands and the complex–forming agent $c(P_2O_7^{4-})$: (Cit^{3-}): $c(Co^{2+})$ 1:2:1, citrate and mixed cobalt complexes dominate in the solution, therefore the kinetic parameters are similar to those given in Table.3.7, that is, reactions 3.7-3.9 mainly occur at the

cathode. With an increase in the concentration of $P_2O_7^{4-}$ relative to citrate, pyrophosphate and mixed complexes already predominate in the solution, hence the mechanism of the cathode process changes, as indicated by the corresponding kinetic criteria (Table 3.8).

Table 3.8

Kinetic parameters of cathode reactions in the system Co^{2+}-Cit^{3-}- $P_2O_7^{4-}$- H_2O (*c*, mole/dm³: Co^{2+} – 0,01; Cit^{3-} – 0,02; Na_2SO_4 – 1); *s*=10^{-2} V/s

$c(P_2O_7^{4-})$, mole/dm³	E_c, V	αz	X_s	X_c
0,01	−0,44	1,02	0,50	0,8
0,02	−0,50	0,72	0,56	
0,03	−0,49	0,62	0,9	

The linear nature of the dependence in the coordinates of i_p - √s, as well as the independence of i_p / √s from the potential sweep rate (Fig. 3.24) at the concentration of ions $P_2O_7^{4-}$- = 0.01 mole/ dm3 indicate the irreversibility of the cathode process and complications of the subsequent chemical stage.

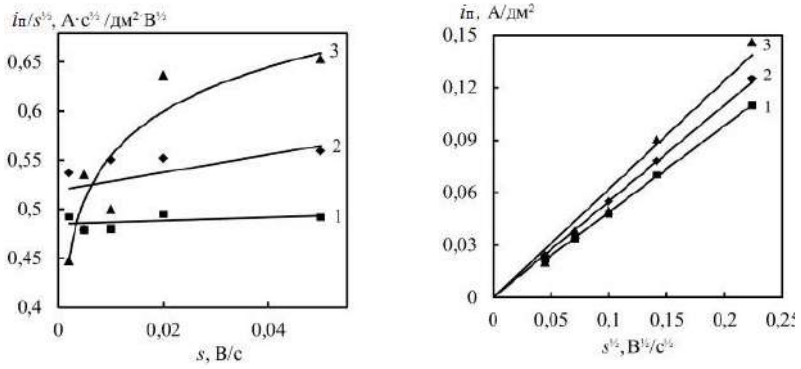

а *б*

Figure 3.24 - Dependence of the characteristic criterion i_p / √s (a) i -th of the peak current density ip (b) recovery of cobalt on the potential sweep rate against the background of 1M Na_2SO_4 from solution, mole/dm³: Co^{2+} – 0,01; Cit^{3-} – 0,02; $P_2O_7^{4-}$ – 0,01 (1), 0,02 (2), 0,03 (3)

With a further increase in the concentration of pyrophosphate ions in solution greater than 0.01 mole/ dm3, the mechanism changes

to a slowdown in the adsorption stage, which is probably due to an increase in the charge of the complex ions.

The values of i_p /s decrease with the concentration of $P_2O_7^{4-}$-ion, and the wave current density practically does not depend on $c(P_2O_7^{4-})$ (Fig. 3.24 a), this is evidence of the discharge at the cathode of cobalt pyrophosphate complexes. To establish the total chemical formula of the substance involved in the discharge stage, the order of the electrode reaction was calculated by the $P_2O_7^{4-}$ ions, which was p = 0, which confirms the preliminary conclusion.

The value of the concentration criterion X_c (Table 3.8), as well as the nature of the dependencies in the coordinates i_p – c (Fig. 3.25 b) indicate the presence of the following chemical reaction, the contribution of which to the overall cathode process increases with an increase in the concentration of pyrophosphate ions.

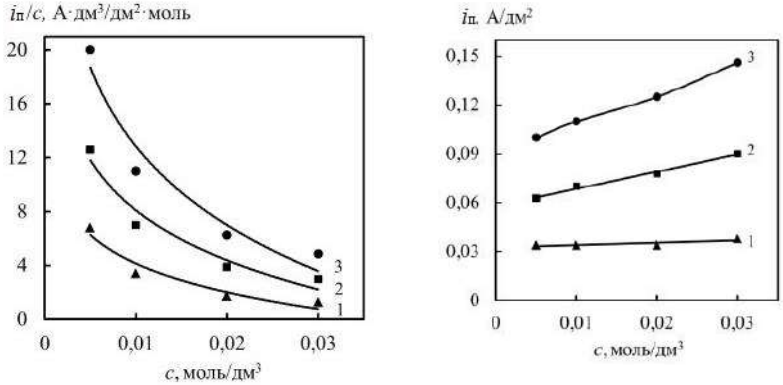

а *б*

Figure 3.25 - Dependence of the characteristic criterion i_p/s (a) and the current density of the peak i_p (b) reduction of cobalt from $c(P_2O_7^{4-})$ on the background of 1M Na_2SO_4 from solution, mole/dm³: Co^{2+} – 0,01; Cit^{3-} – 0,02; *s*, V/s: 1 – $5 \cdot 10^{-3}$, 2 – $2 \cdot 10^{-2}$, 3 – $5 \cdot 10^{-2}$

The totality of the experimental data obtained, taking into account the ionic equilibria in the Co^{2+}-Cit^{3-}-$P_2O_7^{4-}$-H_2O system, the values of the instability constants of pyrophosphate, citrate and mixed cobalt complexes and the results presented in the scientific literature [149], suggests that the reduction of cobalt from citrate-

pyrophosphate electrolyte occurs mainly from mixed $[P_2O_7Co(Cit)]^{5-}$ complexes ($K_н = 2{,}5 \cdot 10^{-10}$) and can be represented as a complex of sequential reactions:

$$[P_2O_7Co(Cit)]^{5-}{}_L \leftrightarrow [CoP_2O_7]^{2-}{}_L + Cit^{3-} \quad (3.13)$$

$$[CoP_2O_7]^{2-}{}_L \leftrightarrow [CoP_2O_7]^{2-}{}_S \quad (3.14)$$

$$[CoP_2O_7]^{2-}{}_S + 2e \rightarrow Co_S + P_2O_7^{4-} \quad (3.15)$$

$$Co_S \rightarrow Co_{КГ} \quad (3.16)$$

in which the indices $(\,)_L$, $()_S$ and $()_{kg}$ means particles in solution, on the surface of the electrode and in the crystal bed, respectively.

Electrochemical behavior of systems

Co^{2+}-Cit^{3-}-WO_4^{2-}-H_2O, Co^{2+}-Cit^{3-}-MoO_4^{2-}- H_2O,

Co^{2+}-Cit^{3-}-WO_4^{2-}-$P_2O_7^{4-}$-H_2O та Co^{2+}-Cit^{3-}-MoO_4^{2-}-$P_2O_7^{4-}$-H_2O

Cathodic reduction of tungstate and molybdenum ions (M - Mo or W) is a multistage process [150-153]:

$$MO_4^{2-} + 2H_2O + 2e \rightarrow MO_2(WO_2) + 4OH^-, \quad (3.17)$$

$$MO_2 + 2H_2O + 4e \rightarrow M(W) + 4OH^-, \quad (3.18)$$

and most often ends with the first stage of the formation of molybdenum oxide or tungsten (IV), which blocks the surface through a higher resistivity (8.8 × 10-7 Ohm * m) compared to metal. This explains the presence of a wave, not a peak, and a decrease in the limiting current on the polarization dependences [154].

In the Co^{2+}-Cit^{3-}-WO_4^{2-}-H_2O system, unlike Co^{2+}-Cit^{3-}-H_2O, peaks appear on the polarization dependences, the height of which practically does not depend on the concentration of tungstates, and the potential range is within –(0.8–0.9) V (Fig. 3.26).

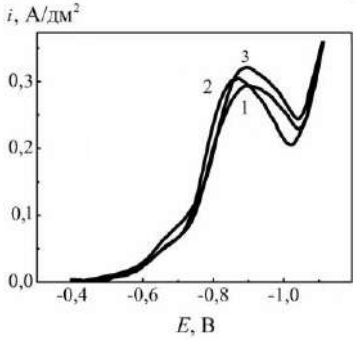

Figure 3.26 - Cathode voltammograms of a steel electrode against a background of 1M Na_2SO_4 in solutions of the composition, mol/dm3: Co^{2+} – 0,01; Cit^{3-} – 0,01; WO_4^{2-} – 0,002 (1), 0,005 (2), 0,01 (3); $s = 1 \cdot 10^{-2}$ V/s, $T = 293$ K

The clearly expressed peak of the voltammogram of the Co^{2+}-Cit^{3-}-WO_4^{2-}-H_2O system indicates a conjugate metal reduction process originating from an unstable complex $[WO_4Co(Cit)]^{3-}$. This is confirmed by the increase in the peak current density compared to the Co^{2+}-Cit^{3-}-H_2O system, which is accompanied by a shift in the peak and half-peak potentials in the positive direction. The values of the product of the transfer coefficient by the number of electrons az and the Semerano criterion X_s are calculated (Table 3.9), as well as the nature of the dependence $i_p / \sqrt{s}$ - s (Fig. 3.27, a), indicate the irreversibility of the cathode process.

Table 3.9

Kinetic parameters of cathode reactions in the system Co^{2+}-Cit^{3-}-WO_4^{2-}-H_2O (*c*, моль/дм³: Co^{2+}– 0,01; Cit^{3-} – 0,01; Na_2SO_4 – 1)

$c(WO_4^{2-})$, mole/dm³	E_c, V	αz	X_s	X_c
0,002	−0,38	0,79	0,69	0,97
0,005	−0,36	0,94	0,61	
0,01	−0,35	0,79	0,58	

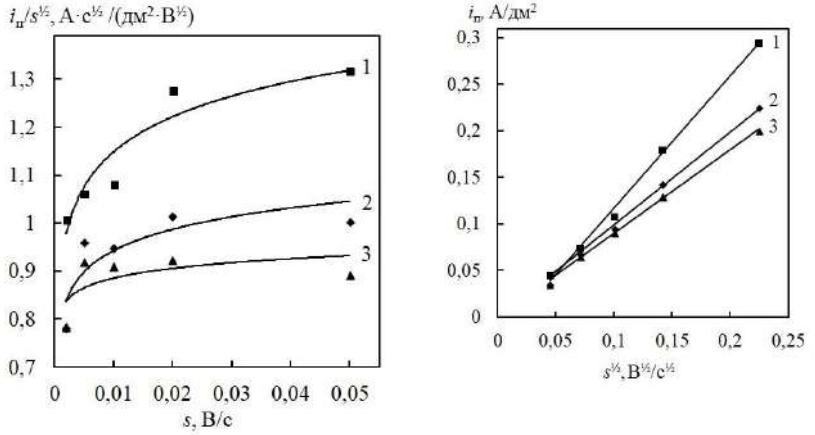

а *б*

Figure 3.27 - Dependence of the characteristic criterion $i_p / \sqrt{s}$ (a) and the current density of the peak i_p (b) with the half-recovery of cobalt and tungsten on the rate of potential sweep against the background of 1M Na_2SO_4 from solution, mole/dm3: Co^{2+} – 0,01; Cit^{3-} – 0,01; WO_4^{2-} – 0,002 (1), 0,005 (2), 0,01 (3)

The dependences of the characteristic criterion $i_p / \sqrt{s}$ (Fig. 3.27) and the peak current density on the scanning rate of the potential indicate the inhibition of the preliminary chemical reaction at all concentrations of tungstate ions.

The dependences of i_p / c and i_p on the concentration of tungstate ions (Fig. 3.28), as well as the values of the concentration criterion X_c (Table 3.9) confirm the inhibition of the preliminary chemical reaction.

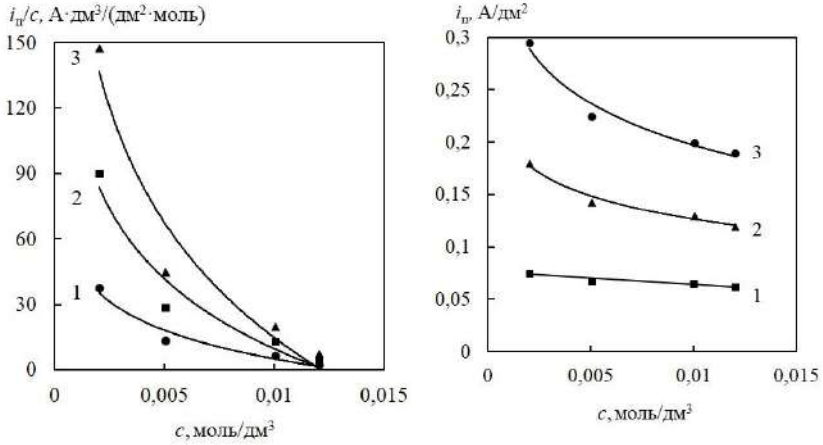

а *б*

Figure 3.28 - Dependence of the characteristic criterion i_p/s (a) and the current density of the peak i_p (b) of cobalt and tungsten co-deposition on $c(WO_4^{2-})$ against a background of 1M Na_2SO_4 from solution, mole/dm3: Co^{2+} – 0,01; Cit^{3-} – 0,01; *s*, V/s: $1 – 5\cdot10^{-3}$, $2 – 2\cdot10^{-2}$, $3 – 5\cdot10^{-2}$

The polarization dependencies of the steel electrode in solution of Cit^{3-}-MoO_4^{2-}- H_2O at 0,002 M Na_2MoO_4 (Fig.3.29) there is a plateau, as for Co^{2+}-Cit^{3-}-H_2O (figure 3.20), while increasing the concentration of molybdate there is a pronounced peak in the potentials(0,7–0,85) V.

The course of the dependencies i_p–$\sqrt{s}$ or $i_p/\sqrt{s}$–s (Fig. 3.30) with varying concentrations of MoO_4^{2-}-ions, and the value αz and criterion Semerano X_s indicate the irreversibility of the process and product adsorption.

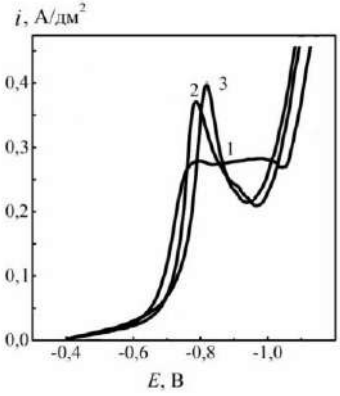

Figure 3.29 - Cathode voltammograms of a steel electrode on the background of 1M Na_2SO_4 in solutions of the remaining load, mole/dm3: Co^{2+} – 0,01; Cit^{3-} – 0,01; MoO_4^{2-} – 0,002 (1), 0,005 (2), 0,01 (3); $s = 1 \cdot 10^{-2}$ V/s, T = 293 K

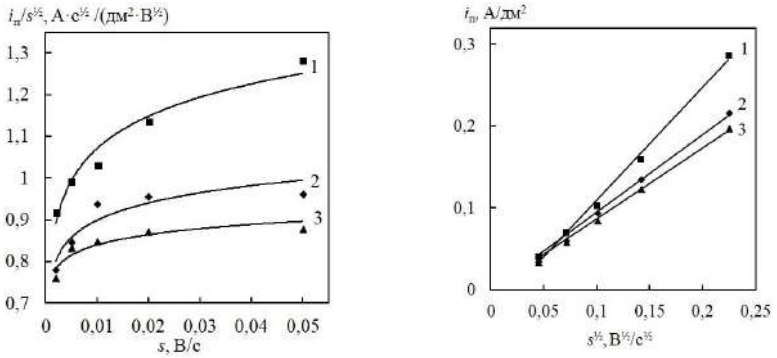

а *б*

Figure 3.30 - Dependence of the characteristic criterion $i_п / \sqrt{s}$ (a) and the current density of the peak $i_п$ (b) of cobalt and molybdenum co-deposition on the potential sweep rate against the background of 1M Na_2SO_4 from ratsovr, mole/dm3: Co^{2+} – 0,01; Cit^{3-} – 0,01; MoO_4^{2-} – 0,002 (1), 0,005 (2), 0,01 (3)

The value of the concentration criterion X_c (Table 3.10), as well as the nature of the dependencies in the coordinates $i_п – c$ (Fig. 3.31), indicate a preliminary chemical reaction, the contribution of which to the overall cathode process increases with an increase in the con-

centration of molybdenum ions in solution. And the concentration dependence of $i_п/c$ confirms the assumption of the presence of a chemical stage.

Таблица 3.10

Кинетические параметры катодных реакций в системе Co^{2+}-Cit^{3-}-MoO_4^{2-}-H_2O (*c*, mole/dm^3: Co^{2+}– 0,01; Cit^{3-} – 0,01; Na_2SO_4 – 1)

$c(MoO_4^{2-})$, mole/dm^3	E_c, V	αz	X_s	X_c
0,002	−0,38	0,43	0,65	1,0
0,005	−0,36	0,47		
0,01	−0,35	0,53		

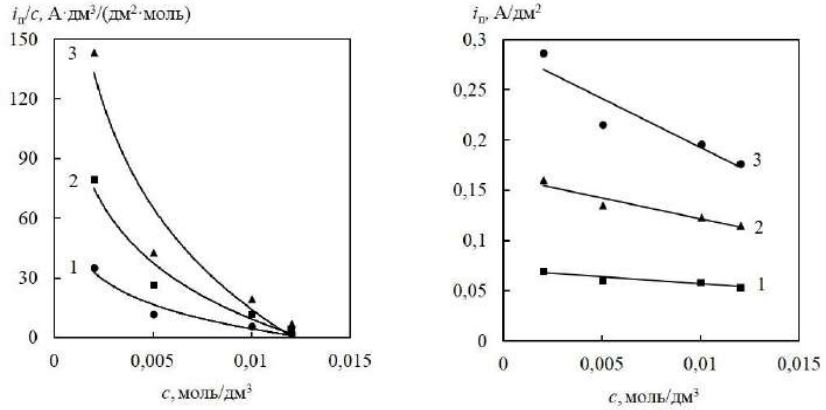

а *б*

Figure 3.31 - Dependence of the characteristic criterion $i_п$ / c (a) and the current density of the peak $i_п$ (b) of cobalt and molybdenum co-deposition on $c(MoO_4^{2-})$ against the background of 1M Na_2SO_4 from solution, mole/dm3: Co^{2+} – 0,01; Cit^{3-} – 0,01; *s*, V/s: 1 – $5\cdot10^{-3}$, 2 – $2\cdot10^{-2}$, 3 – $5\cdot10^{-2}$

Since the co-deposition of tungsten and malben show antagonism towards each other, their recovery from the individual complex compounds of composition $[WO_4Co(Cit)]^{3-}$ and $[MoO_4Co(Cit)]^{3-}$.

Thus, based on the analysis of data sets and the nature of the polarization dependence can be concluded about the braking phase charge transfer is complicated by adsorption of the product and prior chemical reaction. The above factors are the basis for the conclusion that the process of reduction of cobalt with tungsten or molybdenum occurs as a sequential course of reactions:

$$[MeO_4Co(Cit)]^{3-}{}_L \leftrightarrow [MeO_4Co(Cit)]^{3-}{}_S \quad (3.19)$$

$$[MeO_4Co(Cit)]^{3-}{}_S + 2e + 2H_2O \xrightarrow{k_s} [MeO_2Co(Cit)]^{-}{}_S + 4OH^- \quad (3.20)$$

$$[MeO_2Co(Cit)]^{-}{}_S + 2e \leftrightarrow Co|MeO_2 + Cit^{3-} \quad (3.21)$$

$$Co|H_2O + e \leftrightarrow Co|H_{ад} + OH^- \quad (3.22)$$

$$Co|MeO_2 + 4H_{ад} \leftrightarrow Co + Me + 2H_2O, \text{ де Me – Mo, W.} \quad (3.23)$$

Stationary potentials of the steel electrode in solutions Co^{2+}-Cit^{3-}-$P_2O_7^{4-}$-WO_4^{2-}-H_2O are shifted towards values of –(0.7-0.8) In comparison with the Co^{2+}-Cit^{3-}-WO_4^{2-}-H_2O system. The peaks on the polarization dependences degenerate into waves, the current density of which decreases by a factor of 2 (Fig. 3.32). The slope of the voltammograms becomes more gentle, which indicates a slowdown in the discharge stage and adsorption complications of the process.

The calculated values of αz and the Semerano X_s criterion (Table 3.11), as well as a significant decrease in αz with an increase in the concentration of WO_4^{2-}-ions indicate a deceleration of the charge transfer stage, that is, the irreversibility of the cathode process. However, the growth of az for the system under study in comparison with Co^{2+}-Cit^{3-}-MO_4^{2-}-H_2O indicates a joint reduction of cobalt and refractory metal at least to an intermediate oxide.

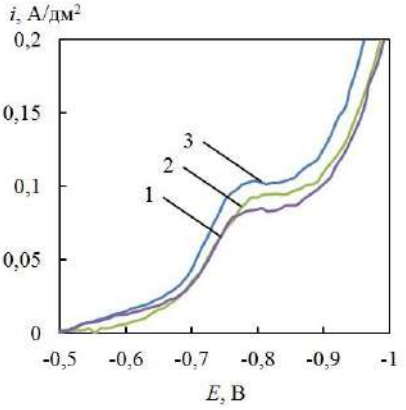

Figure 3.32 - Cathode voltammograms of a steel electrode against a background of 1M Na_2SO_4 in solutions of the composition, mole/dm3: Co^{2+} – 0,01; Cit^{3-} – 0,01; $P_2O_7^{4-}$ – 0,02; WO_4^{2-} – 0,002 (1), 0,005 (2), 0,01 (3); $s = 1 \cdot 10^{-2}$ V/s, $T = 293$ K

Table 3.11

Kinetic parameters of cathode reactions in the system Co^{2+}-Cit^{3-}-$P_2O_7^{4-}$- WO_4^{2-}-H_2O (*c*, mole/dm^3: Co^{2+}– 0,01; Cit^{3-} – 0,01, $P_2O_7^{4-}$ – 0,02; Na_2SO_4 – 1), $s = 1 \cdot 10^{-2}$ V/s

$c(WO_4^{2-})$, mole/dm^3	E_c, V	αz	X_s	X_c
0,002	−0,48	1,29	0,65	1,0
0,005	−0,46	1,21		
0,01	−0,45	1,04		

The course of the dependences of $i_п - \sqrt{s}$ and $i_п / \sqrt{s}$ - s (Fig. 3.33) with varying concentrations of WO_4^{2-}-ions testifies to the inhibition of adsorption processes.

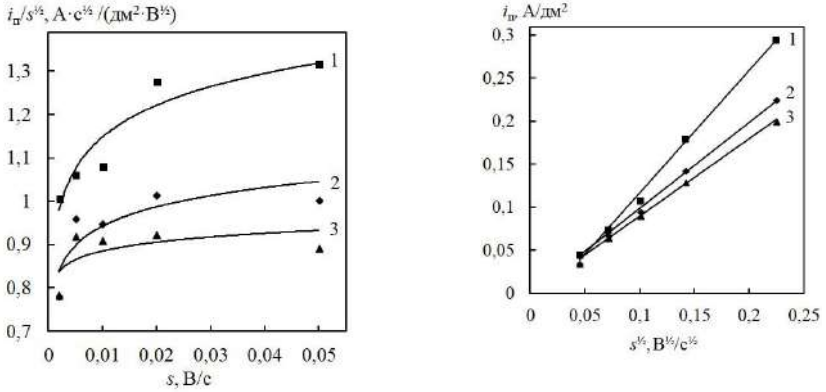

а *б*

Figure 3.33 - Dependence of the characteristic criterion $i_п / \sqrt{s}$ (a) and the current density of the peak $i_п$ (b) of cobalt and tungsten co-deposition on the potential sweep rate on the background. 1M Na_2SO_4 in solutions of the composition, mole/dm3: Co^{2+} – 0,01; Cit^{3-} – 0,01; $P_2O_7^{4-}$ – 0,02; WO_4^{2-} – 0,002 (1), 0,005 (2), 0,01 (3)

The value of the concentration criterion X_c (Table 3.11), as well as the nature of concentration dependences in the coordinates $i_п / c$ and $i_п - c$ (Fig. 3.34), also indicate a complication of the adsorption of the reagent. The peak current density in the range of low potential sweep rates is linear, which confirms the assumption of adsorption inhibition.

Thus, the analysis of the totality of the obtained characteristic criteria (Table 3.11), as well as the dependence of peak currents,

indicate the irreversibility of the process complicated by the adsorption of the reagent.

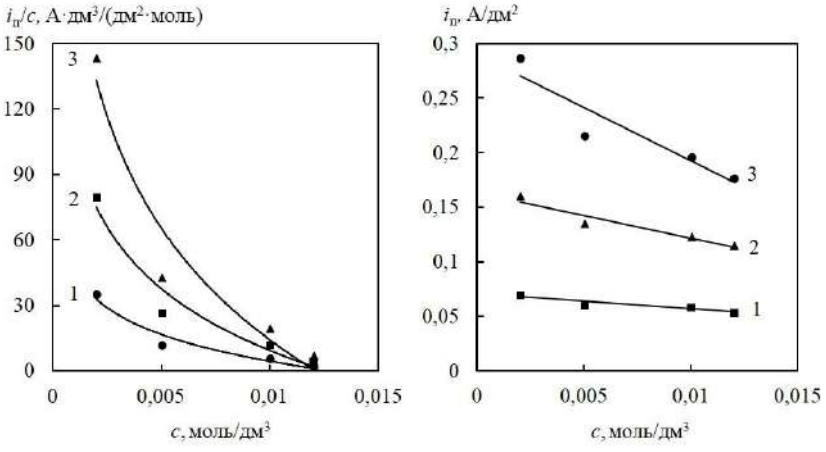

а *б*

Figure 3.34 - Dependence of the characteristic criterion $i_п$ / c (a) and the current density of the peak $i_п$ (b) of cobalt and tungsten co-deposition reduction from c(WO_4^{2-}) against the background of 1M Na_2SO_4 in solutions of the composition, mole/dm3: Co^{2+} – 0,01; Cit^{3-} – 0,01; $P_2O_7^{4-}$ – 0,02; *s*, V/s: 1 – $5\cdot10^{-3}$, 2 – $2\cdot10^{-2}$, 3 – $5\cdot10^{-2}$

The stationary potentials of the steel electrode in solutions of Co^{2+}-Cit^{3-}-$P_2O_7^{4-}$-MoO_4^{2-}-H_2O naturally shift towards more negative values compared to the Co^{2+}-Cit^{3-}-MoO_4^{2-}-H_2O system, the peaks on the polarization dependences degenerate into waves whose current density decreases by 3.5 times (Fig. 3.35). The slope of the voltammograms becomes more gentle, which indicates a slowdown in the discharge stage and adsorption complications of the process.

The dependence of $i_п$ – s (fig.3.36 b) has a linear character and the peak current density increases with increasing s, the characteristic criterion $i_п/\sqrt{s}$ – *s* (Fig. 3.36 a), as well as the kinetic parameters (αz, X_s) (Table 3.12) indicate that the discharge stage is complicated by the adsorption process.

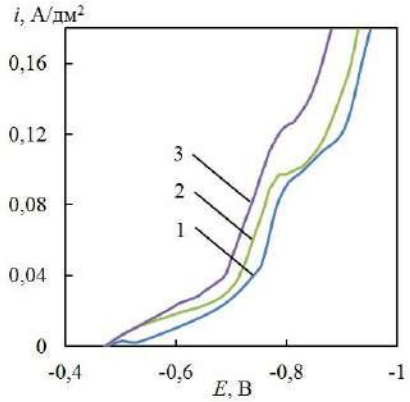

Figure 3.35 - Cathode voltammograms of a steel electrode against a background of 1M Na_2SO_4 in solutions of the composition, mole/dm3: Co^{2+} – 0,01; Cit^{3-} – 0,01; $P_2O_7^{4-}$ – 0,02; MoO_4^{2-} – 0,002 (1), 0,005 (2), 0,01 (3); $s = 1 \cdot 10^{-2}$ V/s, $T = 293$ K

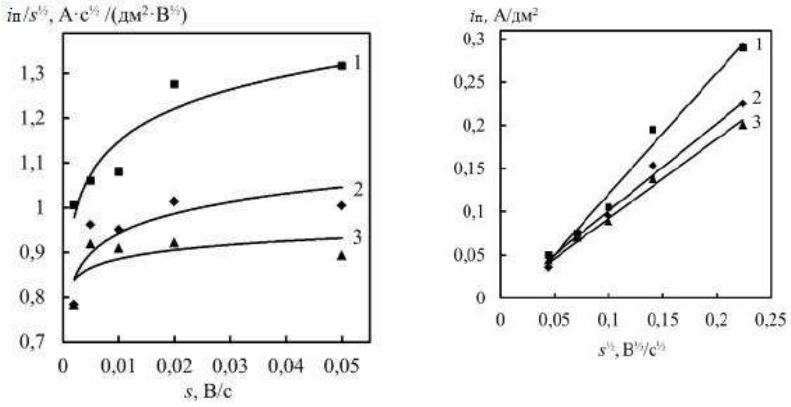

а *б*

Figure 3.36 - Dependence of the characteristic criterion $i_п / \sqrt{s}$ (a) and the current density of the peak $i_п$ (b) of cobalt and molybdenum co-deposition on the potential sweep rate against the background of 1M Na_2SO_4 in solutions of the composition, mole/dm3: Co^{2+} – 0,01; Cit^{3-} – 0,01; $P_2O_7^{4-}$ – 0,02; MoO_4^{2-} – 0,002 (1), 0,005 (2), 0,01 (3)

At the same time, the growth of az for the system under study in comparison with the tungstate-containing system indicates the joint reduction of cobalt and refractory metal, and the reduction of

molybdenum is more complete compared to tungsten.the reduction in comparison with tungstate-containing indicates the joint reduction of cobalt and refractory metal, and the reduction of molybdenum is more complete compared to tungsten.

Table 3.12

Kinetic parameters of cathode reactions in the system Co^{2+}-Cit^{3-}-H_2O (*c*, mole/dm³: Co^{2+}– 0,01; Cit^{3-} – 0,01, $P_2O_7^{4-}$– 0,02; Na_2SO_4 – 1)

$c(MoO_4^{2-})$, mole/dm³	E_c, V	αz	X_s	X_c
0,002	−0,48	1,37	0,6	1,0
0,005	−0,46	1,39	0,55	
0,01	−0,45	1,57	0,48	

The concentration dependences (Fig. 3.37) and the value of the concentration criterion of X_c confirm the inhibition of the adsorption of the reagent.

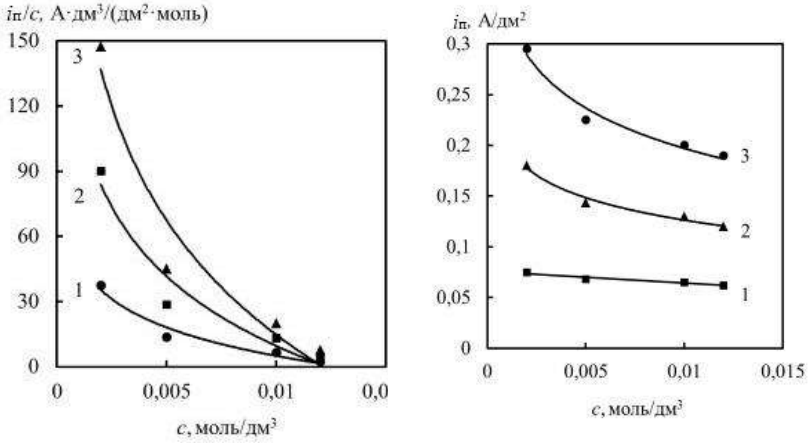

а *б*

Figure 3.37 - Dependence of the characteristic criterion $i_п$ / c (a) and the current density of the peak $i_п$ (b) of cobalt and molybdenum co-deposition on c(MoO_4^{2-}) against the background of 1M Na_2SO_4 in solutions of the composition, mole/dm³

Thus, based on the analysis of the totality of data and the nature of the polarization dependencies, it can be concluded that the cathode process is inhibited at the discharge stage, complicated by the adsorption of the reagent.

The above factors are the basis for the conclusion that the process of updating cobalt with tungsten or moliden occurs according to a sequential scheme, including ionic equilibria in solutions, the formation of complexes and polyanions with the participation of cobalt and oxometalates. MoO_4^{2-} (WO_4^{2-}) (Fig. 3.38).

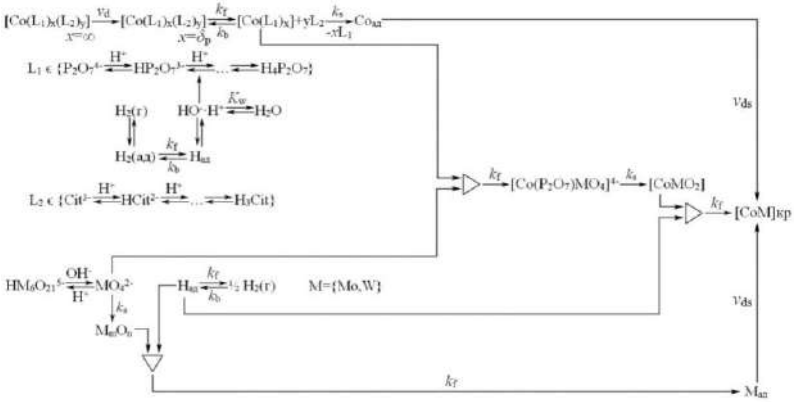

Figure 3.38 - Diagram of the process of co-deposition of cobalt with tungsten or molybdenum from a citrate-pyrophosphate electrolyte

The scheme of the process of co-deposition of cobalt with tungsten or molybdenum from a citrate-pyrophosphate electrolyte reflects the adsorption of intermediates on the cathode surface, the preliminary chemical stage of ligand release, the delayed stage of cobalt discharge with tungsten or molybdenum, including the formation of intermediate oxides of refractory metals that can be reduced by hydrogen atoms. The scheme takes into account ionic equilibria in solutions, namely: hydrolysis reactions, the formation of complexes and polyanions involving cobalt, zirconium and oxometalates MoO_4^{2-} (WO_4^{2-}).

2.2.3 Electrochemical behavior of systems Co^{2+}-Cit^{3-}-$P_2O_7^{4-}$-WO_4^{2-}- MoO_4^{2-}-H_2O, Co^{2+}-Cit^{3-}- $P_2O_7^{4-}$-WO_4^{2-}-ZrO^{2+}- H_2O та Co^{2+}-Cit^{3-}-$P_2O_7^{4-}$-MoO_4^{2-}- ZrO^{2+}- H_2O

The polarization dependences obtained on a steel electrode in the Co^{2+}-Cit^{3-}-$P_2O_7^{4-}$-WO_4^{2-}- MoO_4^{2-}-H_2O system against the background of a 1M sodium sulfate solution with fixed concentrations of ligands, cobalt (II) and tungstate and varying the content of molybdates at a potential sweep rate of $1 \cdot 10^{-1}$ V/s (Fig. 3.39) are characterized by the presence of limit current waves in potential intervals from –(0.75-0.85) V.

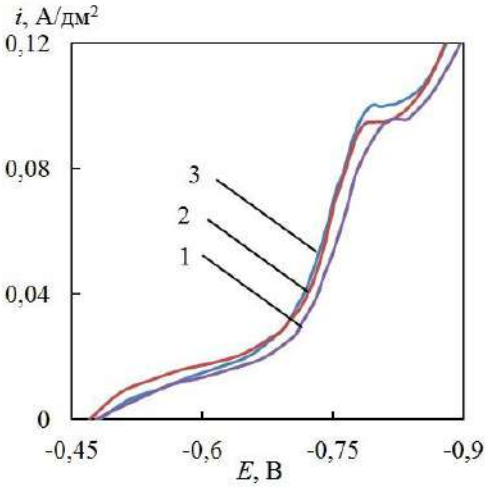

Figure 3.39 - Cathode voltammograms of a steel electrode against a background of 1M Na_2SO_4 in solutions of the composition, mole/dm3: Co^{2+} – 0,01; Cit^{3-} – 0,02; $P_2O_7^{4-}$ – 0,02; WO_4^{2-} – 0,002; MoO_4^{2-} –0,001 (1), 0,0025 (2), 0,005 (3); $s = 1 \cdot 10^{-2}$ V/s, T = 293 K

Linear dependences of $i_п$ on the potential sweep rate proceed from the origin (Fig. 3.40), the concentration criterion X_c = 1.0, as well as the Semerano criterion X_s ((Table 3.13) characterize the process as irreversible.

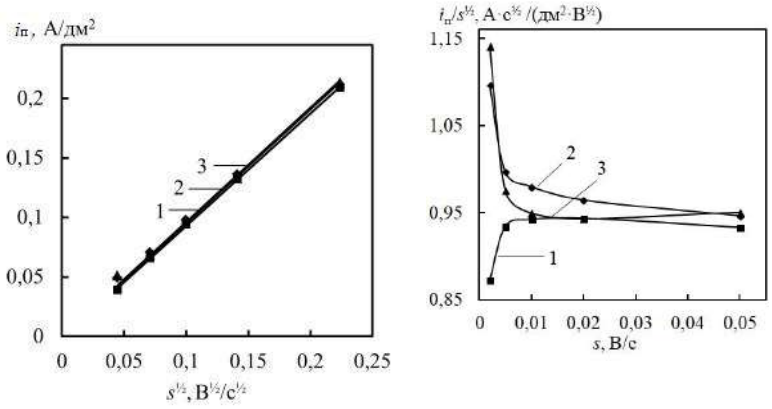

а *б*

Figure 3.40 - Dependence of the characteristic criterion $i_п$ / √s (a) and the current density of the peak $i_п$ (b) of the ratio Co, Mo and W on the scanning speed on a potential background of 1M Na_2SO_4 in solutions of the composition, mole/dm3: Co^{2+} – 0,01; Cit^{3-} – 0,02; $P_2O_7^{4-}$ – 0,02; WO_4^{2-} – 0,002; MoO_4^{2-} –0,001(1), 0,0025(2), 0,005(3)

Graphoanalytical processing of polarization measurement data in coordinates $i_п/\sqrt{s} - s$ (Fig. 3.40 a) indicates a change in the mechanism of co-reduction of cobalt with molybdenum and tungsten depending on the concentration of MoO_4^{2-}. If the concentration of molybdates is less than tungstate (Fig. 3.40, Dependence 1), the discharge stage is accompanied by a chemical reaction, and with an increase in the ratio of $c(MoO_4^{2-})/c(WO_4^{2-})$ in the electrolyte in favor of the molybdates, the chemical reaction already precedes the discharge stage. Taking into account the oxidizing properties of oxomethylates and the stability of the corresponding complexes, it can be assumed that this reaction is associated with the displacement of tungstates by molybdates from complex ions. In addition, it should be noted that the delayed stage of discharge is hindered by the adsorption of reactive particles, since the wave current density depends on the concentrations of alloy-forming components [154].

Table 3.13

Kinetic parameters of cathode reactions in the system Co^{2+}- Cit^{3-}- WO_4^{2-}- MoO_4^{2-}- $P_2O_7^{4-}$- H_2O (*c*, моль/дм³: Co^{2+}– 0,01; Cit^{3-} – 0,01; $P_2O_7^{4-}$ – 0,02; WO_4^{2-} – 0,002; Na_2SO_4 – 1)

$c(MoO_4^{2-})$, mole/dm³	E_c, V	αz	X_s	X_c
0,001	−0,42	1,46	0,6	1,0
0,0025	−0,53	1,43	0,55	
0,05	−0,57	1,54	0,54	

The peak current density (Fig. 3.41 b) does not depend on the concentration of MoO_4^{2-} ions-- with varying potential sweep rate, which indicates the reduction of molybdates from complex particles, and not free MoO_4^{2-} ions- and delayed adsorption of reaction particles

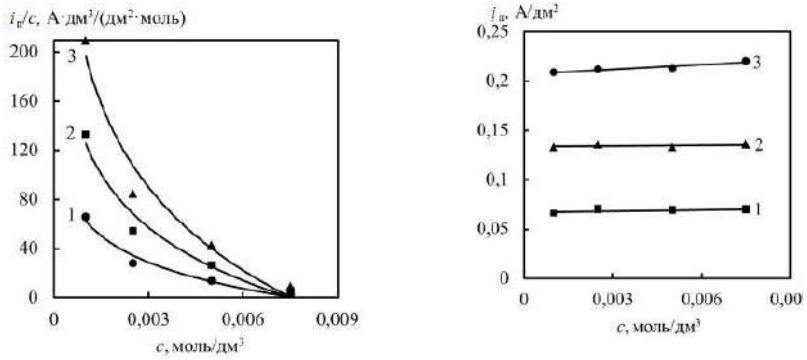

а *б*

Figure 3.41 - Dependence of the characteristic criterion $i_п$ / c (a) and the current density of the peak $i_п$ (b) of Co deposition, Mo i W vid c(MoO42–) on the background of 1M Na_2SO_4 in solutions of the composition, mole/dm3: Co^{2+} – 0,01; Cit^{3-} – 0,01; $P_2O_7^{4-}$ – 0,02;WO_4^{2-} – 0,002; *s*, V/s: 1 – $5\cdot10^{-3}$, 2 – $2\cdot10^{-2}$, 3 – $5\cdot10^{-2}$

The polarization dependences obtained on a steel electrode in the Co^{2+}-Cit^{3-}-$P_2O_7^{4-}$-WO_4^{2-}-ZrO^{2+}-H_2O system against the background of a 1M sodium sulfate solution with fixed concentrations of ligands, cobalt (II) and tungstate and varying the content of ZrO^{2+} ions at a potential sweep rate of $1\cdot10^{-2}$ V/s (Fig. 3.42) are characterized by

the presence of limit current waves in potential intervals from –(0.6-0.9) V.

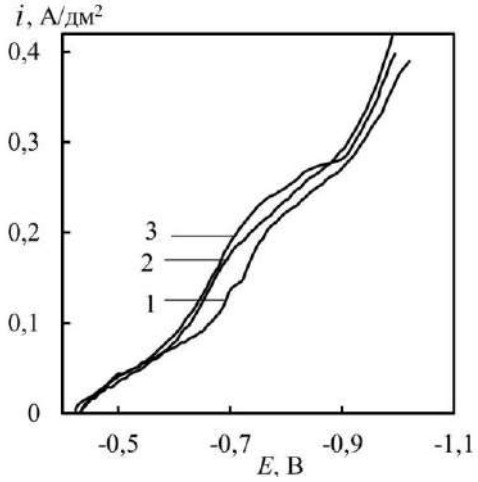

Figure. 3.42 - Cathode voltammograms of a steel electrode on the background of 1M Na_2SO_4 in solutions of the composition, mole/dm^3:Co^{2+} – 0,01; Cit^{3-} – 0,02; $P_2O_7^{4-}$ – 0,02; WO_4^{2-} – 0,002; ZrO^{2+} –0,001 (1), 0,005 (2), 0,01 (3); $s = 1 \cdot 10^{-2}$ V/s, T = 293 K

The dependence of the $i_п$ on the potential sweep rate is linear, but does not follow from the origin (Fig. 3.43 a), which indicates the irreversibility of the process. Analysis of the dependences of $i_п/\sqrt{s}$ on the potential sweep rate (Fig. 3.43 b), as well as the product of the transfer coefficient by the number of electrons az and the Semerano X_s criterion (Table 3.14), allow us to conclude that the process of metal co-recovery is irreversible. However, it follows from Fig. 3.43 b that, depending on the concentration of ZrO^{2+} ions, there is a change in the inhibition of individual stages of the general cathode process. With the ratio $c(WO_4^{2-})/c(ZrO^{2+})$ as 2:1, $i_п/\sqrt{s}$ grows insignificantly in the entire s interval (Fig.3.43, b dependence 1), and, consequently, the deceleration of the discharge stage is accompanied by delayed adsorption.

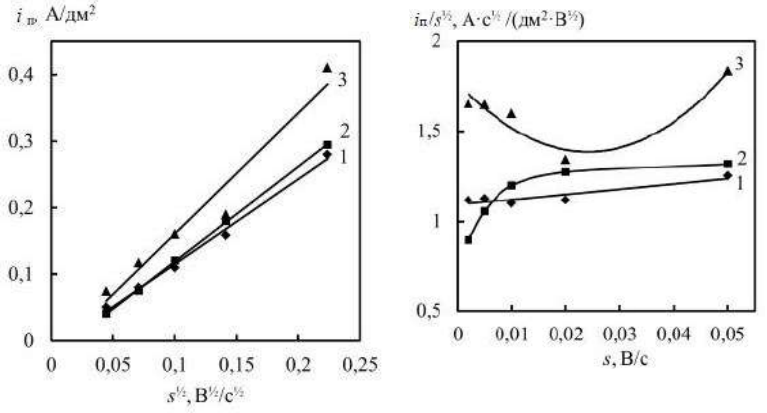

а *б*

Figure 3.43 - The dependence of the characteristic criterion $j_п$ / √s (a) and the current density of the peak $i_п$ (b) of the co-deposition of cobalt, tungsten and zirconium on the sweep rate of the potential on the background. 1M Na_2SO_4 in solutions of the composition, mole/dm3: Co^{2+} – 0,01; Cit^{3-} – 0,02; $P_2O_7^{4-}$ – 0,02; WO_4^{2-} – 0,002; ZrO^{2+} –0,001 (1), 0,005 (2), 0,01 (3)

Table 3.14

Kinetic parameters of cathode reactions in the system Co^{2+}-Cit^{3-}-$P_2O_7^{4-}$-WO_4^{2-}-Zr^{4+}-H_2O (*c*, mole/dm³: Co^{2+}– 0,01; Cit^{3-} – 0,01, $P_2O_7^{4-}$ – 0,02, WO_4^{2-} – 0,002; Na_2SO_4 – 1)

$c(ZrO^{2+})$, mole/dm³	E_c, V	αz	X_s	X_c
0,001	−0,49	1,67	0,50	0,15
0,002	−0,46	0,87	0,49	
0,005	−0,43	0,86	0,50	

An increase in the concentration of ZrO^{2+} ions relative to tungstates to the level of 5:2 (Fig. 3.43, b dependence 2) leads to an increase in adsorption complications only in the range s 2 – 20 mV/s. With a ratio of $c(WO_4^{2-})/c(ZrO^{2+})$ as 1:5 (Figure 3.43, and dependence 3), the mechanism changes depending on the potential sweep rate: in the range s = 2-20 mV/s, the discharge stage is accompanied by a chemical reaction, and the acceleration of potential scanning enhances the contribution of adsorption..

The concentration dependences (Fig. 3.44) also indicate a change in the complications of the chemical reaction to the adsorption of the reagent depending on the rate of potential unfolding. In addition, it should be noted that complex ions containing zirconium (IV), and not free ZrO^{2+} cations, are involved in the cathode process.

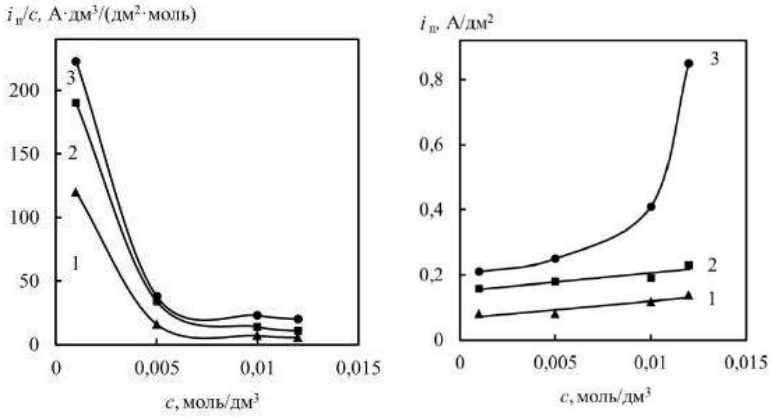

а *б*

Figure 3.44 - Dependence of the characteristic criterion $i_п$ / c (a) and the current density of the peak $i_п$ (b) of the co-deposition of cobalt, tungsten and zirconium on $c(ZrO^{2+})$ against the background of 1M Na_2SO_4 in solutions of the composition, mole/dm³: Co^{2+} – 0,01; Cit^{3-} – 0,01; WO_4^{2-} – 0,002; $P_2O_7^{4-}$ – 0,02; *s*, V/c: 1 – $5\cdot10^{-3}$, 2 – $2\cdot10^{-2}$, 3 – $5\cdot10^{-2}$

The polarization dependences obtained on a steel electrode in the Co^{2+}-Cit^{3-}-$P_2O_7^{4-}$-MoO_4^{2-}-ZrO^{2+}-H_2O system against the background of a 1M sodium sulfate solution with fixed concentrations of ligands, cobalt (II) and molybdenum and varying the content of ZrO^{2+} ions at a potential sweep rate of $1\cdot10^{-2}$ V/s (Fig. 3.45) are characterized by the presence of limit current waves in potential intervals from –(0.6-0.9) V.

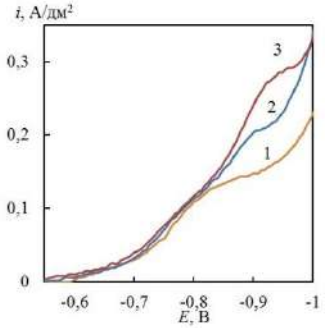

Figure 3.45 - Cathode voltammograms of a steel electrode against a background of 1M Na_2SO_4 in solutions of the composition, mol/dm³: Co^{2+} – 0,01; Cit^{3-} – 0,02; $P_2O_7^{4-}$ – 0,02; MoO_4^{2-} – 0,002; ZrO^{2+} –0,001 (1), 0,005 (2), 0,01 (3); $s = 5 \cdot 10^{-3}$ V/s, $T = 293$ K

The dependence of $i_п/\sqrt{s}$ on the potential sweep rate (Fig. 3.46 a) on the concentration of ZrO^{2+} ions indicates the limiting stage of charge transfer and the chemical reaction of dissociation of complexes. The dependence of ip on the potential sweep rate is nonlinear and does not go out of the origin (Fig. 3.46 b). The product of the transfer coefficient by the number of electrons az and the Semerano criterion X_s (Table 3.15), allow us to conclude that the process of metal co-recovery is irreversible.

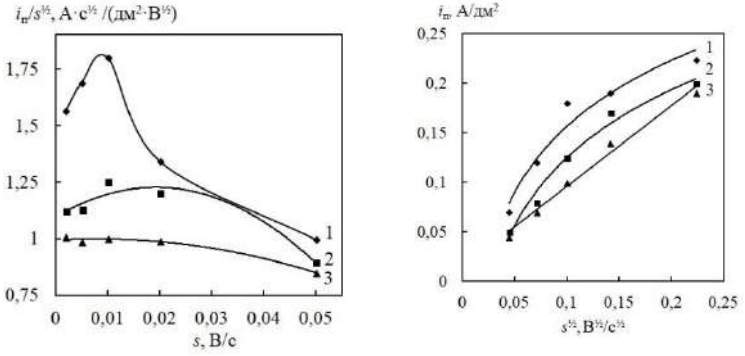

а *б*

Figure 3.46 - Dependence of the characteristic criterion $i_п$ / √s (a) and the current density of the peak $i_п$ (b) of co-deposition of cobalt, molybdenum and zirconium on the rate of potential sweep on the background. 1M Na_2SO_4 in solutions of the composition, mole/dm³: Co^{2+} – 0,01; Cit^{3-} – 0,02; $P_2O_7^{4-}$ – 0,02; MoO_4^{2-} – 0,002; ZrO^{2+} –0,001 (1), 0,005 (2), 0,01 (3)

Table 3.15

Kinetic parameters of cathode reactions in the system Co^{2+}-Cit^{3-}-$P_2O_7^{4-}$-MoO_4^{2-} - ZrO^{2+}- H_2O (*c*, mole/dm³: Co^{2+}– 0,01; Cit^{3-} – 0,01; $P_2O_7^{4-}$ – 0,02; MoO_4^{2-} – 0,002; Na_2SO_4 – 1)

$c(ZrO^{2+})$, mole/dm³	E_c, V	αz	X_s	X_c
0,001	−0,48	0,85	0,49	0,5
0,002	−0,46	1,40	0,41	
0,005	−0,45	1,81	0,46	

Concentration dependences (Fig. 3.47) indicate a complication of the chemical reaction depending on the rate of potential unfolding.

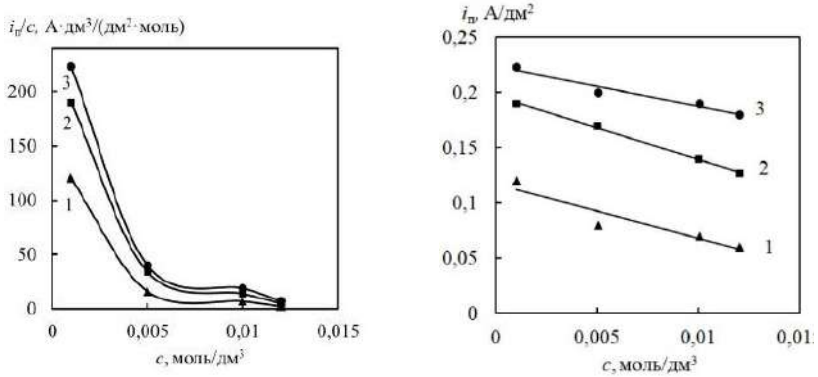

а *б*

Figure 3.47 - Dependence of the characteristic criterion $i_п$ / c (a) and the current density of the peak $i_п$ (b) of the co-deposition of cobalt, molybdenum and zirconium on $c(ZrO^{2+})$ from a solution, against the background of 1M Na_2SO_4 in solutions of the composition, mole/dm³: Co^{2+} – 0,01; Cit^{3-} – 0,01; MoO_4^{2-} – 0,002; $P_2O_7^{4-}$ – 0,02; *s*, V/s: 1 – $5\cdot10^{-3}$, 2 – $2\cdot10^{-2}$, 3 – $5\cdot10^{-2}$

The totality of the results obtained allows us to present the mechanism of co-deposition of metals into alloys and composites Co-Mo-WO_x, Co-Mo-ZrO_2, Co-W-ZrO_2 by a generalized scheme (Fig. 3.48), which reflects the adsorption of intermediates on the cathode surface, the preliminary chemical stage of ligand release, the delayed stage of cobalt discharge with tungsten, molybdenum and zirconium, including the formation of intermediate oxides of refractory metals capable of being reduced by ad atoms of hydrogen. The scheme takes into account ionic equilibria in solutions, namely:

hydrolysis reactions, the formation of complexes and polyanions involving cobalt, zirconium and oxometalates MoO_4^{2-} (WO_4^{2-}).

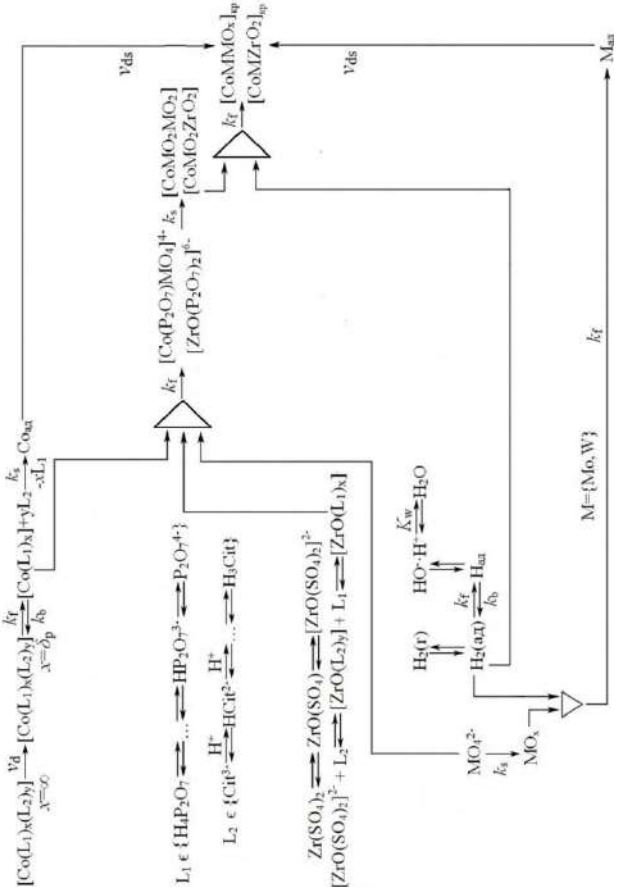

Figure 3.48 - Diagram of the deposition process of electrolytic composite coatings based on cobalt with refractory metals of citrate-pyrophosphate electrolyte: : v_{ds}, v_d - rates of surface and volumetric diffusion of components from solution (x=∞) to the surface of the electrode (x=0) or reaction layer (x= δ_p); k_s, k_f, k_b - rate constants of electrochemical, forward and reverse chemical reactions

The proposed scheme allows us to identify ways to control the deposition of cobalt-based alloys and composites with refractory metals, namely, varying the ratio of concentrations of electrolyte components and electrolysis modes that contribute to a more complete flow of both chemical and electrochemical reactions..

The established parameters of complex compounds of cobalt, molybdenum, tungsten and zirconium, kinetic patterns and the stages of the process of joint recovery of the extracted metals, as well as the proposed schemes, form the basis for the development of electrolytes and modes of electrochemical deposition of cobalt-based alloys and composites with refractory metals. This scheme opens up possibilities for controlling the electrodeposition process in the systems under consideration by varying the methods (direct or pulsed current) and polarization parameters for the targeted synthesis of coatings with alloys or composites of a given composition.

3.3 Features of the use of citrate-pyrophosphate electrolytes for the production of CEC

One of the prerequisites for obtaining high-quality galvanic coatings is the electrical conductivity of electrolyte solutions the high level of which contributes to the uniform distribution of the electric field in the electrolyte, reduces electricity consumption and allows you to obtain high-quality coatings.

Based on the analysis of the experimentally determined temperature dependence of electrical conductivity (Table 3.16), it can be argued that complex citrate-pyrophosphate electrolytes for deposition of coatings based on cobalt alloys have a sufficiently high scattering capacity.

Table 3.16

Electrical conductivity of citrate-pyrophosate electrolytes of CEP deposition

Coatings	Electrical conductivity of electrolytes ($Ом^{-1}·м^{-1}$) at temperatures (K)			
	298	303	313	323
Co-Mo-WO_x	$7,4·10^{-2}$	$8,2·10^{-2}$	$9,6·10^{-2}$	$1,1·10^{-1}$
Co-Mo-ZrO_2,	$5,8·10^{-2}$	$6,9·10^{-2}$	$7,6·10^{-2}$	$8,7·10^{-2}$
Co-W-ZrO_2	$5,6·10^{-2}$	$5,9·10^{-2}$	$6,7·10^{-2}$	$7,4·10^{-2}$

The activation energy of the electrical conductivity of complex electrolytes, calculated for graphical analysis of the temperature dependence of electrical conductivity, is in the range of 22-29 kJ / mole, which is a sign of the mass transfer processes in the diffuse mode. An increase in temperature reduces the inhibition of diffusion processes and contributes to an increase in operating current densities, information about the temperature dependence of the electrical conductivity of electrolytes is in demand when determining the operating parameters of technological processes.

Since the experimentally determined values of the electrical conductivity of solutions for the deposition of the coatings under study are in the range of $\chi = 0{,}055 - 0{,}07$ ohms$^{-1}\cdot$ m^{-1}, the temperature range of 25-30 ° C can be considered optimal.

An important technological parameter of electrochemical deposition of composite coatings is the distribution of local velocities over the substrate surface, which in turn is determined by the current distribution over the treated surface [155]. In relation to this process, such an indicator is the scattering capacity, which is understood as the ability of the electrolyte to change the primary current distribution due only to geometric parameters.

A Hull cell with a collapsible cathode located at an angle to the anode was used to measure the electrolyte scattering capacity (RH). When using a Hull cell, the RZ is estimated by the distribution curves of the metal mass gain from the interelectrode distance, plotted in the coordinates δ_i/δ_{cp}–l_i, where δ_i is the mass gain of the i-th plate of the collapsible cathode,

δ_{cp} is the average mass gain calculated as $\Sigma\ \delta_i/n$, (n is the number of plates, which usually ranges from 6 to 10); l_i is the distance from the collapsible cathode plate to the anode. According to Gost 9.309–86, RH measurements are recommended to be made in a cell using a collapsible cathode consisting of 10 plates. The scattering capacity is calculated by the formula:

$$RH = \left(1 - \frac{(B_1 - 1) + (B_2 - 1) + \cdots + (B_n - 1)}{6{,}37}\right) 100,$$

where 6.37 is the coefficient due to the primary current distribution.

Measurements in the Hull cell allow more accurate modeling of the surface of a complex profile.

The electrical conductivity of the electrolyte was measured in a conductometric cell using the E7-13 device with a variation in the electrolyte temperature t = 298 – 323 K.

Before performing the experiment, the cell for measuring electrical conductivity was thoroughly washed, steamed and rinsed with a research solution. To determine the stable $C_к$ Cell, The Resistance R_{KC} of a standard solution of 0.1 mole/dm^3 of potassium chloride, whose specific electrical conductivity χ_{KCl}=0,01288 Ohms^{-1}·cm^{-1} at a temperature t = 298 K, was measured, and the $C_к$ was calculated using the equation [163]:

$$C_к = \chi_{KCl} \cdot R_{KCl.}$$

The value of the electrical conductivity Hel of the studied electrolyte solutions was calculated from the value of the rel resistance [163]:

$$\chi_{ел} = C_к / R_{ел.}$$

The results of the RH measurements indicate that with an increase in the current density of the electrolyte for deposition of composite coatings, the Co-Mo Shop decreases (Fig. 3.49). However, in the range of current densities of 0.5–2.0 A/ dm^2, the value of this parameter is more than 85%.

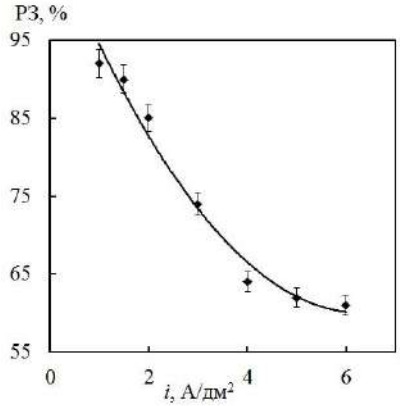

Figure 3.49 - Effect of current density on the scattering capacity of electrolyte No. 5 deposition of composite coating Co-Mo-WO$_x$

The ability of the citrate-pyrophosphate electrolyte of the application of the Co-Mo-ZrO_2 CEP to evenly distribute metal over the electrode surface was determined at different current densities. The resulting CEP have a uniform matte dark gray color, only on the first and second sections of the cathode, which were closer to the anode, it is noticeable at the edges of the darkening of the coatings, which is associated with an excess of the boundary current density on these sections and excessive hydrogen release.

The dependence of the distribution of metals across the cathode sections at current densities of 5-8 A/dm^2 is uneven (Fig. 3.50, dependences 1-3). Thus, in the first and second sections of the cathode, the sediment mass gain is almost twice as much as in the 3-6 sections, which is explained by the influence of electrochemical parameters on the scattering capacity.

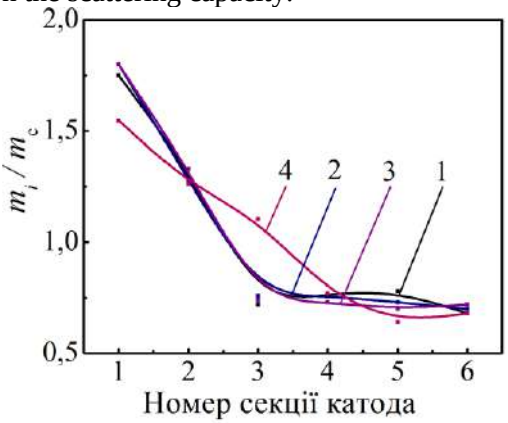

Figure 3.50 - Dependence of the cathode mass gain on the section number, electrolyte No. 3 (1-3) and electrolyte No. 3 + 50 g/dm^3 Na_2SO_4 (4) at current densities, A/dm^2: 1 – 5; 2 – 6, 5; 3, 4 – 6

The polarizability during deposition of the composite coating Co-Mo-ZrO_2 is low, since the formation occurs at high current densities (3 - 10 A / dm^2). This explains the significant difference in the mass gain on the cathode sections located in the Hula cell at different distances from the anode (Fig.4.37), which indicates an insufficiently high scattering capacity of the electrolyte. Therefore, an electrically

conductive additive is introduced to increase the scattering capacity of the working electrolyte. - 50 g/dm^3 Na_2SO_4. This somewhat improves the scattering ability, that is, it contributes to a more uniform distribution of metal over the cathode surface (Fig. 3.50, dependence 4). The results of the measurements of the scattering capacity indicate that with an increase in the current density, the RH of the electrolyte for deposition of the composite coating Co-Mo-ZrO_2 increases slightly (Fig.3.51).

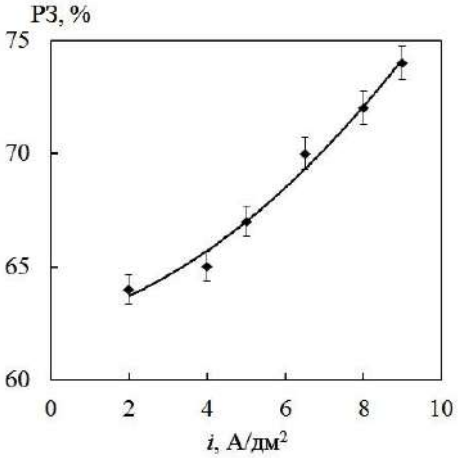

Figure 3.51 - Effect of current density on the scattering capacity of citrate-pyrophosphate electrolyte No. 3 for deposition of composite coatings Co-Mo-ZrO_2

Результаты проведенных измерений рассеивающей способности электролита №5 для осаждения покрытия Co-W-ZrO_2 свидетельствуют о том, что с повышением плотности тока РЗ электролита снижается (рис.4.39). Такое поведение может быть связано с аморфизацией структуры КЭП Co-Mo-WO_x і Co-W-ZrO_2.

The results of the measurements of the scattering capacity of electrolyte No. 5 for deposition of the Co-W-ZrO_2 coating indicate that with an increase in the current density, the HP of the electrolyte decreases (Fig 3.52). This behavior may be due to the amorphization of the structure of the CEP Co-Mo-WO_x and Co-W-ZrO_2.

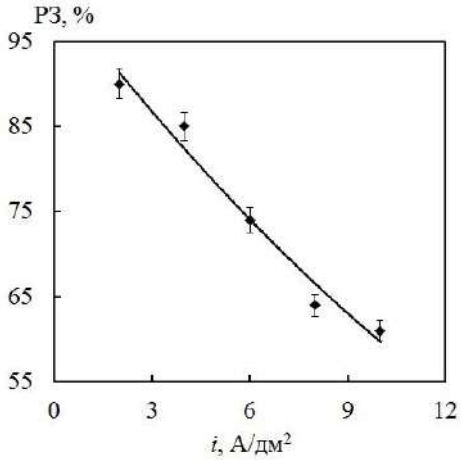

Figure 3.52 - Effect of current density on the scattering capacity of citrate-pyrophosphate electrolyte No. 5 for deposition of composite coating Co-W-ZrO_2 But when Co-W-ZrO_2 CEP is deposited at a current density of up to 4 A/dm^2, the value of this parameter is more than 85%.

3.4 Selection of anode material for electrodeposition of multicomponent cobalt-based CEP

Electrodeposition of composite coatings based on cobalt alloys from citrate-pyrophosphate electrolytes is sensitive to changes in their composition, therefore, requirements such as corrosion resistance, absence of oxidation reactions of electrolyte components leading to changes in the composition of the electrolyte are imposed on anode materials. For electroplating processes, anodes made of the same metal as coatings are usually used. However, when electrolytic deposition of multicomponent coatings is carried out, the selection of a soluble anode made of several metals is complicated by different dissolution rates of the components, and, accordingly, the enrichment of the electrolyte with only one type of ions.

To determine the characteristics of electrode processes, polarization dependences for different anode materials are obtained. Since the reduction of metals is not the only process, such dependencies are cumulative and are characterized by the simultaneous course of all anode reactions.

The vast majority of scientists conduct experimental studies using an inert electrode [156], and platinum or stainless steel is most often used. Taking into account the need to identify the influence of the concentration of alloy-forming components on the composition of coatings, this approach is quite justified, since inert electrodes do not affect the content of electrode-active particles in the electrolyte [157]. The peculiarities of electrodeposition of cobalt-based composite coatings consist, in particular, in the difference not only of cathodic reactions, but also of the anodic behavior of outlined metals, therefore, the use of soluble anodes in this case is the subject of an extensive separate study. However, in this work, the possibility of using inert stainless steel anodes is proved and the anode current density intervals are justified, at which the course of the anode reaction has an insignificant effect on the structure and number of electro-active particles.

When deposition of composite coatings Co-Mo-WO_x, Co-Mo-ZrO_2,
Co-W-ZrO_2 anode potential on steel X18H10T shifts in a positive direction with an increase in the cathode current density and does not exceed 1.9 V in the range of the studied current densities $i_к$ (2.0 - 12.0 A / dm^2) (Table 3.17).

Studies of the anodic behavior of various electrode materials in solutions of electrolytes deposition of composite coatings allow us to draw the following conclusion. The absence of any active processes on the anode made of steel X18N10T in the range of potentials up to +0.8 V for Co-Mo-WO_x and +1.2 V Co-Mo-ZrO_2, Co-W-ZrO_2 confirms the possibility of using these anodes as inert.

Table 3.17

Anode potential under current when coating alloys (anode - steel X18H10T; $S_A : S_K = 10 : 1$)

Coatings	Anode potential under current E_a, V					
	polarization current density $i_к$, A/dm^2					
	2,0	4,0	6,0	8,0	10,0	12,0
Co-Mo-WO_x	1,42	1,50	1,58	1,66	1,74	1,82
Co-W-ZrO_2	1,48	1,61	1,70	1,78	1,85	1,79
Co-Mo-ZrO_2	1,43	1,54	1,62	1,69	1,75	1,90

As is known [158], the use of insoluble anodes makes it possible to improve the quality of coatings and the efficiency of the cathode process. Cobalt anodes dissolve to form Co^{2+} at low polarization at a high rate, as evidenced by the rapid increase in current density on voltammograms (Fig. 3.53-3.55).

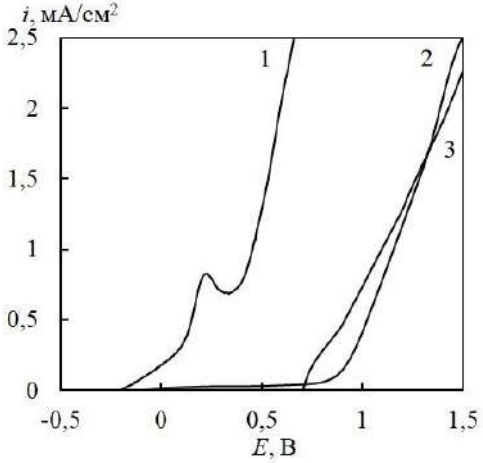

Figure 3.53 Anode voltammograms on cobalt (1), graphite (2) and steel X18N10T (3) electrodes in an electrolyte solution for the formation of composite coatings Co-Mo-WO_x; $s = 2 \cdot 10^{-3}$ V/s

The formation of soluble cobalt anodes can only provide compensation for cobalt costs during electrolysis and prolongation of the electrolyte resource [159, 160], but, on the other hand, leads to a violation of the ratio of concentrations of complex holes in solution, since it is not possible to achieve the appropriate rate of dissolution of cobalt with refractory metals (cycronium) when using folded anodes. Also, after the use of soluble anodes, staining and a decrease in the electrolyte resource are observed. This is due to the formation of hydroxide ions in the side reaction of hydrogen evolution and the lack of the possibility of compensating for their effect on the pH from the anode reaction, since oxygen release, accompanied by acidification of the solution, does not occur on the soluble anode.

Anode polarization dependences for graphite anode (Fig. 3.53 - 3.55 dependence 2) have a plateau at potentials of 0.7 - 0.9 V for Co-

Mo-WO_x, Co-Mo-ZrO_2, Co-W-ZrO_2 CEP, which indicates the impossibility of using them as an anode material.

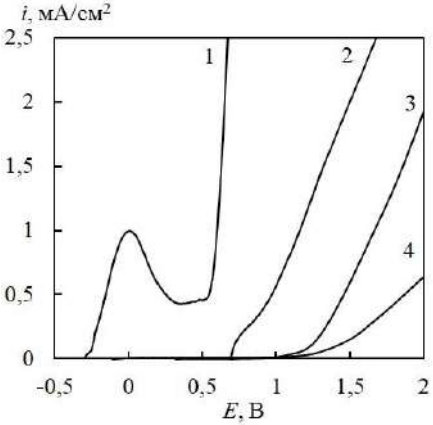

Figure 3.54 Анод Anode voltammograms on cobalt (1), graphite (2), steel X18N10T (3) and zirconium (4) electrodes in an electrolyte solution for the formation of composite coatings. Co-Mo-ZrO_2; s = 2×10^{-3} V/s

Therefore, it is advisable to use inert stainless steel anodes for the process, and the anode current density, as can be seen from Fig. 3.55, should be maintained at 0.2 □ 0.3 A / dm^2, that is, the ratio of the area of the anode to the cathode should be $S_A : S_K = 10 : 1$ [161].

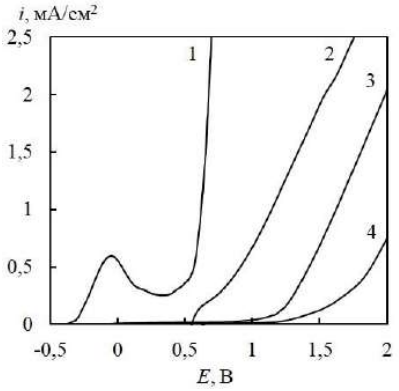

Figure 4.42 Анод Anode voltammograms on cobalt (1), graphite (2), steel X18N10T (3) and zirconium (4) electrodes in an electrolyte solution for the formation of composite coatings. Co-W-ZrO_2; s = 2×10-3 V/s

According to the results of the study, it was found that the anode material affects the efficiency of the process: during the deposition of coatings Co-Mo-WO_x in galvanostatic mode at I = 4 A/dm^2 with a cobalt anode sun is higher than tungsten (table. 3.18).

Table 3.18 the Influence of anode material on the content of components of composite electrolytic coatings of Co-Mo-WO_x and the current output in galvanostatic and pulse modes of electrolyte No. 5

Anode	Содержимое компонентов, масс. %			ВТ,%
	Co	Mo	W	
Galvanostatic mode (i = 4 A/dm^2)				
Cobalt	82,3	16,2	1,5	71
Tungsten	86,1	11,8	2,1	34
impulse mode (i = 10 A/dm^2, t_i = 5 ms, $t_п$ = 20 ms)				
Cobalt	77,4	16,3	6,3	85
Tungsten	79,4	15,3	5,3	33

The study of the effect of the anode material on the deposition of Co-Mo-WO_x CEP in pulsed mode, at i = 10A/dm^2 with a pulse duration of 5 ms and a pause of 20 ms confirms (Table 3.18) that the use of a cobalt anode allows to increase the total content of refractory components by 2% and increase BC.

The tungsten anode during electrolysis is covered with a thick oxide film and acts as an insoluble anode, and for its activation it is necessary to use appropriate means, change the component composition of the electrolyte by introducing activator ions, etc., which will certainly affect the performance of the process and the quality of coatings.

Chapter 3

APPLICATION OF POLYLIGAND ELECTROLYTE COMPOSITE COATINGS

The nature and methods of formation and properties of composite coatings are inextricably linked and are links of the same chain. In particular, there are significant differences in the structure and properties of metallurgical and galvanic alloys, as well as the concentration ratios of the components, especially considering their redistribution in the surface layers and the bulk of the material [162]. Electrolytic composite coatings in their phase composition, surface morphology, and, accordingly, properties, significantly differ from alloys obtained by thermal means, which significantly expands the technical capabilities of electrolytic alloys and their areas of application. The influence of the main external and internal factors on the formation of the composition and properties of multicomponent coatings is well known and logical [163-165].

4.1 Composite electrolytic coatings Co-Mo-WO_x

4.1.1 Electrolyte for the formation of composite coatings Co-Mo-WOx

To determine the rational composition of the complex citrate-pyrophosphate electrolyte, the Co-Mo-WOx composite coatings were applied to a stainless steel substrate in a galvanostatic mode. The concentration ratio of the alloy-forming components of the electrolyte Co^{2+}:WO_4^{2-}:MoO_4^{2-} was varied in the range 1: 1: 1 - 1: 2: 2 [166].

Table 4.1

Compositions of electrolytes for the deposition of composite coatings Co-Mo-WO_x

Electrolyte composition	Concentration, mol / dm^3						
	1	2	3	4	5	6	7
$CoSO_4$	0,1	0,1	0,1	0,1	0,2	0,2	0,2
Na_2WO_4	0,06	0,12	0,16	0,3	0,16	0,16	0,16
Na_2MoO_4	0,04	0,08	0,12	0,3	0,08	0,08	0,08
$Na_3C_6H_5O_7$	0,2	0,2	0,2	0,3	0,2	0,3	0,4
$K_4P_2O_7$	0,3	0,3	0,3	0,2	0,4	0,5	0,7

From poly-ligand citrate-pyrophosphate electrolytes at pH 8.5–10.0, shiny homogeneous composite coatings with high adhesion to the substrate are deposited. The content of molybdenum in the composition of coatings, as well as VT (Fig. 4.1), increases with a decrease in the total concentration of oxometallates $c(Co^{2+})/c(WO_4^{2-} + MoO_4^{2-})$.

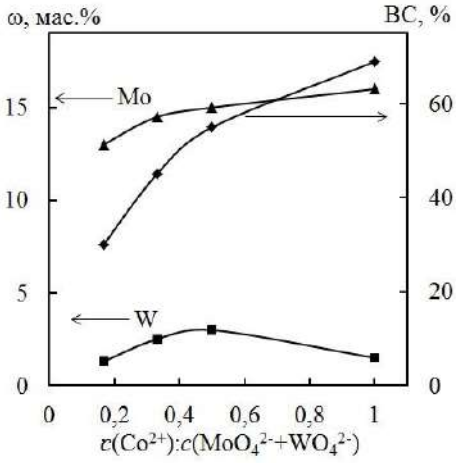

Figure 4.1 - Dependence of the composition of composite coatings Co-Mo-WO_x and VT on the ratio of the concentrations of complexing agents at i = 4 A / dm^2, pH = 9.0

This fact can be explained by the following circumstances: with an excess of oxometallates, their polymerization occurs; therefore, the true concentration of monoforms participating in the formation of heteronuclear complexes decreases. At a high concentration of oxometallate, the latter can act as ligands for cobalt, which also somewhat reduces the content of refractory metals in CEC with Co-Mo-WO_x alloys.

From electrolyte No. 4 with an increased content of oxometallates, shiny composite coatings of a gray-blue tint are deposited, which probably indicates an incomplete reduction of oxometallates and the presence of tungsten and molybdenum oxides in the coatings (the so-called "molybdenum blue"), therefore, an increase in the concentration of refractory components in the electrolyte above this value is impractical.

An integral part of determining the rational content of ligands in the composition of the electrolyte is the procedure for establishing the effect of their concentration on the content of refractory components in the composition of composite coatings. When performing this study, we used electrolytes with a stable content of complexing agents, mol / dm^3: c (Co^{2+}) = 0.2; c (WO_4^{2-}) = 0.16; c (MoO_4^{2-}) = 0.08 at pH = 9.5 (Figure 4.2).

It was found that an increase in the concentration of citrate and pyrophosphate leads to an increase in the number of ligands in the composition of the complexes and the total negative charge of the particles. In view of this, the strength of the complexes increases, and energy complications are observed at the discharge stage. On the other hand, difficulties increase at the stage of transporting particles to the cathode surface (migration component of the transfer) and, accordingly, the process is inhibited. Both reasons lead to a decrease in BT, since an increase in the concentration of ligands does not significantly affect the hydrogen discharge.

An increase in the concentration of ligands has a less effect on the precipitation of cobalt, since its constants for the formation of complexes increase to a lesser extent in comparison with refractory metals. Therefore, the total content of cobalt in the composition of the composite coating increases. As a consequence, on a surface

enriched with cobalt, due to its catalytic activity in the reaction of hydrogen evolution, the hydrogen current efficiency increases [167]

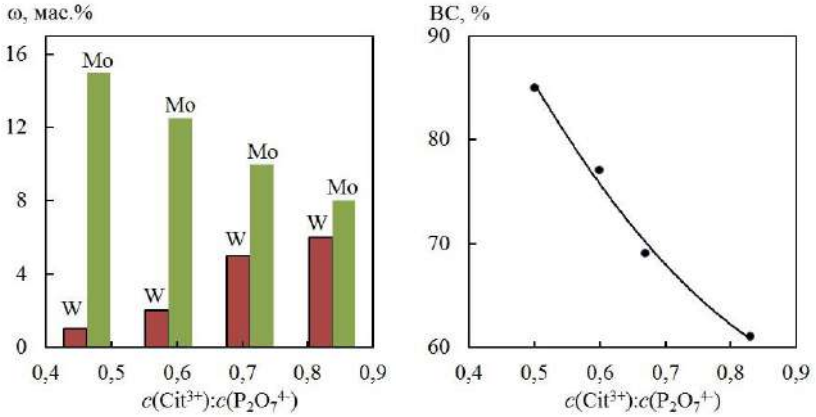

Figure 4.2 - Influence of the ratio of ligand concentrations on the total content of tungsten and molybdenum in composite coatings Co-Mo-WO_x (*а*) and VT (*б*) (i = 4 A/dm^2)

An important condition for the synthesis of high-quality composite coatings Co-Mo-WO_x of a given composition is the stability of the electrolyte pH, since the acidification of the medium leads to the polymerization of oxoanions, and the formation of hydroxides and / or other cobalt hydroxo compounds is possible in the alkaline region [230]. Thus, in particular, in the pH range 1–6, coatings are formed with a low level of adhesion to the substrate, a low content of refractory components, and a current efficiency of 15–43% (Fig. 4.3).

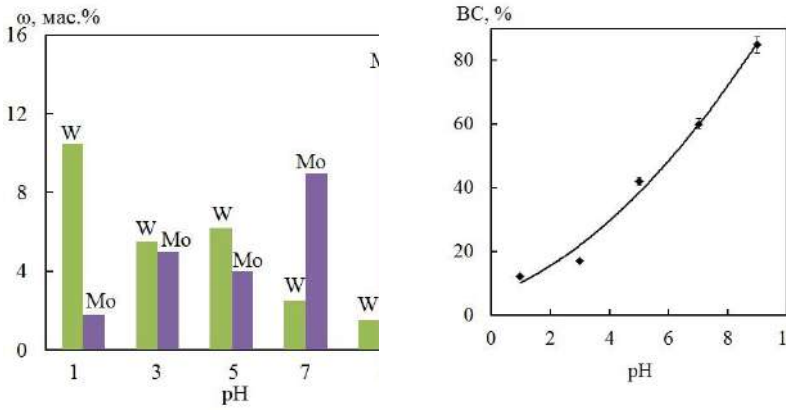

а *б*

Figure 4.3 - Influence of acidity of citrate-pyrophosphate electrolyte on the composition of composite coatings Co-Mo-WO_x (a) and VT (b) at i = 4 A / dm^2

However, as the pH of the electrolyte rises to 8–10, both the current efficiency and the total content of refractory metals increase. It turned out to be interesting that the total content of refractory components in the range of pH = 1 - 6 remains practically constant ω (W + Mo) ≠ f (pH), but as the solution alkalizes, ω (Mo) increases and ω (W) decreases.

4.2.2 Formation of composite coatings Co-Mo-WO_x in galvanostatic mode

In addition to the electrolyte composition, the current density and deposition time have a significant influence on the formation of high-quality composite coatings Co-Mo-WOx. With an increase in the current density, the content of refractory components in the composition of the obtained coatings changes symbatically (Fig. 4.4). Thus, composite coatings obtained from electrolyte at i = 6 A / dm^2 contain 5–6% more tungsten and molybdenum than at i = 2 A / dm^2.

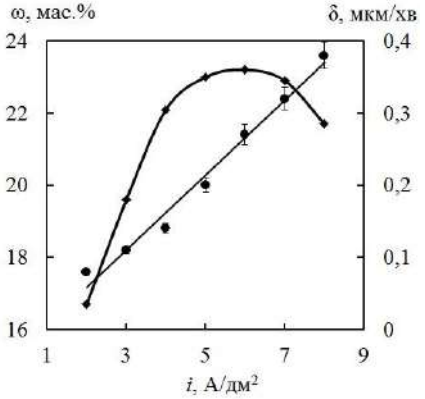

Figure 4.4 - Influence of current density on the total content of tungsten with molybdenum and the deposition rate of Co-Mo-WO_x coatings

Also, with an increase in the cathode current density, the rate of CEC deposition also naturally increases. Note that the dependence ω = f (i) has an extreme character with a maximum at i = 6 A / dm^2. The same value is the upper limit of the cathodic current density, above which the quality of the coatings decreases (burning of the deposit and deterioration of adhesion due to an increase in the rate of the partial reaction of hydrogen evolution are observed). The dissipative power of the electrolyte at the indicated current density is only 61%.

The selection of the lower limit of the current density was carried out experimentally by visual assessment of the quality of the resulting precipitation. By current densities lower than 2 A / dm^2, the coatings have a blue-brown color, which is inherent in tungsten and molybdenum oxides of intermediate oxidation states.

The effect of the deposition time of Co-Mo-WO_x composite coatings on their composition is shown in Fig. 4.5, a. The results obtained can be explained as follows: in the initial seconds of electrolysis, a thin continuous monolayer of cobalt is electrochemically deposited on the sample surface. After that, refractory metals are coprecipitated into the Co-Mo-WO_x coating competitively due to changes in the rates of partial reduction reactions of individual components with a change in polarization.

With an increase in the electrolysis belt, this leads to a gradual enrichment of the coating with molybdenum due to a decrease in the tungsten content.

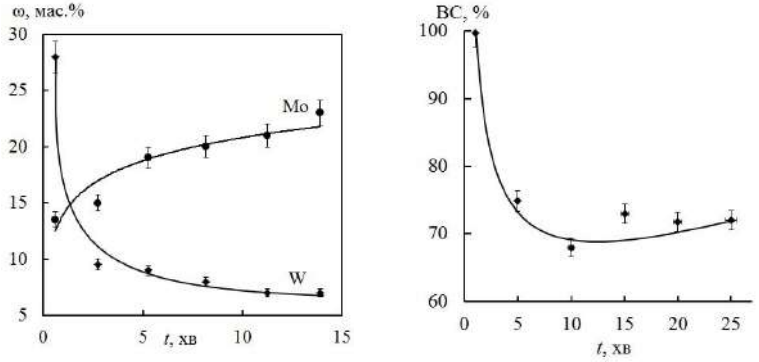

а *б*

Figure 4.5 - Influence of the deposition time on the content of tungsten and molybdenum (a) and BC (b) of the Co-Mo-WO_x coating

To determine the efficiency of the process, the effect of the deposition time on the current efficiency was established (Fig. 4.5, b). So the current efficiency of composite coatings Co-Mo-WOx practically does not depend on the electrolysis time and is at a fairly high level in the range of 70-80%.

4.1.2 Formation of composite coatings Co-Mo-WO_x in pulsed mode

The use of a galvanostatic mode, as well as a variation in the composition of electrolytes, does not allow obtaining high-quality composite coatings Co-Mo-WOx with a total content of refractory components of more than 20%. The use of a non-stationary mode contributes to the enrichment of coatings with alloying components and a decrease in the content of non-metallic impurities. In addition, it was found that the use of a non-stationary electrolysis mode allows obtaining a more uniform perfect surface of coatings with fewer micropores and cracks (Fig. 4.6), which has a positive effect on the functional characteristics of composite coatings, as shown in [168].

Pulse electrolysis is a promising method for the deposition of composite coatings, since it allows improving the technological process without changing the composition of the electrolyte by redistributing the rates of electrochemical and chemical stages during polarization and current interruption.

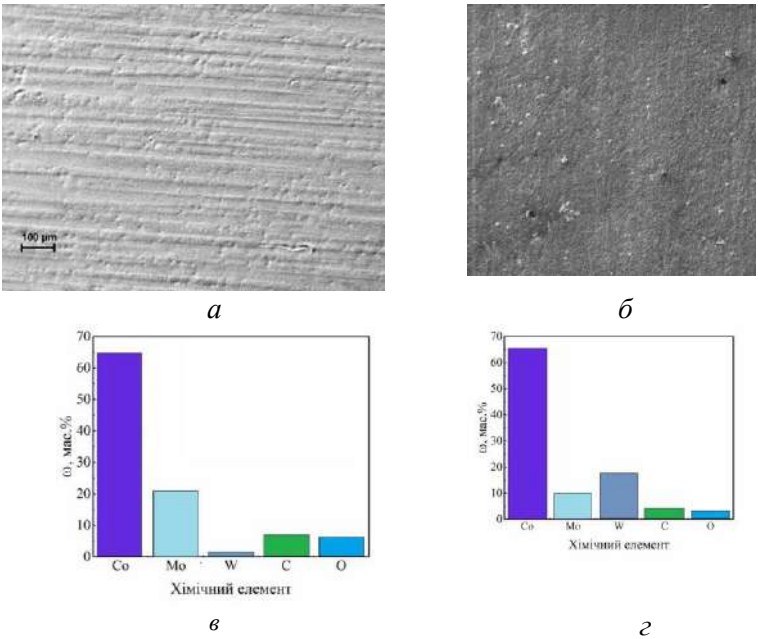

Figure 4.6 - Surface microstructure (x100) (a, b) and component composition (c, d) of composite coatings (wt.%) Co-Mo-WOx, deposited and electrolyte No. 4, i = 4 A / dm2 in stationary (a , c) and pulsed $t_i = 2$ • ms, $t_p = 10$ ms (b, d) modes. Temperature T = 50 ° C

To determine the efficiency of the process, the influence of the current density on the content of refractory components and the current efficiency of the VT composite coating was established (Fig. 4.7). Yes, the current efficiency Co-Mo-WO_x practically does not depend on the amplitude of the pulse current and is at a rather high level of 70–80%. With an increase in the cathodic current density, the composite coating is enriched with refractory components.

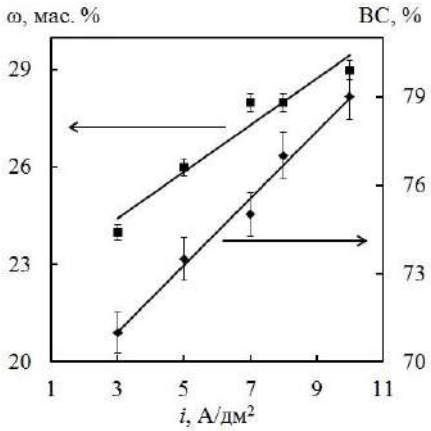

Figure 4.7 - Influence of the pulse current density on the content of refractory metals in composite coatings Co-Mo-WOx and current efficiency at t_i = 5 ms, t_p = 10 ms. Temperature T = 50 ° C

With an increase in the amplitude of the pulsed current, refractory metals are composited in the CEC Co-Mo-WOx competitively due to a change in the rate of partial reactions of reduction of individual components with a change in polarization, which leads to a gradual enrichment of composite coatings Co-Mo-WOx with tungsten due to a decrease in the content of molybdenum (Fig. 4.8) and, accordingly, a slight increase in the percentage of oxygen (up to 8 wt.%) due to the formation of tungsten oxides WO_x.

From the analysis of the dependences (Fig. 4.7, 4.8), it can be concluded that the deposition of Co-Mo-WO_x coatings most effectively occurs at a pulse current density u = 4 - 10 A / dm^2.

In pulsed electrolysis during a current pulse, the partial rates of metal and hydrogen evolution are redistributed in favor of metals. This leads to a decrease in the likelihood of alkalization of the near-cathode layer, as a result of which the formation of cobalt hydroxides on the surface of the electrode is inhibited. Estimating the distribution of components over the surface of the coatings (Fig. 4.9, a), it can be concluded that the composition of the composite coatings is rather uniform (Fig. 4.9, b). During the pause, first, there is a replenishment of the near-electrode layer with electrode active

particles due to diffusion and a kind of relaxation of the composition of this layer and the resulting precipitation. Secondly, conditions are created for the chemical reduction of intermediate oxides of molybdenum and tungsten by ad-hydrogen atoms.

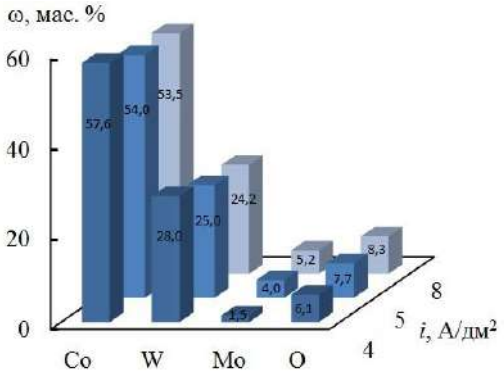

Figure 4.8 - Influence of current density on the composition of composite coatings Co-Mo-WOx, deposited from electrolyte No. 5; current amplitude t_i = 5 • ms, t_p = 5 • ms

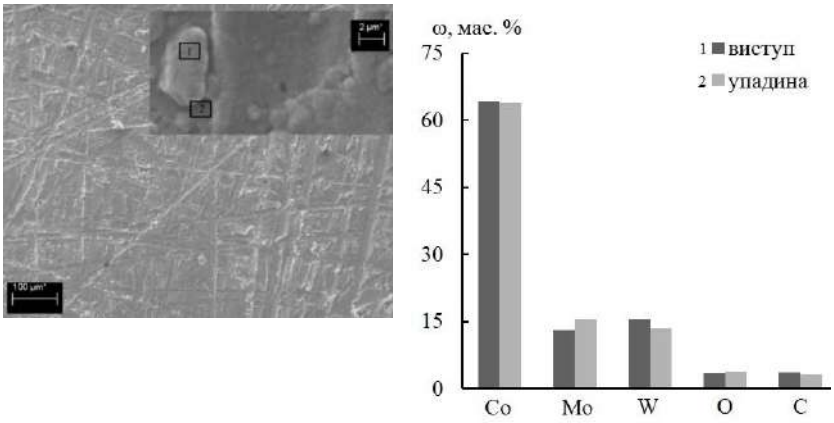

а *б*

Figure 4.9 - Morphology (a) and elemental composition (wt%) (b) of Co-Mo-WO_x composite coatings obtained by pulsed electrolysis t_i = 5 ms, t_p = 5 ms, i = 10 A/dm^2, T = 60 °C.

An increase in the pulse duration above 20 ms leads to an increase in the overvoltage of the release of refractory metals into coatings and a deterioration in their quality [169], and the duration of pauses leads to a decrease in the productivity (HT) of electrolysis. In these circumstances, it is necessary to analyze the effect of the pulse duration (Fig. 4.10) on the metal content and the efficiency of the process. The course of the dependences is quite predictable, since for a fixed pause time, an increase in the pulse duration reduces the contribution of the chemical stage of reduction to the implementation of the cathodic process, which leads to a decrease in the content of refractory components.

In this case, with an increase in the pulse duration over 10 ms, the tungsten content decreases with a simultaneous increase in the molybdenum content (Table 4.2.). Analysis of the effect of the pulse frequency on the composition of the coatings reflects (Fig. 4.11) the general trend for the inclusion of refractory metals in the composition of composite coatings.

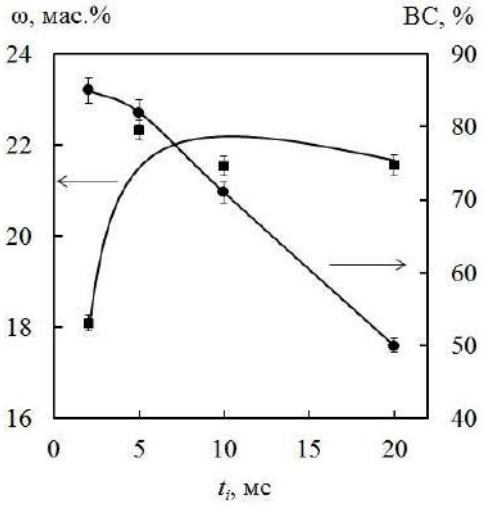

Figure 4.10 - Influence of the pulse duration on the current output of the pulse duration on the current output and the content of refractory components of composite coatings Co-Mo-WO_x in a pulsed electrolysis mode at i = 10 A/dm^2, t_p = 20 ms. Temperature T = 25 ° C, pH = 8. Electrolyte No. 1

As seen from Fig. 4.11 with an increase in the pulse frequency from 30 to 90 Hz, the current efficiency and the content of refractory metals in the composite coatings Co-Mo-WOx increase.

Table 4.2

Content of refractory components in Co-Mo-WOx coatings when varying the pulse duration in the pulsed electrolysis mode at i = 10 A / dm^2, tp = 20 ms. Temperature T = 25 ° C. Electrolyte No. 1

Metal content, wt. %	Pulse duration, ms			
	2	5	10	20
Mo	15,7	16,3	18,8	18,5
W	5,9	6,0	3,7	3,4

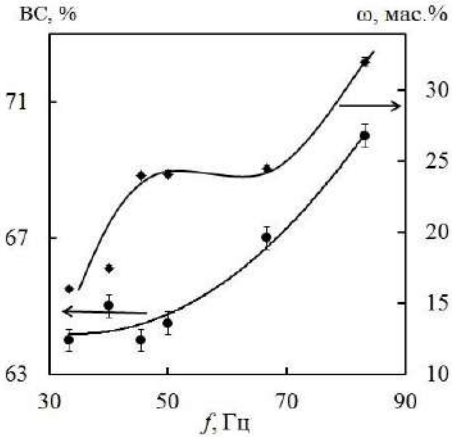

Figure 4.11 - Influence of the pulse frequency on the current efficiency of composite coatings Co-Mo-WOx at i = 4 A / dm2. Temperature T = 25 ° C, pH = 8.

The maximum content of these metals is observed at a frequency of 88 Hz (ti = 2 ms, tp = 10 ms), and with a further increase in f, the mass fraction of Mo, W and in the CEC composition decreases. It was found that an increase in the pulse duration above the proposed value leads to an increase in the overvoltage of the release of refractory metals into the composition of composite coatings and, accordingly, to a deterioration in the quality of coatings, and the duration of pauses leads to a decrease in the productivity of electrolysis.

The results of studying the distribution of the metal content over the thickness of Co-Mo-WOx ECCs obtained by pulsed current on copper substrates revealed a tendency towards a decrease in the percentage of tungsten in the direction from the substrate to the coating surface (Fig. 4.12, a). It is essential that this is reflected in the change in surface morphology (Fig. 4.12, b). With an increase in the content of molybdenum in composite coatings Co-Mo-WOx, the percentage of tungsten decreases, which proves the competitive reduction of metals. The surface morphology also changes: the grain size decreases slightly, but large globules and conglomerates appear (Fig. 4.12, b).

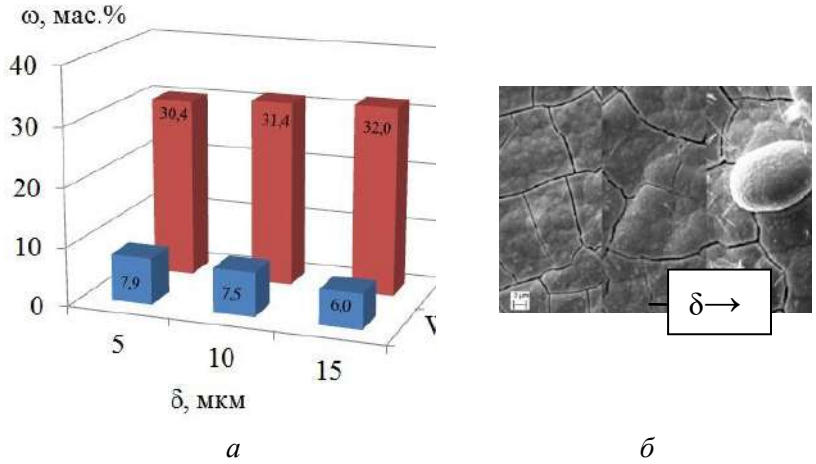

а *б*

Figure 4.12 - Distribution of metals by thickness (a) and change in surface morphology (b) of Co-Mo-WOx composite coatings. Pulse electrolysis i = 4 A / dm2, ti = 5 ms, tp = 10 ms. Electrolyte No. 5, T = 25 ° C

4.2 Composite electrolytic coatings Co-Mo-ZrO_2

4.2.1 Electrolyte for the formation of composite coatings Co-Mo-ZrO_2

To determine the rational composition of the citrate-pyrophosphate electrolyte, composite Co-Mo-ZrO_2 coatings were deposited on a copper substrate by varying the concentrations of the solution components [170].

From polyligand citrate-pyrophosphate electrolytes at pH 6.4–10, shiny homogeneous coatings with high adhesion to the substrate are deposited [171]. From electrolyte No. 5 (Table 4.3), the highest quality shiny CECs of a gray shade are deposited, therefore, an increase in the concentration of oxomolybdates in the electrolyte above 0.06 mol/dm^3 is inappropriate.

For citrate-pyrophosphate electrolytes used for the deposition of a composite coating Co-Mo-ZrO_2, it is characteristic that the degree of protonation of ligands (citrate and pyrophosphate) decreases with increasing pH. Accordingly, the strength of the corresponding complexes of cobalt will increase, and the potential for its reduction will shift towards approaching the reduction potentials of molybdate ions and zirconium [172] (Fig. 4.13).

Table 4.3

Compositions of electrolytes for the deposition of composite coatings Co-Mo-ZrO_2

Electrolyte composition	Concentration, mol / dm^3				
	1	2	3	4	5
$CoSO_4$	0,1	0,1	0,1	0,15	0,15
Na_2MoO_4	0,02	0,02	0,02	0,06	0,06
$Zr(SO_4)_2$	0,05	0,05	0,05	0,1	0,05
$Na_3C_6H_5O_7$	0,2	0,2	0,1	0,25	0,2
$K_4P_2O_7$	0,2	0,1	0,1	0,1	0,1

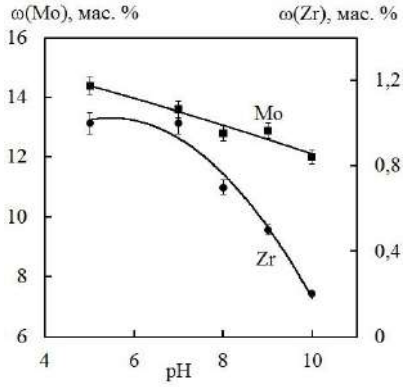

Figure 4.13 - Influence of solution acidity on the elemental composition of composite coatings Co-Mo-ZrO_2, deposited in a pulsed mode: i = 8 A / dm2, ti = 5 ms, tp = 10 ms. Temperature T = 25 ° C.

However, attention should be paid to the fact that with the transition to the alkaline region, the danger of the formation of cobalt hydroxides in the electrolyte increases, which leads to their undesirable inclusion in the composition of the coatings. In addition, the acidity of the solution has a significant effect on ionic equilibria in solutions of oxometalates, and with increasing pH, polyoxometalates dissociate into mono-forms, the sizes of which, as well as the ability to form heteronuclear complexes, are significantly higher [171]. However, the reduction of monooxomolybdates bound into stable complexes, like zirconium (IV), which in an alkaline medium exists mainly in the form of the $HZrO^{3-}$ oxoanion, is complicated. Consequently, the effect of electrolyte pH on the coating composition seems ambiguous and requires research.

According to the results of the experiments, it was found that the content of refractory components in composite coatings Co-Mo-ZrO_2 decreases with increasing pH of the solution.

In parallel with the metal reduction reaction, the hydrogen evolution reaction also proceeds, which has a significant effect on the current efficiency of composite coatings. Since the reduction of hydrogen from an alkaline solution proceeds at more negative potentials, an increase in the CEC current efficiency with an increase in the pH of the electrolyte looks quite natural (Fig. 4.14)

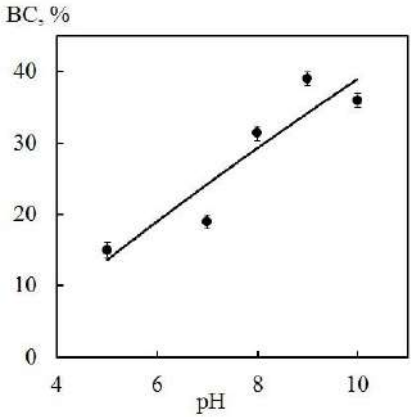

Figure 4.14 - Influence of solution acidity on the current efficiency of Co-Mo-ZrO_2 composite coatings deposited in a pulsed mode: i = 8 A / dm^2, ti = 5 ms, tp = 10 ms. Temperature T = 25 ° C.

4.2.2 Formation of composite coatings Co-Mo-ZrO_2 in galvanostatic mode

It is known from the literature [172] that in the galvanostatic mode, zirconium is not deposited into coatings with cobalt and molybdenum. But we found that from a complex citrate-pyrophosphate electrolyte, fine-crystalline uniform coatings with composites Co-Mo-ZrO_2 (Fig. 4.15) are formed in a wide range of direct current density. With an increase in the current density, the zirconium content in the composition of the composite coating changes symbatically, and the dependence of the molybdenum content has an extreme character with a maximum at i = 6 A/dm^2. However, low values of the current efficiency at high current densities do not allow the efficient use of the galvanostatic mode for the deposition of a composite electrolytic coating Co-Mo-ZrO_2 (Fig. 4.15)

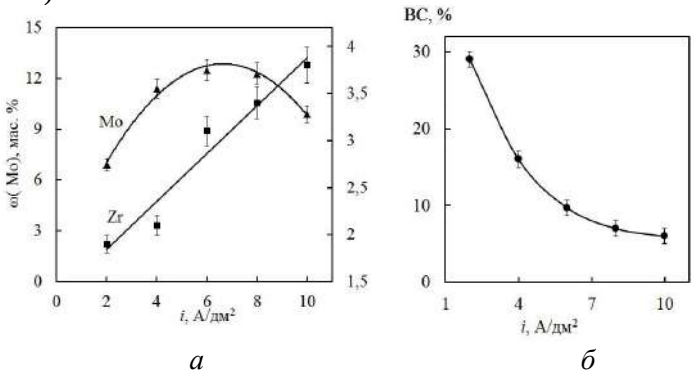

а *б*

Figure 4.15 - Influence of current density on the content of molybdenum and zirconium (a) and VT (b) of the composite coating Co-Mo-ZrO_2, precipitated from electrolyte No. 5

The effect of the deposition time of Co-Mo-ZrO_2 composite coatings on their composition is shown in Fig. 4.16.

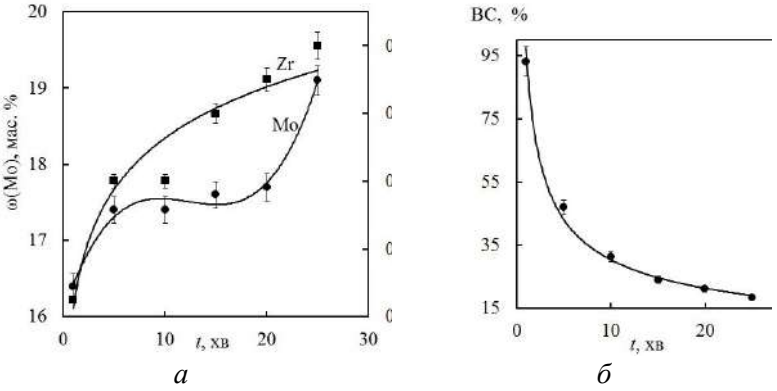

а *б*

Figure 4.16 - Influence of deposition time on the content of molybdenum and zirconium (a) m VT (b) composite electrolytic coating Co-Mo-ZrO_2 precipitated from electrolyte No. 1

Experimental studies have shown the absence of zirconium in the composition of the composite coating after the first minute of electrolysis, which is probably due to the catalytic effect of the cobalt sublayer on the discharge of oxomolybdates. Further incorporation of zirconium occurs already in the Co84-Mo16 coating and the Co-Mo-ZrO_2 CEC is formed. With an increase in the deposition time, an increase in the content of zirconium up to 0.8 wt.% Is observed with a simultaneous enrichment with molybdenum up to 17-19 wt.%.

To determine the efficiency of the process, the effect of the deposition time on the current output of the CEC was established (Figure 4.16, b). The current efficiency of Co-Mo-ZrO_2 decreases with the deposition time, since an increase in the content of molybdenum with zirconium in the Co-Mo-ZrO_2 coating provides a decrease in the hydrogen overvoltage and, as a consequence, a high catalytic activity in the reaction of hydrogen evolution.

4.2.3 Formation of a Co-Mo-ZrO_2 composite coating in a pulsed mode

The study of the effect of electrolysis modes on the composition, structure, and current efficiency of Co-Mo-ZrO_2 coatings, as well as the establishment of their relationship with the properties of synthesized coatings, is the basis for recommendations on the use of

materials. The use of the galvanostatic mode of deposition of Co-Mo-ZrO_2 coatings, as well as varying the composition of electrolyte components, does not allow obtaining high-quality coatings with a high current efficiency. Therefore, to improve these properties, it is proposed to use pulsed electrolysis.

An increase in the amplitude of the pulse current density, as well as the constant one, from 5 to 12 A/dm^2 with a constant pulse and pause duration, contributes to the enrichment of composite coatings with refractory metals - ω (Mo) to 16.2 wt% and ω (Zr) to 2, 1 wt% (Fig. 4.17).

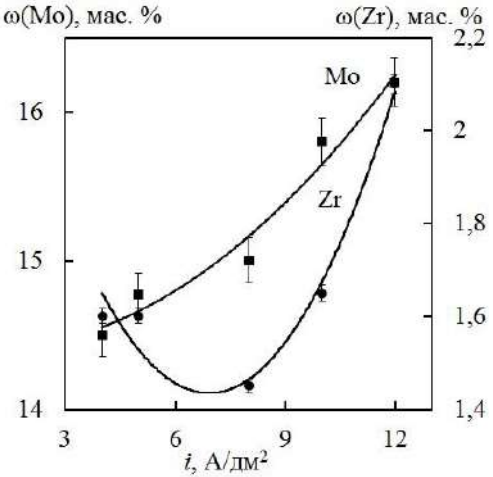

Figure 4.17 - Influence of the pulse current density on the content of molybdenum and zirconium in the composite electrolytic coating Co-Mo-ZrO_2 precipitated from electrolyte No. 3 at t_i = 2 ms, t_p = 10 ms, T = 25 ° C

The enrichment of composite coatings with alloying components with increasing current density is quite predictable, since the reduction of these metals is at least a two-step process and requires greater polarization and is accompanied by chemical reduction of intermediate molybdenum oxides by adsorbed hydrogen atoms Had. Indeed, it has been experimentally established that the range of deposition potentials of the Co-Mo-ZrO2 composite coating is - (1.8–2.8) V (Fig. 4.18).

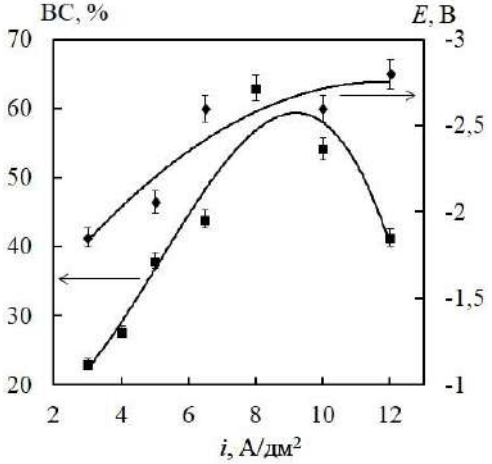

Figure 4.18 - Influence of current density on VT and potential of deposition of composite coatings Co-Mo-ZrO2 from electrolyte No. 3 in pulsed mode at ti = 2 ms, tp = 10 ms, T = 25 ° C

Thus, with an increase in the current density, the electrode potential shifts in the negative direction, which increases the partial reduction rate of zirconium (IV) and oxomolybdates.

The dependence of the current efficiency of the composite coating on the current density is extreme (Fig. 4.18): VT increases from 20% and reaches 63% with an increase in the current density from 5 to 8 A/dm^2; however, a further increase in i reduces the current efficiency to 44%. This behavior can be associated with the intensification of the side reaction of hydrogen evolution with significant fluctuations in the cathodic potential.

Energy parameters and conditions of electrolysis have a significant effect on the microstructure of the CEC surface. Indeed, at a current density of 3 A/dm^2, room temperature and a t / tp = 2/10 ms ratio, light coatings with a microglobular structure are formed (Fig. 4.19, a). An increase in the current density up to 8 A / dm2, all other things being equal, completely changes the surface morphology - microcracks appear due to an increase in internal stresses in the coatings, separate spheroidal conglomerates and globules are formed (Fig. 4.19, b) and occurs by a change in the CEC color.

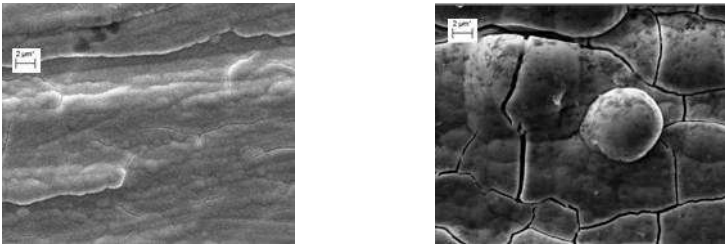

а *б*

Figure 4.19 - Micrographs (× 3000) of the surface of the Co-Mo-ZrO2 ECC precipitated from a citrate-pyrophosphate electrolyte in a pulsed mode at ti = 2 ms, tp = 10 ms, i, A / dm2: a - 3, b - 8; T = 20 - 25 ° C

Evaluating the distribution of components over the surface of composite coatings, we can conclude that the composition of the ECC is not uniform: Co dominates on the ridges, while in the depressions the oxygen concentration is significantly higher than the average one (Fig. 4.20). An increase in the current density does not lead to a significant increase in the percentage of refractory components, although the oxygen concentration naturally increases. In contrast to two-component Co-W coatings [173], the tungsten content decreases with increasing current amplitude. The time parameters of pulse electrolysis (pulse and pause duration) affect the composite composition and the deposition efficiency of the Co-Mo-ZrO2 coating. The minimum impulse value should be sufficient to achieve the potential for co-deposition of metals in the CEC, and the maximum one should be sufficient to ensure high-quality coating and electrolysis efficiency.

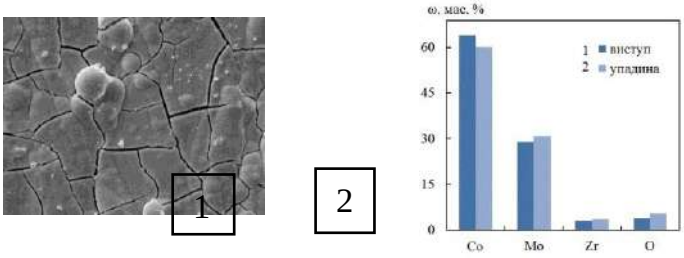

а *б*

Figure 4.20 - Morphology (a) and elemental composition (wt%) (b) of Co-Mo-ZrO_2 composite coatings obtained by pulsed current

i=4 A/dm^2 at t_i=5 ms, t_p=10 ms, T = 25 °C.

It was found that with an increase in the pulse time from 0.5 to 5.0 ms at a steady current density amplitude (i = 8 A / dm^2) and a constant pause duration of 10 ms, the molybdenum content in Co-Mo-ZrO_2 composite coatings decreases from 15, 9 to 13.7 mass. %, and zirconium, on the contrary, increases from 0.8 to 1.5 wt.% (Fig. 4.21). This is due to an increase in the effective current due to complete signal processing, due to which the deposition potential of zirconium in the composite coating is achieved. This dependence also shows different mechanisms of the deposition of zirconium and molybdenum in composite coatings under the studied conditions.

An extension of the pause from 5 to 50 ms at a steady current density and pulse duration (2 ms) provides an increase in the zirconium content in composite coatings from 0.8 to 2.1 mass%, followed by a decrease in ω (Zr) at high currents (Fig. 4.22).

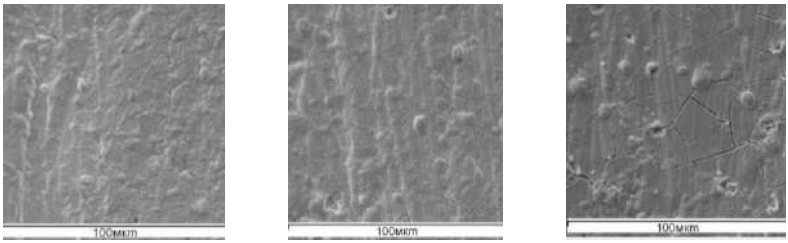

а *б* *в*

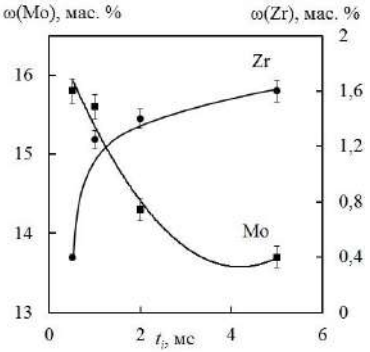

г

Figure 4.21 - Influence of the pulse duration on the morphology (ti: 2 (a), 5 (b), 10 (c) ms) and the content of molybdenum and zirconium (d) in the Co-Mo-ZrO_2 CEC, deposited from electrolyte No. 3 by a pulse current 8 A / dm^2 at tp = 10 ms, T = 25 ° C

Thus, the maximum concentration of zirconium in the ECC is achieved at the ratio ti / tp = 2/10 ms. At the same time, the content of molybdenum in the composite coating increases from 16.0 to 22.0 wt% with an increase in the pause duration due to a more complete course of the chemical reaction of reduction of intermediate oxides formed during polarization. The current efficiency decreases from 60 to 36% with an increase in the pulse time, and an increase in the pause has a positive effect on the efficiency of the Co-Mo-ZrO2 CEC deposition. Thus, the current efficiency reaches 78% at tp 50 ms and ti 2 ms.

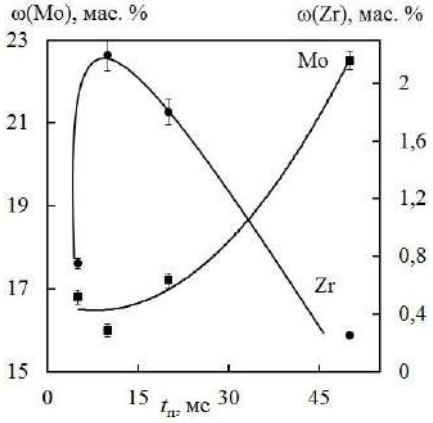

Figure 4.22 - Influence of the pause duration on the content of molybdenum and zirconium in CEC Co-Mo-ZrO_2 deposited from electrolyte No. 3 with a pulse current of 8 A / dm2 at ti = 2□10-3 s, T = 25 ° C

The maximum content of refractory metals in the CEC composition (Figure 4.23, a) is observed at a pulse frequency of 88 Hz (ti / tp = 2/10 ms), and with a further increase in frequency, the mass fraction of Mo, Zr and the oxygen content decrease.

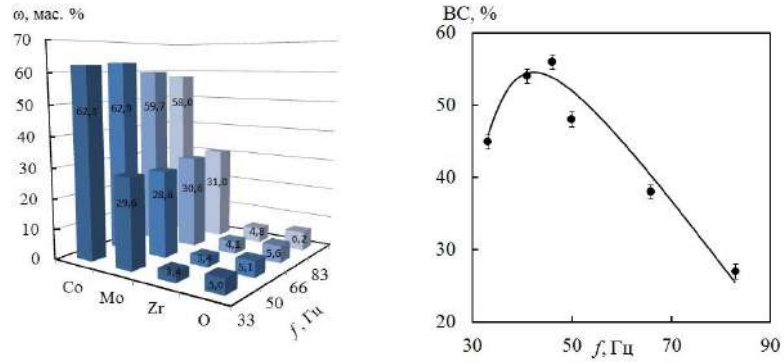

а *б*

Figure 4.23 - Impact of the pulse frequency on the composition (a) and VT (b) of the Co-Mo-ZrO2 ECC, deposited from electrolyte No. 3 with a pulse current of 4 A / dm2, T = 25 ° C.

With an increase in the pulse frequency from 30 to 50 Hz, the current efficiency of the Co-Mo-ZrO_2 composite coatings increases (Fig. 4.23, b), and a further increase in the pulse frequency leads to a sharp decrease in VT.

An increase in the electrolyte temperature to 50 °C contributes to an increase in the content of cobalt and zirconium in the Co-Mo-ZrO_2 CEC with a decrease in the percentage of molybdenum (Fig. 4.24)

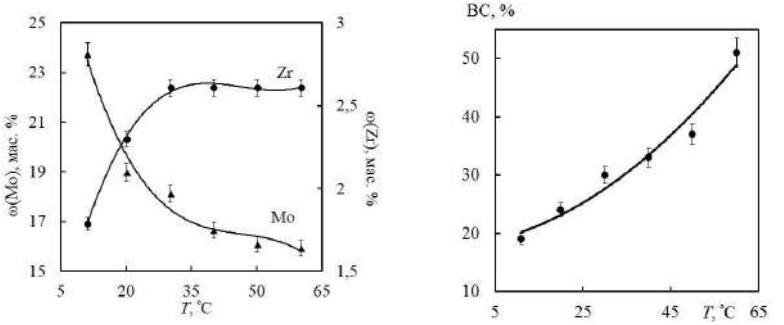

а *б*

Figure 4.24 - Effect of temperature on the composition (a) and BC (b) of Co-Mo-ZrO2 composite coatings, deposited from electrolyte No. 3 with a pulse current of 4 A/dm2, ti = 5ms, tp = 10 ms, T = 25 ° C.

The increase in the current efficiency of Co-Mo-ZrO_2 with increasing temperature (Fig. 4.24, b) can be explained not only by the acceleration of diffusion of electrode-active particles to the cathode surface and an increase in the limiting current density at which deposition of high-quality coatings is possible, but also by the acceleration of combined reactions recovery of metals in CEC.

The results of studying the distribution of metals over the thickness of Co-Mo-ZrO_2 coatings deposited by a pulsed current on a copper substrate revealed a tendency towards an increase in the content of molybdenum and zirconium (Fig. 4.25, a). The surface of the Co-Mo-ZrO_2 composites becomes more developed and microglobular with increasing coating thicknesses (Fig. 4.25, b). During the formation of zirconium-containing CECs, molybdenum and zirconium compete with cobalt, and the Co-Mo-ZrO2 coatings are enriched in refractory components from the substrate to the surface.

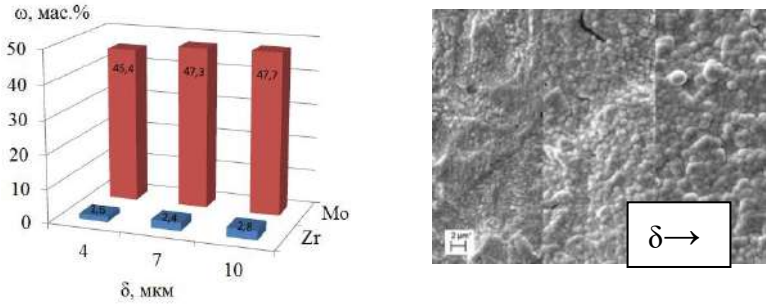

а *б*

Figure 4.25 - Distribution of metals over thickness (a) and change in surface morphology (b) of Co-Mo-ZrO2 composite coatings deposited from electrolyte No. 5 with a pulse current of 4 A / dm^2 at ti = 5 ms, tp = 10 ms, T = 25 °C

4.3 Electrolyte for the formation of composite coatings Co-W-ZrO2

To determine the optimal composition of the electrolyte, composite electrolytic coatings Co-W-ZrO2 were applied to a St3 steel substrate in a galvanostatic mode [236]. The concentration ratio

of the salts of the alloying components in the Co^{2+}:WO_4^{2-}:ZrO^{2+} electrolyte was varied in the range 1: 2: 1 - 1: 5: 2.

From polyligand citrate-pyrophosphate electrolytes at pH 6–10, shiny homogeneous composite coatings with high adhesion to the substrate are deposited [173].

Table 4.4

Compositions of electrolytes for the deposition of a composite coating Co-W-ZrO_2

Electrolyte composition	Concentration, mol / dm^3				
	1	2	3	4	5
$CoSO_4$	0,1	0,1	0,1	0,1	0,15
Na_2WO_4	0,02	0,02	0,02	0,02	0,06
$Zr(SO_4)_2$	0,05	0,1	0,05	0,05	0,05
$Na_3C_6H_5O_7$	0,2	0,2	0,2	0,3	0,2
$K_4P_2O_7$	0,2	0,2	0,1	0,1	0,1

An increase in the concentration of pyrophosphate ions in solution contributes to the enrichment of CEC with tungsten and zirconium due to a decrease in the content of cobalt (Fig. 4.26, a), which confirms the previously established fact of the competitive reduction of the mentioned metals. This can be explained by an increase in the number of ligands in the composition of cobalt complexes, and, accordingly, in the total negative charge of electrode-active particles, an increase in the strength of the complexes, which causes inhibition of cobalt reduction. Very interesting is the dependence of the content of alloying metals in the CEC Co-W-ZrO_2 on the concentration of zirconium (IV) sulfate (Fig. 4.26, b). On the contrary, with an increase in the concentration of zirconium (IV) in the electrolyte, the content of this metal in the coatings decreases. The same pattern was found for cobalt, while the percentage of tungsten in the Co-W-ZrO_2 CEC increases. The reason for this behavior should be sought in the tendency of zirconium to form sulfate complexes, the probability of the formation of which increases with an increase in the concentration of sulfates in relation to other ligands. Indeed, from electrolyte No. 2 (Table 4.4) with an increased content of zirconium (IV) sulfate, loose matte coatings of a

gray hue were obtained, therefore, the optimal concentration of Zr $(SO_4)_2$ 0.05 mol/dm^2.

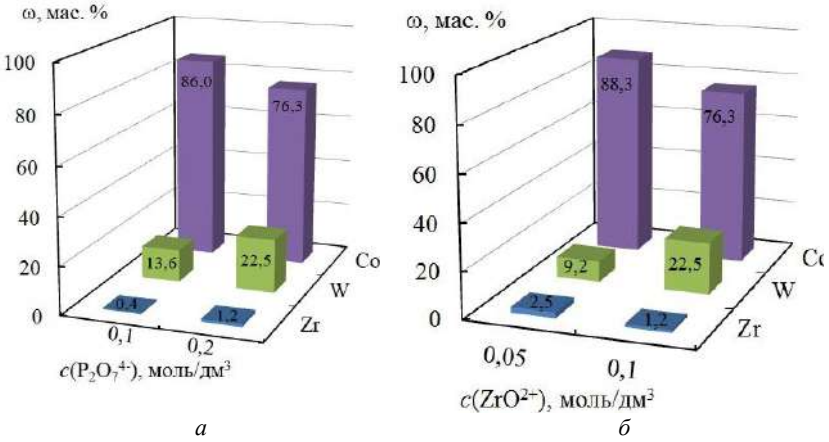

а *б*

Figure 4.26 - Dependence of the composition of Co-W-ZrO2 composite coatings on the concentration of pyrophosphate ions (a) and ZrO2 + (b), current 4 A/dm^2, pH 9.0

It is known from practice that the acidity of the electrolyte has a significant effect on the productivity of the electrodeposition process - the current efficiency and the quality of the coatings. Even a slight change in the pH of the electrolyte can lead to disruption of the electrolysis process and the deposition of poor-quality coatings.

For the citrate-pyrophosphate electrolytes used in this study for the deposition of the Co-W-ZrO_2 CEC, it is characteristic that with an increase in pH, the degree of protonation of ligands (citrate and pyrophosphate) decreases, and, accordingly, the strength of the corresponding cobalt complexes increases, and the potential of its reduction becomes negative. side and approach the renewal potentials of tungstates and zirconium [202]. Therefore, there is an increase in the content of W and Zr in the CEC Co-W-ZrO_2 precipitated from the investigated electrolytes at pH> 7 (Fig. 4.27, a).

On the other hand, stronger complexes are discharged with greater complications, and accordingly, the process of coating formation is inhibited, which leads to a decrease in VT (Fig. 4.27, b).

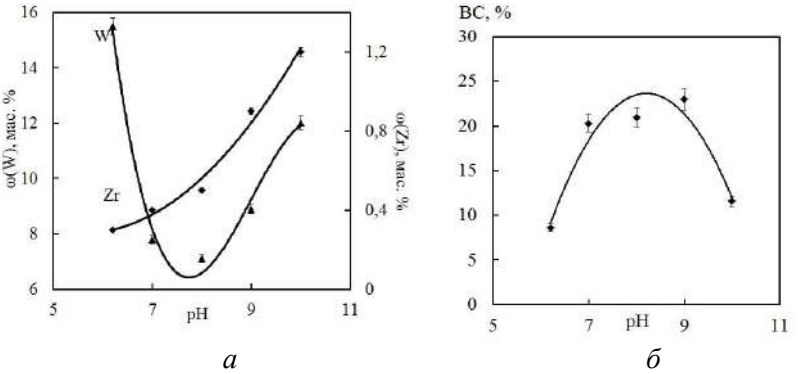

а *б*

Figure 4.27 - Effect of solution acidity on the elemental composition (a) and VT (b) of composite coatings Co-W-ZrO_2, deposited with a pulse current of 8 A / dm^2 at ti = 5 ms, tp = 10 ms. Temperature T = 25 ° C.

One of the general reasons for the decrease in the stability of the electrolyte is the alkalization of the near-electrode layer as a result of the side reaction of hydrogen evolution, which consumes up to 80% of the current in the processes under consideration. On the basis of the studies carried out, it was found that the optimal pH range for the formation of composite coatings Co-W-ZrO_2 is 7–9 [232].

Alkalization of the solution to pH more than 9 leads to a sharp decrease in the current efficiency of the composite Co-W-ZrO_2 coating, and after reaching pH 10, an insoluble precipitate of cobalt hydroxides is formed in the electrolyte and at the electrode layer, and, as a consequence, deterioration of the quality of the coatings.

4.3.1 Formation of composite coatings Co-W-ZrO_2 in galvanostatic mode

The study of the effect of electrolysis modes on the composition, structure, and current efficiency of the Co-W-ZrO_2 CEC is the basis for recommendations on the technology of composite coatings. With an increase in the current density, the content of refractory components in the composition of the composite coating practically does not change and remains in the range of 8.7 - 10.0 wt.% (Fig. 4.28). At current densities less than 2 A/dm^2, coatings of a blue-

brown color, characteristic of nonstoichiometric tungsten oxides, are deposited. Therefore, the lower limit of the current density should be considered 3 A/dm^2.

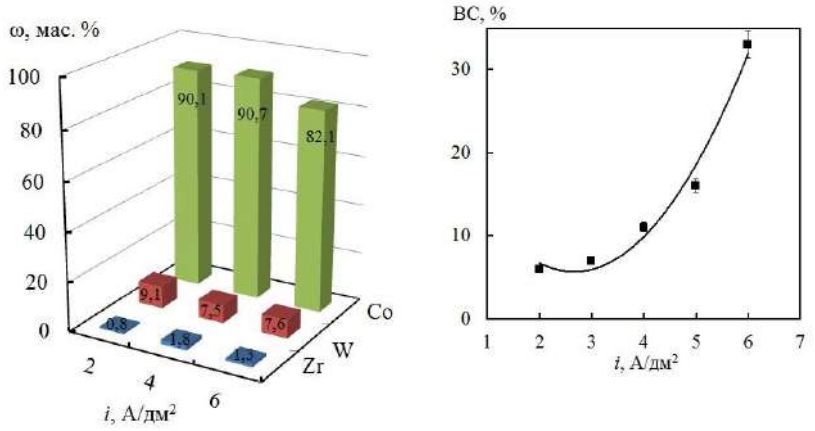

а *б*

Figure 4.28 - Effect of current density on the content of tungsten and zirconium (a) and BC (b) of the Co-W-ZrO_2 composite coating

Note that the dependence ω = f (i) is linear in the range of current densities from 3 to 6 A / dm^2 [174]. The latter value should be considered the upper limit of the cathodic current density, above which the quality of the composite coatings decreases - there is burning of the deposit and deterioration of adhesion due to an increase in the rate of the partial reaction of hydrogen evolution.

The effect of the deposition time of Co-W-ZrO_2 composite coatings on their composition is shown in Fig. 4.29, a. The results obtained can be explained as follows: in the first seconds of electrolysis, a continuous thin (monolayer) cobalt is electrochemically deposited on the sample surface. After the first minute of electrolysis, no zirconium was found in the composition of the Co-W-ZrO_2 coatings, which is probably due to the catalytic effect of the cobalt sublayer on the oxo-tungstate discharge. Further incorporation of zirconium occurs already in the Co72-W28 coating. After 5 minutes of deposition, the zirconium content in the Co-W-ZrO2 ECC is ~ 1.0 wt. %, but with an increase in the electrolysis time, a decrease in the content of zirconium in the coatings to 0.4

wt.% is observed with a simultaneous depletion in tungsten to 12 wt. % (Fig. 4.29, a).

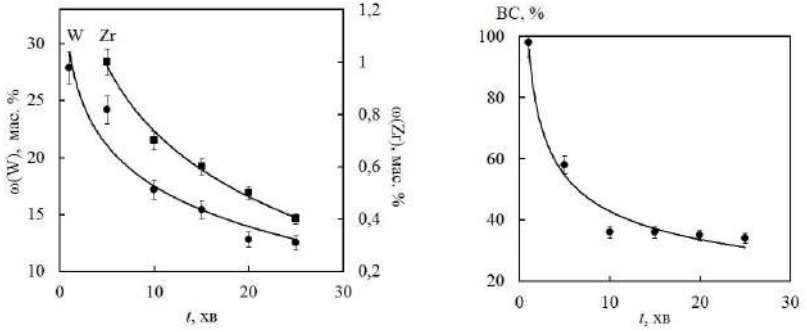

а *б*

Figure 4.29 - Influence of the deposition time on the content (a) of tungsten and zirconium and BC of composite coatings Co-W-ZrO_2 (b) deposited at a current density of 6 A / dm^2

The current efficiency of the Co-W-ZrO_2 composite coating after 10 minutes of deposition is practically independent of the electrolysis time and is within 35-40% (Figure 4.29, b).

4.3.2 Formation of composite coatings Co-W-ZrO_2 in a pulsed mode

The use of a galvanostatic mode for the deposition of Co-W-ZrO_2 CEC, as well as varying the composition of electrolytes, does not allow obtaining high-quality composite coatings with a Zr content of more than 0.7 wt. %. Therefore, pulsed electrolysis was used, which makes it possible to improve the technological process without changing the composition of the electrolyte.

To determine the efficiency of the process, the effect of the current density on the composition of the coatings (Fig. 4.30, a) and the current efficiency of the VT (Fig. 4.30, b) was established. At a current density of 4 A / dm^2, coatings with a tungsten content of 22 wt% were obtained. 10 A / dm^2. Co-W-ZrO_2 coatings contain non-metallic impurities, in particular, oxygen and carbon, which is associated with the presence of citrates in the electrolyte, as well as the inclusion of incompletely reduced oxides of refractory metals in the matrix of the composite coating. The carbon content in the

composition of Co-W-ZrO_2 coatings practically does not depend on the current density and ranges from 3.5 to 3.7 wt.%. At the same time, the oxygen content with a current density increases from 5.7 to 10.9 wt.%, And the percentage of tungsten decreases, in contrast to two-component Co-W alloys [175]

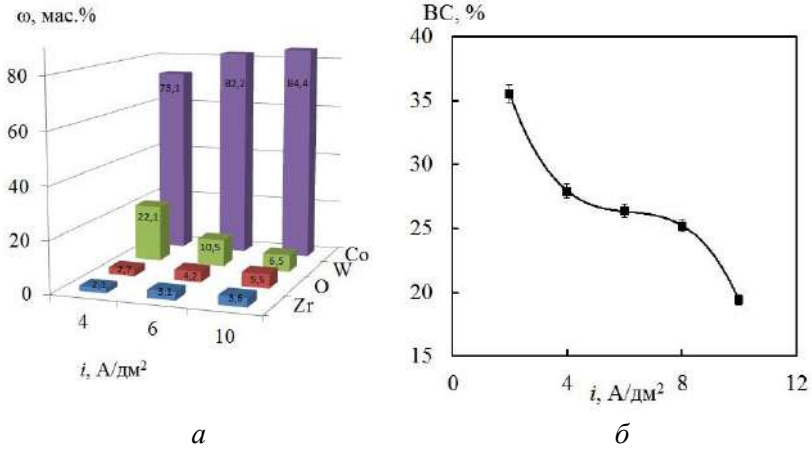

а *б*

Figure 4.30 - Effect of current density on the composition (a) and BC (b) of the Co-W-ZrO_2 CEC, deposited in a pulsed mode at ti = 2 ms, tp = 10 ms. Temperature T = 25 ° C, pH = 8

Based on the experimental results, it has been established that for the deposition of high-quality composite coatings Co-W-ZrO_2, the optimal pulse current amplitude range is from 4 to 8 A/dm^2.

To determine the efficiency of the process, the influence of the current density on the current output of the alloys VT was established (Figure 4.30, b). It has been established that the current efficiency of the Co-W-ZrO_2 composite coating is significantly lower than that of VT Co-Mo-WOx, which is explained by the lower oxidizing ability of tungstates and zirconium in comparison with molybdates.

An increase in the oxygen concentration in the composition of the composite coating leads to a decrease in the content of the crystalline phase of solid solutions and an increase in the percentage of the amorphous component of the deposits (Fig. 4.31). The peculiarities of the formation of the structure of the coatings have a

direct effect on the surface morphology, with the most significant effect being the cathodic current density. So, with an increase in the current density, the rate of nucleation of crystallization centers increases to a greater extent in comparison with the rate of crystal growth, therefore, the grain size decreases and the CEC becomes fine-grained (Fig. 4.31)

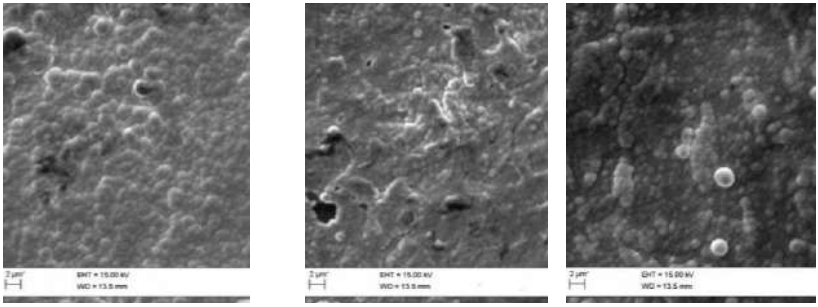

а *б* *в*

Figure 4.31 - Effect of current density on the morphology of Co-W-ZrO2 coatings deposited with a pulsed current with a density, A/dm^2: 4 (a), 6 (b), 10 (c) at ti = 2 ms, tp = 10 ms. Temperature T = 25 °C, pH = 8

An increase in the cathode current density and more than 10 A/dm^2 leads to the formation of loose Co-W-ZrO_2 coatings due to the increased influence of diffuse complications in comparison with the charge transfer stage. In addition, alkalization of the near-cathode layer occurs and the likelihood of the formation of cobalt hydroxides increases, which are included in the composition of the coatings and deteriorate their quality.

Analysis of the effect of the pulse duration on the composition of the Co-W-ZrO_2 coatings (Fig. 4.32, a) makes it possible to state an increase in the content of zirconium and cobalt and a decrease in the percentage of tungsten with an increase in the polarization time. At the same time, the current efficiency decreases (Figure 4.32, b) with lengthening the pulse time. This behavior can be explained by the intensification of the side reaction of hydrogen reduction with an increase in the polarization time.

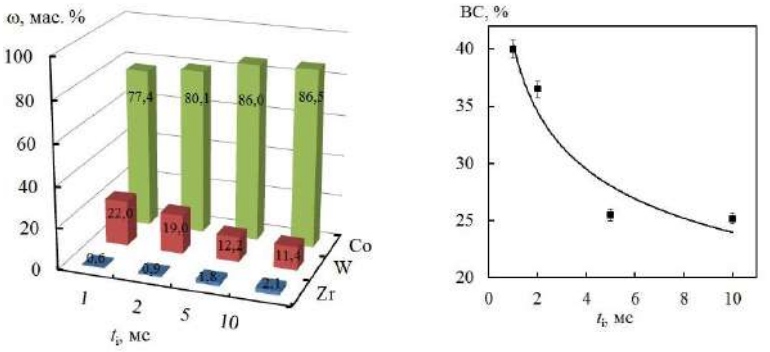

а *б*

Figure 4.32 - Impact of the pulse duration on the composition (a) and BC (b) of the Co-W-ZrO_2 CEC, deposited with a pulse current of 6 A / dm^2 at tp = 10 ms. Temperature T = 25 ° C, pH = 8

The effect of the pulse alternation frequency on the coating composition (Fig. 4.33, a) reflects the general trend of an increase in the tungsten content and a decrease in the percentage of zirconium in the Co-W-ZrO_2 CEC, which fully correlates with the effect of the pulse time.

The optimal content of refractory metals in the composition of the Co-W-ZrO_2 composite coating is observed at frequencies of 70–90 Hz (ti = 2–5 ms, tp = 10 ms), and with a further increase in the pulse frequency, the mass fraction of Zr in the composition of composite materials decreases. tungsten grows. The HT of composite coatings Co-W-ZrO2 increases with an increase in the pulse frequency from 30 to 90 Hz (Fig. 4.33, b), in contrast to the CEC Co-Mo-WOx and Co-Mo-ZrO_2 [240].

The electrolyte temperature has a significant effect on the surface morphology and chemical composition of the CEC. Thus, coatings with small microcracks are formed at room temperature. For the Co-W-ZrO_2 CEC, the temperature dependence has the following form: the mass fraction of zirconium is no more than 0.5 wt% and decreases with an increase in the electrolyte temperature, and the temperature dependence of the tungsten content in the coating composition passes through a minimum (Fig. 4.34)

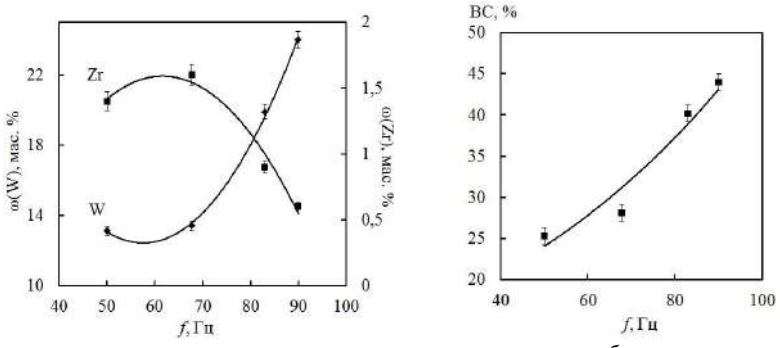

а *б*

Figure 4.33 - Impact of the pulse frequency on the composition (a) and BC (b) of composite coatings Co-W-ZrO_2, deposited with electrolyte No.3 with a pulse strum 4 A/dm^2, T = 25 °C, pH = 9

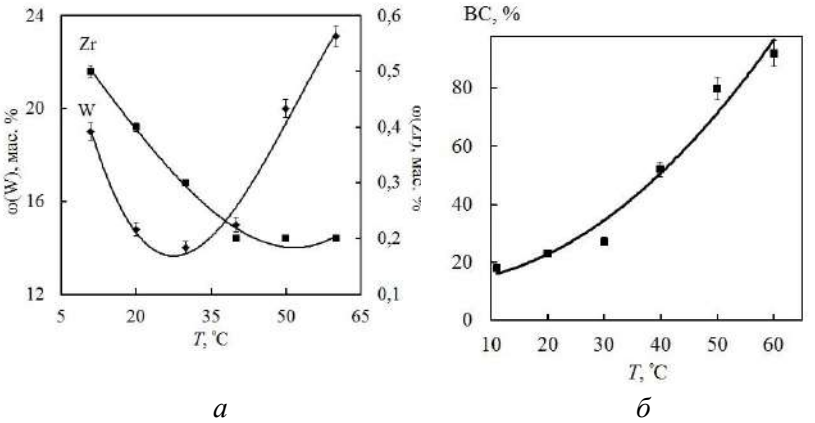

а *б*

Figure 4.34 - Effect of temperature on the composition (a) and VT (b) of Co-W-ZrO_2 composite coatings deposited from electrolyte No. 4 with a pulse current of 8 A / dm2 at ti = 5 ms, tp = 10 ms, pH = 7

The different effect of temperature on the composition of the Co-Mo-ZrO_2 and Co-W-ZrO_2 CECs can be explained by the differences in the coating formation mechanism due to a number of reasons. First, the rather high content of refractory metals in the coating at low temperatures (up to 20 °C) is associated with an insignificant contribution of hydrolysis to the general multistage process of CEC

formation. Second, the equilibrium reduction potentials of molybdates are higher than those of tungstates, and, therefore, an increase in the limiting current density for obtaining high-quality coatings with increasing temperature will affect to a greater extent precisely the systems containing tungsten [176].

Thus, temperature has an ambiguous effect on the formation of composite coatings. On the one hand, as the temperature rises, the rate of ion diffusion increases, which makes it possible to increase the current density at which dendrites and spongy deposits have not yet begun to form. In addition, an increase in the electrolyte temperature leads to an increase in the crystal growth rate, which contributes to the formation of coarse-grained structures.

An increase in the current output with an increase in the electrolyte temperature can be explained not only by the acceleration of the diffusion of electrode-active particles to the cathode surface and the corresponding boundary current density, but also by the acceleration of conjugate metal reduction reactions. For the Co-W-ZrO_2 composite coating, the current efficiency reaches 90% at 60 °C. The results of studying the distribution of the content of alloy-forming metals over the thickness of the Co-W-ZrO_2 coatings obtained by pulsed current revealed a tendency towards a decrease in the percentage of tungsten and zirconium content in the direction from the substrate to the surface (Fig.4.35, a)

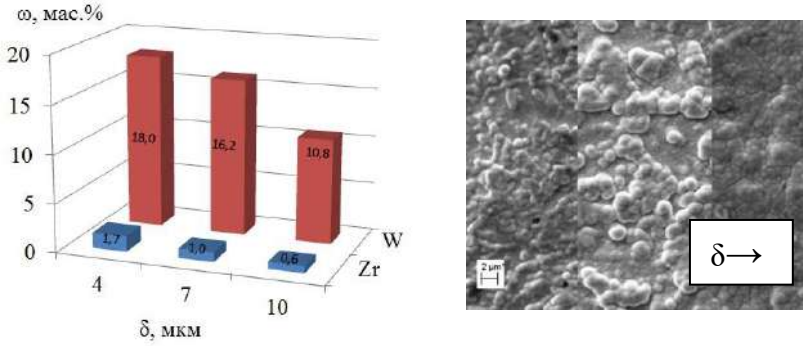

а *б*

Figure 4.35 - Distribution of metals over thickness (a) and changes in surface morphology (b) Co-W-ZrO_2 CEC, deposited from electrolyte No. 4 with a pulse current of 4 A / dm2 at ti = 5 ms, tp = 10 ms, T = 25 °C

It is essential that this is reflected in the change in surface morphology with increasing thickness (Fig. 4.35, b). On the surface of Co-W-ZrO_2 composite coatings, an increase in the size of globules with a coating thickness of 10 μm and a peculiar leveling of the surface profile are observed.

Based on the results obtained, it can be stated that tungsten and zirconium compete with cobalt in the deposition of Co-W-ZrO_2 CEC. Consequently, the electrolysis time, and, accordingly, the thickness of the coatings becomes a lever for controlling the composition of the surface layers.

4.4 Scattering power and electrical conductivity of citrate-pyrophosphate electrolytes for CEP deposition

One of the prerequisites for obtaining high-quality galvanic coatings is the electrical conductivity of electrolyte solutions (χ), a high level of which contributes to a uniform distribution of the electric field in the electrolyte, a decrease in energy consumption and allows obtaining high-quality coatings. Based on the analysis of the experimentally determined temperature dependence of electrical conductivity (Table 4.5), it can be argued that complex citrate-pyrophosphate electrolytes for the deposition of coatings based on cobalt alloys will have a sufficiently high scattering power.

Table 4.5

Electrical conductivity of citrate-pyrophosate electrolytes for CEC deposition

Coating	Electrical conductivity of electrolytes ($Ohm^{-1} \cdot m^{-1}$) at temperatures (K)			
	298	303	313	323
Co-Mo-WO_x	$7{,}4 \cdot 10^{-2}$	$8{,}2 \cdot 10^{-2}$	$9{,}6 \cdot 10^{-2}$	$1{,}1 \cdot 10^{-1}$
Co-Mo-ZrO_2,	$5{,}8 \cdot 10^{-2}$	$6{,}9 \cdot 10^{-2}$	$7{,}6 \cdot 10^{-2}$	$8{,}7 \cdot 10^{-2}$
Co-W-ZrO_2	$5{,}6 \cdot 10^{-2}$	$5{,}9 \cdot 10^{-2}$	$6{,}7 \cdot 10^{-2}$	$7{,}4 \cdot 10^{-2}$

The activation energy of electrical conductivity of complex electrolytes, calculated from a graphical analysis of the temperature dependence of electrical conductivity, is in the range of 22–29 kJ / mol, which is a sign of the course of mass transfer processes in a

diffuse mode. An increase in temperature reduces the inhibition of diffusion processes and contributes to an increase in operating current densities; information on the temperature dependence of the electrical conductivity of electrolytes is in demand when determining the operating parameters of technological processes.

Since the experimentally determined values of the electrical conductivity of solutions for the deposition of the investigated coatings are in the range χ = 0.055 - 0.07 $Ohm^{-1}m^{-1}$, the temperature range of 25–30 °C can be considered optimal.

An important technological parameter of the electrochemical deposition of composite coatings is the distribution of local velocities over the substrate surface, which in turn is determined by the current distribution over the treated surface [177]. With regard to this process, such an indicator is the scattering ability, which is understood as the ability of the electrolyte to change the primary current distribution, due only to geometric parameters. The results of the measurements of the SA indicate that with an increase in the current density, the SA of the electrolyte for the deposition of composite coatings Co-Mo-WOx decreases (Fig. 4.36). However, in the range of current densities 0.5–2.0 A / dm^2, the value of this parameter is more than 85%.

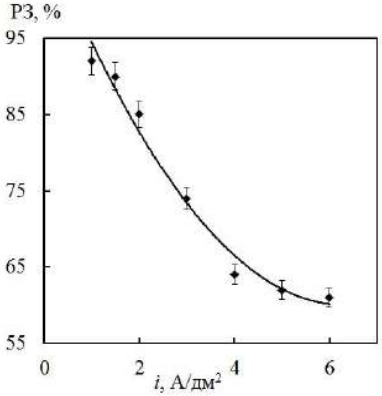

Figure 4.36 - Influence of the current density on the scattering ability of the electrolyte No. 5 of the deposition of the composite coating Co-Mo-WOx

The ability of the citrate-pyrophosphate electrolyte for deposition of Co-Mo-ZrO^2 CEC to uniformly distribute the metal over the electrode surface was determined at different current densities. The obtained CECs have a uniform matte dark gray color only on the first and second sections of the cathode, which were placed closest to the anode. Darkening of the coating is noticeable along the edges, which is associated with exceeding the limiting current density in these sections and excessive hydrogen evolution. The dependence of the distribution of metals over the sections of the cathode at current densities of 5 - 8 A/dm^2 is nonuniform (Fig. 4.37, dependences 1 - 3). So, in the first and second sections of the cathode, the increase in the mass of the sediment is almost twice as large as in 3 - 6 sections, which is explained by the influence of electrochemical parameters on the scattering ability of the electrolyte.

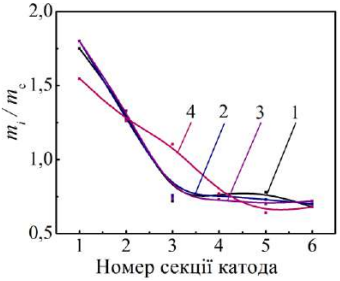

Figure 4.37 - Dependence of the increase in the cathode mass on the section number, electrolyte No. 3 (1 - 3) and electrolyte No. 3 + 50 g / dm^3 Na_2SO_4 (4) at current densities, A/dm^2: 1 - 5; 2 - 6, 5; 3, 4 - 6

The polarization during the deposition of the Co-Mo-ZrO2 composite coating is low, since the formation occurs at high current densities (3 - 10 A / dm2). This explains the significant difference in mass gain on the cathode sections located in the Hull cell at different distances from the anode (Figure 4.37). The results obtained indicate an insufficiently high scattering power of the electrolyte. Therefore, to increase the scattering ability indicator, an electrically conductive additive is introduced to the working electrolyte - 50 g/dm^3 Na_2SO_4. This somewhat improves the scattering power, i.e. promotes a more uniform distribution of metal over the cathode surface (Fig. 4.37, dependence 4). The results of the performed measurements of the

scattering ability indicate that with an increase in the current density of the SA of the electrolyte for the deposition of the composite coating Co-Mo-ZrO_2, it slightly increases (Fig. 4.38).

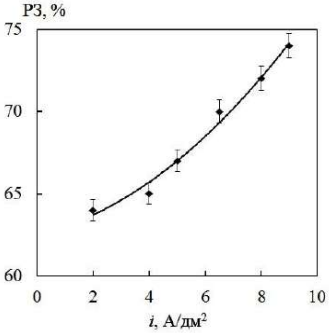

Figure 4.38 - Influence of current density on the scattering ability of citrate-pyrophosphate electrolyte No. 3 for the deposition of composite coatings Co-Mo-ZrO_2

The results of the measurements of the scattering power of electrolyte No. 5 for the deposition of the Co-W-ZrO_2 coating indicate that with an increase in the current density, the SA of the electrolyte decreases (Fig. 4.39). This behavior can be associated with the amorphization of the structure of composite coatings Co-Mo-WOx i Co-W-ZrO_2.

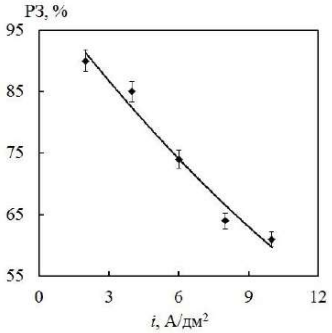

Figure 4.39 - Influence of current density on the scattering ability of citrate-pyrophosphate electrolyte No. 5 for the deposition of a composite coating Co-W-ZrO_2

But during the deposition of composite coatings Co-W-ZrO_2 at a current density of up to 4 A / dm2, the value of this parameter is more than 85%.

4.5 Choice of anode material for CEC deposition Co-Mo-WOx, Co-Mo-ZrO_2 and Co-W-ZrO_2

The electrodeposition of composite coatings based on cobalt alloys from citrate-pyrophosphate electrolytes is sensitive to changes in their composition. Therefore, such requirements are imposed on anode materials for electrolysis as corrosion resistance, the absence of oxidation reactions of electrolyte components, leading to a change in the composition of the electrolyte. For electroplating processes, anodes of the same metal as the coatings are usually used. However, when electrolytic deposition of multicomponent coatings is carried out, the selection of a soluble anode made of several metals is complicated by the different dissolution rates of the components, and, accordingly, the enrichment of the electrolyte with only one type of ions.

To determine the characteristics of electrode processes, polarization dependences were obtained for different anode materials. Since the reduction of metals is not the only process, such dependences are cumulative and are characterized by the simultaneous flow of all anodic reactions.

The overwhelming majority of scientists conduct experimental research using an inert electrode [178], and most often they use platinum or stainless steel. Taking into account the need to reveal the influence of the concentration of alloy-forming components on the composition of the coatings, this approach is quite justified, since inert electrodes do not affect the content of electrode-active particles in the electrolyte [179].

The peculiarities of the electrodeposition of composite coatings based on cobalt are, in particular, in the difference not only of cathodic reactions, but also of the anodic behavior of the metals used; therefore, the use of soluble anodes in this case is the topic of an extensive separate study.

During the deposition of Co-Mo-WO_x, Co-Mo-ZrO_2, Co-W-ZrO_2 composite coatings, the anode potential on Kh18N10T steel shifts in the positive direction with an increase in the cathodic current density and does not exceed 1.9 V in the range of investigated current densities IR (2 , 0 - 12.0 A / dm^2) (Table 4.6).

Studies of the anodic behavior of various electrode materials in electrolyte solutions for the deposition of composite coatings allow

us to draw the following conclusion. The absence of any active processes on the X18N10T steel anode in the potential range up to +0.8 V for Co-Mo-WOx composite coatings and +1.2 V for Co-Mo-ZrO_2, Co-W-ZrO_2 confirms the fact of the possibility of using these anodes are inert.

Table 4.6

Anode potential under current when coating with alloys (anode - steel X18H10T; S_A: S_K = 10: 1)

coating	Anode potential under current E_a, V polarization current density iк, A / dm^2					
	2,0	4,0	6,0	8,0	10,0	12,0
Co-Mo-WO_x	1,42	1,50	1,58	1,66	1,74	1,82
Co-W-ZrO_2	1,48	1,61	1,70	1,78	1,85	1,79
Co-Mo-ZrO_2	1,43	1,54	1,62	1,69	1,75	1,90

As is known [180], the use of insoluble anodes can improve the quality of coatings and the efficiency of the cathodic process. Cobalt anodes dissolve with the formation of Co^{2+} at low polarization at a high rate, as evidenced by the rapid increase in the current density in voltammograms (Fig. 4.40-4.42)

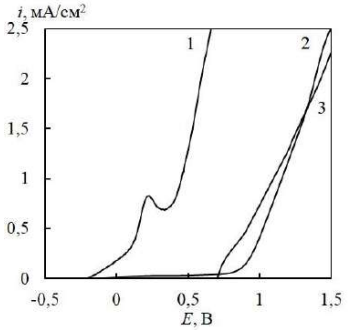

Figure 4.40 - Anodic voltammograms on cobalt (1), graphite (2) and steel X18H10T (3) electrodes in an electrolyte solution for the formation of Co-Mo-WOx composite coatings; s = $2 \cdot 10^{-3}$ V / s

The use of soluble cobalt anodes can only provide compensation for the consumption of cobalt during electrolysis and prolong the life

of the electrolyte [181], but, on the other hand, leads to a violation of the ratio of the concentrations of complexing agents in the solution, since the corresponding rate of dissolution of cobalt with refractory metals (cycronium) fails when using such anodes. Also, after using soluble anodes, alkalization and a decrease in the life of the electrolyte are observed. This is due to the formation of hydroxide ions in the side reaction of hydrogen evolution and the inability to compensate for their effect on pH from the anodic reaction, since oxygen evolution, accompanied by acidification of the solution, does not occur on the soluble anode.

Anodic polarization dependences for a graphite anode (Fig. 4.40 - 4.42 dependence 2) have a plateau at potentials 0.7 - 0.9 V for CEC Co-Mo-WO_x, Co-Mo-ZrO_2, Co-W-ZrO_2, which indicates inability to use them as anode material

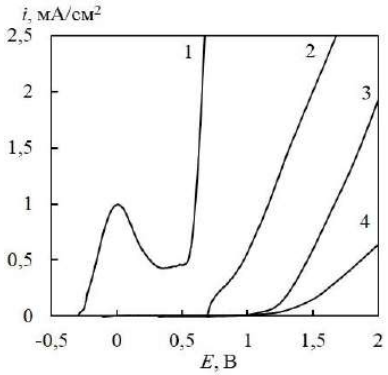

Figure 4.41 - Anodic voltammograms on cobalt (1), graphite (2), steel X18H10T (3) and zirconium (4) electrodes in an electrolyte solution for the formation of Co-Mo-ZrO_2 composite coatings; $s = 2 \cdot 10^{-3}$ V/s

Consequently, for carrying out the process, it is advisable to use inert stainless steel anodes, and the anode current density, as can be seen from Fig. 4.42 should be maintained at the level of 0.2 - 0.3 A/dm^2, i.e. the ratio of the anode to cathode area should be S_A: S_K = 10: 1 [182].

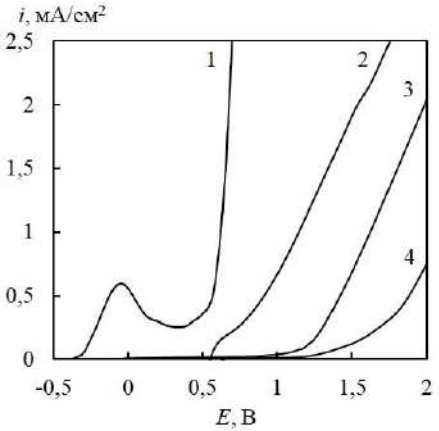

Figure 4.42 - Anodic voltammograms on cobalt (1), graphite (2), steel Kh18N10T (3) and zirconium (4) electrodes in an electrolyte solution for the formation of Co-W-ZrO_2 composite coatings; s = 2 · 10^{-3} V/s

According to the results of the study, it was found that the anode material affects the efficiency of the process: during the deposition of Co-Mo-WOx coatings in the galvanostatic mode at i = 4 A/dm^2 with a cobalt VS anode is higher than with a tungsten anode (Table 4.7).

The study of the influence of the anode material on the deposition of Co-Mo-WOx composite coatings in a pulsed mode at i = 10A / dm^2 with a pulse duration of 5 ms and a pause of 20 ms confirms (Table 4.7) that the use of a cobalt anode allows an increase in the total content of refractory components of 2% and increase the sun.

During electrolysis, the tungsten anode is covered with a thick oxide film and acts as an insoluble anode, and for its activation it is necessary to use appropriate means, change the component composition of the electrolyte by introducing activator ions, etc., which will certainly affect the performance of the process and the quality of coatings.

To obtain high-quality composite coatings Co-Mo-WOx, it is recommended to use the ratio of the concentrations of electrolyte components c(Co^{2+}) : c(MoO_4^{2-}) : c(WO_4^{2-}) = 1,0 : 0,4 : 0,8 and ligands c(Cit^{3-}): c($P_2O_7^{4-}$) = 1,0:2,0; current density 2–8 A/dm^2 with varying temperature in the range of 293–333 K. The low tungsten

content in the composition of composite materials deposited in a stationary mode gives the coatings a fine-crystalline structure and reduces the level of internal stresses. The use of a pulsed mode with a pulse / pause duration ratio, ms: (1 - 10) / (5–20) and a current density amplitude of 4 - 20 A / dm2, makes it possible to obtain composite Co-Mo-WOx coatings with an increased content of refractory metals, in particular tungsten up to 20 wt.%, halving the oxygen content and more uniform distribution of elements over the surface compared to the stationary regime.

Table 4.7

Influence of the anode material on the content of components of composite electrolytic coatings Co-Mo-WO_x and current efficiency in galvanostatic and pulse modes in electrolyte No. 5

Anod	Content of components, wt. %			VT,%
	Co	Mo	W	
Galvanostatic mode (i = 4 A/dm^2)				
Cobalt	82,3	16,2	1,5	71
Tungsten	86,1	11,8	2,1	34
Pulse mode (i = 10 A / dm^2, ti = 5 ms, tp = 20 ms)				
Cobalt	77,4	16,3	6,3	85
Tungsten	79,4	15,3	5,3	33

CEC Co-Mo-ZrO_2 precipitated at a ratio of component concentrations $c(Co^{2+}):c(Cit^{3-}):c(P_2O_74-):c(MoO_4^{2-}):c(Zr^{4+})$ = 1,0:1,4:0 ,7:0,4:0,3. It was found that fine-crystalline Co-Mo-ZrO_2 coatings are formed in the range of direct current densities u = 2 - 8 A / dm^2. With an increase in the current density, the zirconium content in the coating composition changes symbatically, and the molybdenum content has a maximum at u = 6 A/dm^2, but the current efficiency does not exceed 35%. The use of a pulse current with an amplitude of 3 - 10 A / dm^2, a pulse duration ti 1–10 ms and a pause tp 5 - 50 m makes it possible to obtain fine-crystalline composite electrolytic coatings Co-Mo-ZrO_2 containing up to 4 wt. % zirconium and up to 25 wt. % molybdenum at a current output of 50 - 80%.

The optimal ratio of the concentrations of components in electrolytes for the deposition of Co-W-ZrO_2 is $c(Co^{2+})$: $c(Cit^{3-})$:

$c(P_2O_7^{4-}) : c(WO_4^{2-}) : c(Zr^{4+}) = 1 : 3 : 1 : 0,2 : 0,5$. The optimal pH range is 7-9. With an increase in the steady-state current density, the content of refractory components in the Co-W-ZrO2 coating practically does not change and remains in the range of 8.7 - 10.0 wt.%, And the Zr content in the coating composition is not more than 0.7 wt. %, while the current efficiency is up to 30%. It is shown that the use of a unipolar pulse current with an amplitude of 4–8 A / dm2 at a pulse / pause duration ratio of (2–10) / (10) ms ensures the deposition of Co-W-ZrO_2 composite electrolytic coatings with a tungsten content range of 2 -%, zirconium - 1 - 2.5 wt. % and a current output of 40 - 60%.

It was found that the distribution of the content of refractory components in the composition of composite coatings Co-Mo-WOx, Co-Mo-ZrO_2 and Co-W-ZrO_2 over the thickness of the coatings is nonlinear, and changes symbatically to the thickness in the case of Mo and antibate in the case of W. that, in the galvanostatic mode, high-quality CECs based on cobalt with a high content of refractory metals are deposited only at T> 30 °C, while at a pulsed current it allows the temperature to be reduced to T = 20 - 30 °C without loss of quality.

The indicators of the scattering ability and specific electrical conductivity of electrolytes for the deposition of composite coatings Co-Mo-WOx, Co-Mo-ZrO_2 and Co-W-ZrO_2 were established. The electrical conductivity grows linearly with an increase in the electrolyte temperature, but at a temperature of 25–30 ° C, its value is sufficient for the deposition of high-quality coatings on parts of a complex configuration.

The use of inert stainless steel anodes is substantiated. It is shown that the use of combined active anodes is not possible due to the different dissolution rates of coprecipitated metals in composite coatings.

Chapter 4

FUNCTIONAL PROPERTIES OF COMPOSITE ELECTROLYTIC COATINGS BASED ON COBALT WITH REFRACTORY METALS

The functional properties of multicomponent coatings and composites directly depend on the qualitative, quantitative and phase composition, morphology, surface topology and roughness, distribution of components over the surface and coating thickness. In turn, the listed characteristics depend on the composition of the electrolyte and the modes of electrodeposition, which was discussed earlier. Establishing the effect of the composition of the CEC based on cobalt alloys on the relief and surface structure is an indispensable element in predicting the functional properties of the obtained systems.

4.1 Topography and surface roughness of coatings

Along with morphology, an analysis of the topography and determination of the class of surface roughness of electro-deposited films provides rather comprehensive information on the structure of coatings [183].

In materials science, roughness is a characteristic of the surface quality and depends on the processing method (grinding, polishing, etc.) of the material. During the deposition of electroplated coatings, this parameter reflects the degree of roughness of the substrate. At the same time, roughness is the result of a number of processes: nucleation on a substrate of foreign material and subsequent crystal growth during the formation of the coating. The ratio of the rates of

these processes, together with morphology, can be an additional indicator for assessing the degree of surface development [184]. To obtain information on the surface relief, the method of atomic force microscopy was used.

The roughness of the surface of the composite coatings Co-Mo-WOx, Co-Mo-ZrO_2, Co-W-ZrO_2 was determined using a scanning atomic force probe microscope (ACM) NT-206. Scanning was carried out by the contact method using a CSC-37 probe, cantilever B with a lateral resolution of 3 nm [185].

Scanning was carried out on areas of the surface of samples of various areas: 40.0 × 40.0 μm, 20.0 × 20.0 μm, 10.0 × 10.0 μm and 5.0 × 5.0 μm, and the height of the surface relief was fixed with a resolution of 256 × 256 pixels. Areas for scanning were selected in the center of the samples; to take into account the diversity of the surface, the studies were repeated for two areas at a distance of 1500 μm from each other [186].

The visualization of the results was carried out by means of relief reconstruction in the form of 2D and 3D topography maps (the height is reflected in color) and 2D-torsion maps obtained by twisting the measuring console, which reflects surface friction.

The processing of the obtained AFM images was carried out using the Explorer software by analyzing the average amplitude parameters of the surface roughness in accordance with international standards - the arithmetic mean Ra (ISO 4287/1), which determines the surface roughness in the form of a two-dimensional arithmetic value, and the root-mean-square Rq (ISO 4287 / 1), which is the defining characteristic of the surface roughness [187].

Based on the results of the analysis of the surface profile, which was plotted along the section on topographic maps, as well as histograms of the distribution of heights, the angles of inclination of elementary surface sections, and the angles of orientation of the normal to the surface, the size, shape of grains and the presence of anisotropy of properties were determined.

On all structures, the identity of the surface characteristics in different scanning areas was noted, which made it possible to extrapolate the data to the characteristics of the sample under study as a whole.

The surface of the polished St3 steel backing, which is prepared for electrodeposition, is fairly uniform. Analysis of the histograms of the distribution of heights and the distribution of the angles of inclination of the normal to the surface (Fig. 5.1, 5.2) indicates its disordered structure.

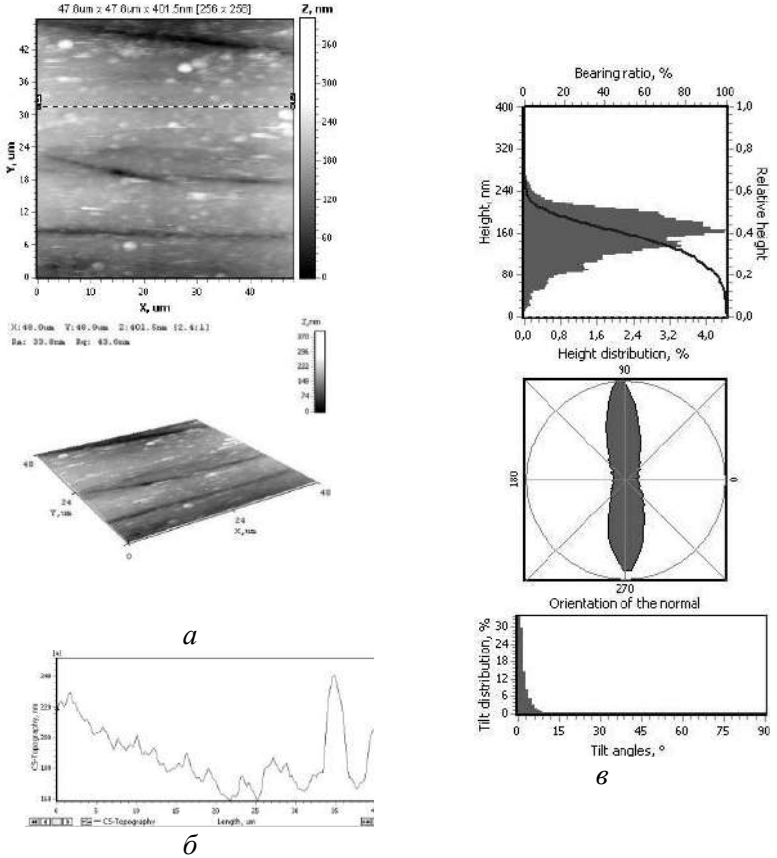

Figure 5.1 - 2D and 3D maps (a), the profile of the surface section between markers 1 and 2 (b), the histogram of the distribution of heights, tilt angles of elementary surface areas and orientation angles (c) for the St3 lining. Scanning area 48 × 48 μm.

Analysis of the profile of the surface section between markers 1 and 2 shows that the grain sizes of the substrate are in the range of 2 - 4 microns (Fig. 5.1, b; 5.2, b). The nature of the histogram of the

orientation angles of the normal to the surface (90 ° → 270 °) indicates the isotropy of the properties of the substrate material (Fig. 5.1, c; 5.2, c).

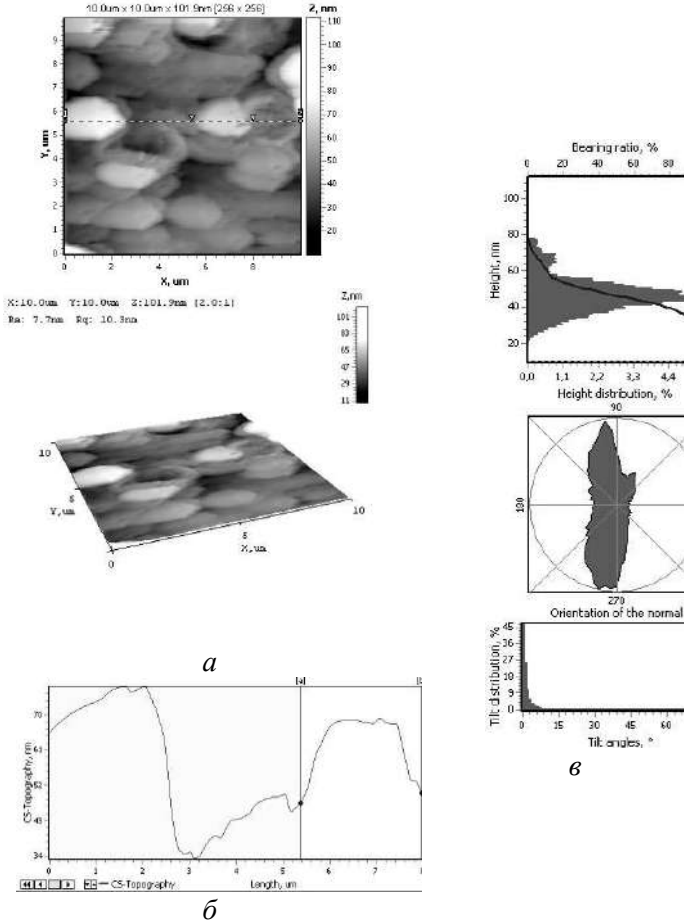

Figure 5.2 - 2D-, 3D-map of the surface (a), the profile of the section between markers 1 and 2 (b) and the histogram of the distribution of heights, inclination angles of elementary surface areas and orientation angles (c) of the St3 substrate. Scanning area 10 × 10 μm.

Composite coatings Co-Mo-WOx (Fig. 5.3, 5.4, a, b) are characterized by a uniformly developed globular surface, the relief which significantly differs from the substrate (Fig. 5.1, 5.2), on which they are

formed. Investigation of the topography of the coating surface with the ratio of alloy-forming metals Co60Mo23W17 using AFM makes it possible to evaluate the grain size and the uniformity of the structure of the surface layers. As seen from Fig. 5.3, the coating consists of spherical grains and is characterized by a sufficiently high density, uniformity of the structure. A small number of peaks up to 870 nm are visualized. As it was established earlier [188], the formation of a spheroidal surface structure is caused by the presence of refractory metals in the obtained CEC.

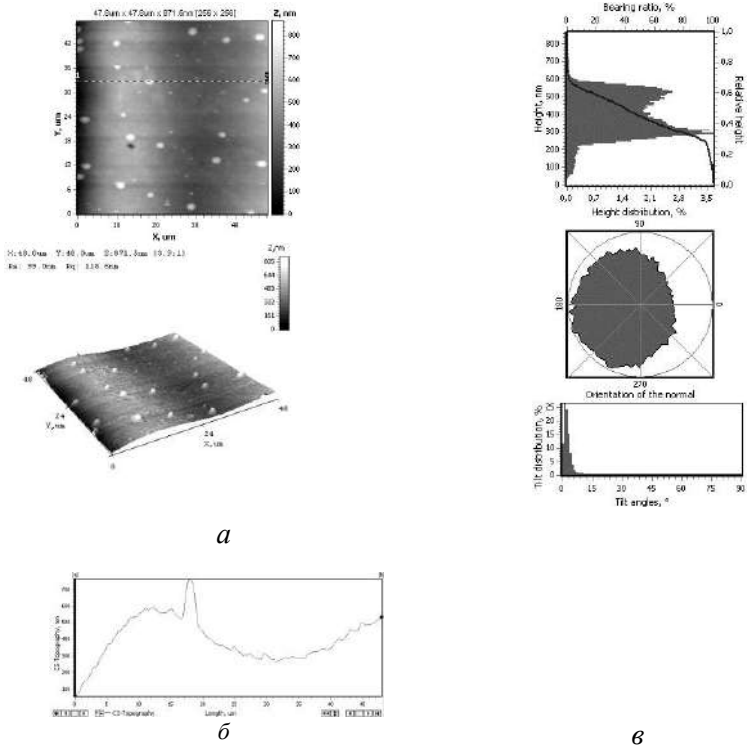

Figure 5.3 - 2D-, 3D-map of the surface (a), the profile of the section between markers 1 and 2 (b) and the histogram of the distribution of heights, angles of inclination of elementary surface sections and angles of orientation (c) CEC based on Co60Mo23W17. Scanning area 48 × 48 μm.

It should be noted that with an increase in the current density and a sufficiently high content of refractory components (39-41 wt%), a

network of cracks forms on the surface of the coatings due to internal stresses. This is due to the high deposition rate and the difference in the type and parameters of the crystal lattice of the alloy-forming metals. Analysis of the AFM data indicates the nanoglobular nature of the surface of Co-Mo-WOx coatings (Fig. 5.4, a, b), on which cone-shaped associates with a diameter of 2-5 μm are formed as a result of coalescence of small globules with a diameter of 20-80 nm.

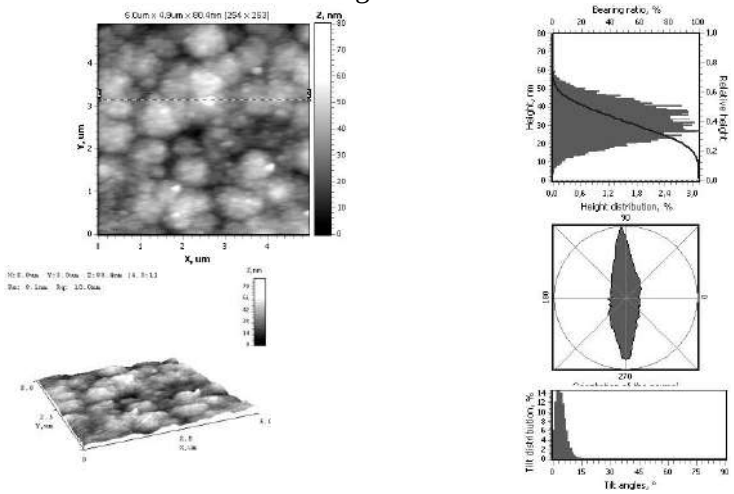

а

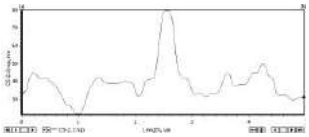

б *в*

Figure 5.4 - 2D-, 3D-map of the surface (a), the profile of the section between markers 1 and 2 (b) and the histogram of the distribution of heights, inclination angles of elementary surface sections and orientation angles (c) of the CEC based on Co60Mo23W17. The scanned area is 5 × 5 μm.

Coatings with the ratio of alloy-forming metals Co62Mo33Zr5, deposited by a pulsed current (i = 4 A / dm^2), differ from both the substrate and the composite electrolytic coating Co60Mo23W17 by a more developed surface. The surface consists of uniformly

distributed conical associates with a diameter of 5-7 microns (Fig. 5.5, 5.6, a, b), the dimensions of which exceed the parameters of the Co60Mo23W17 coating by 1.5-2.5 times.

Profile analysis of surface's cross-section between markers 1 and 2 indicates the formation of small cone-shaped grains with a size of 0.2 - 0.3 microns and their joining into crystallites, the size of which ranges from 1.5 - 3.5 microns (Fig.5.5).

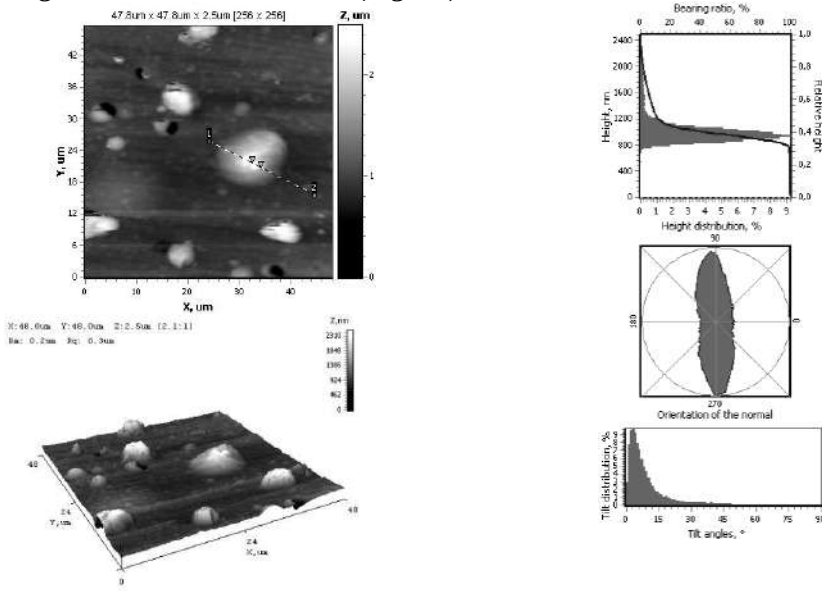

a

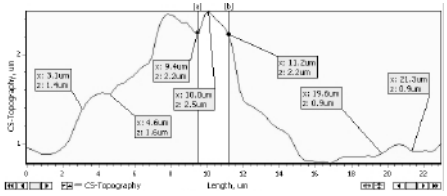

b *c*

Figure 5.5 - 2D-, 3D-map of the surface (a), the profile of the section between markers 1 and 2 (b) and the histogram of the heights' distribution, inclination angles of elementary surface sections and orientation angles (c) of the CEC based on Co62Mo33Zr5. Scanning area 48 × 48 μm

The transition to the nanorelief (scanning area 5 × 5 μm) makes it possible to analyze the surface of detached agglomerates, on which small substructures are observed, the size of which ranges from 1.4 to 1.8 μm. In shape and size, they are similar to the grains of the main surface layer (Fig. 5.6).

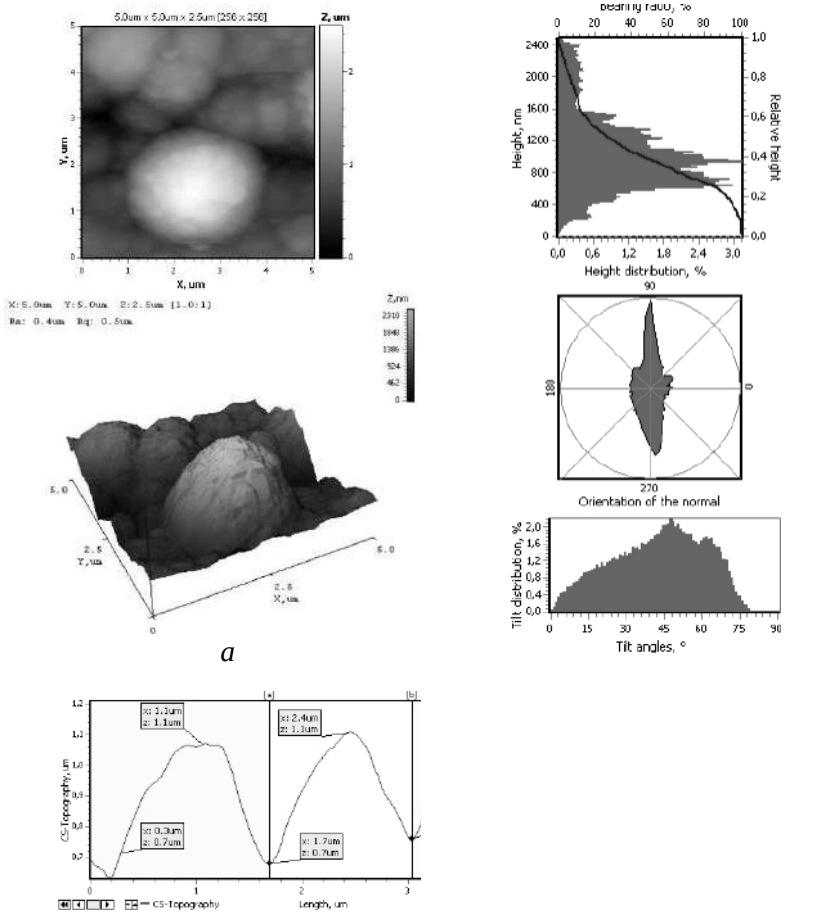

Figure 5.6 - 2D-, 3D-map of the surface (a), the profile of the section between markers 1 and 2 (b) and the histogram of the distribution of heights, inclination angles of elementary surface sections and orientation angles (c) of the CEC based on Co62Mo33Zr5. Scanning area 5 × 5 μm.

The results of studies of the topography of the Co-Mo-ZrO2 CEC with a molybdenum content of 31 at.% And zirconium of 3.5 at.%, Deposited by a unipolar pulse current (i = 6 A / dm^2), also indicate the formation of a more developed surface in comparison with the substrate material. For scanning areas of 48 × 48 μm and 5 × 5 μm, there is a large difference in the heights of the protrusions and depressions of the surface relief compared to the Co62Mo33Zr5 coating (Fig. 5.7, c).

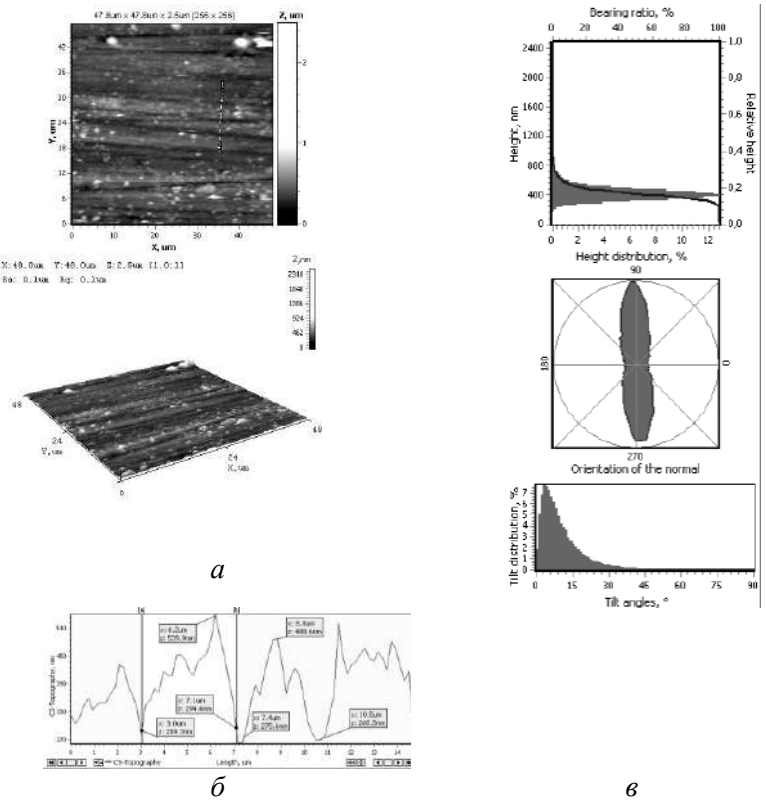

а *б* *в*

Figure 5.7 - 2D-, 3D-map of the surface (a), the profile of the section between markers 1 and 2 (b) and the histogram of the distribution of heights, elementary surface sections' angles of inclination and angles of orientation (c) CEC based on Co65Mo31Zr4. Scanning area 48 × 48 μm.

Profile analysis of surface's cross-section between markers 1 and 2 indicates the formation of small cone-shaped agglomerates, the base diameter of which reaches 1.5 μm (Fig. 5.8, b). Unlike Co-Mo-WOx coatings, the character of the histogram of orientation angles indicates anisotropy of properties within the entire scanning area (Fig. 5.8, c).

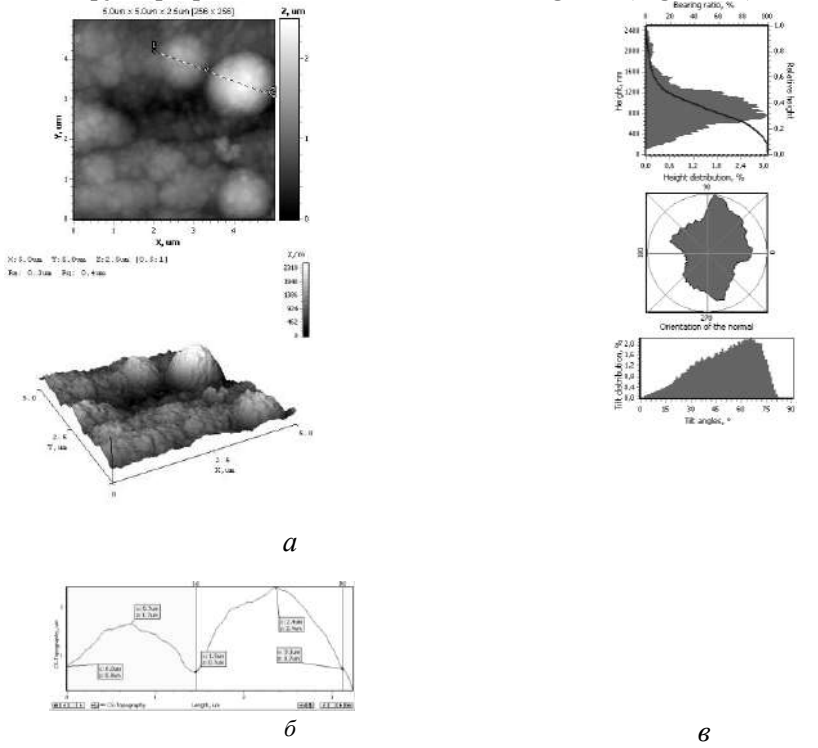

а

б

в

Figure 5.8 - 2D-, 3D-map of the surface (a), the profile of the section between markers 1 and 2 (b) and the histogram of the distribution of heights, inclination angles of elementary surface sections and orientation angles (c) of the CEC based on Co65Mo31Zr4. Scanning area 5 × 5 μm.

The results of contact force microscopy studies of the composite coatings' surface topography with the ratio of alloy-forming metals (mass%) Co91W7Zr2 deposited using a stationary current (Fig. 5.9, 5.10), and Co86W13Zr1 deposited by a pulsed current (Fig. 5.11, 5.12), are in good agreement with the results of scanning electron microscopy (Fig. 4.31). Both methods show that the surface of

coatings formed by unipolar pulsed current (Figs. 5.11, 5.12) is more uniformly developed in comparison with those deposited on direct current (Figs. 5.9, 5.10) [189].

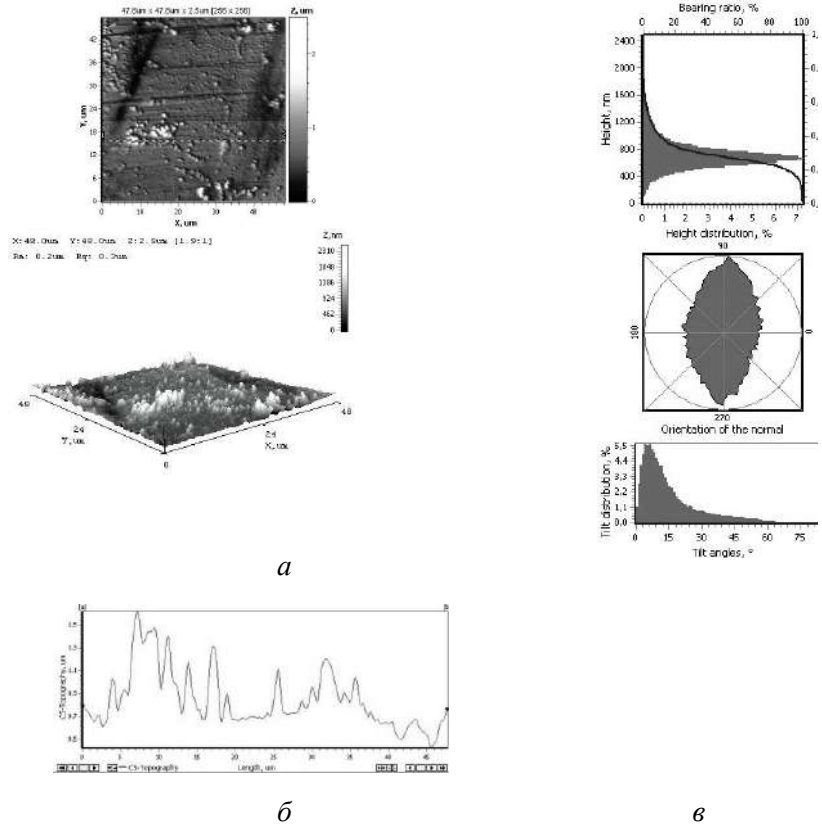

а *б* *в*

Figure 5.9 - 2D-, 3D-map of the surface (a), the profile of the section between markers 1 and 2 (b) and the histogram of the distribution of heights, inclination angles of elementary surface sections and orientation angles (c) of the CEC based on Co91W7Zr$_2$. Scanning area 48 × 48 μm.

The morphology and surface relief of the Co-W-ZrO_2 coatings are similar to those of Co-Mo-ZrO_2 (Fig. 5.7, 5.8). At the same time, it should be noted a decrease in the tungsten content in alloys obtained under the same electrolysis conditions in comparison with the Co-Mo-WOx coatings (Fig. 5.3), as well as a decrease in the percentage of zirconium content in the Co-Mo-ZrO_2 coating (Fig. 5.7).

A decrease in the size of associates (agglomerates) and the absence of cracks in the CEC can be associated with the effect of tungsten on the electrocrystallization process.

The surface relief of the Co-W-ZrO_2 coatings deposited in the galvanostatic mode differs from the substrate regardless of the scanning area, and is more ordered and uniform. On the surface, stand-alone cone-shaped agglomerates with a size of 1 - 4 microns (Fig. 5.9, b) are determined, which are formed by a number of smaller and sharper grains with an average size of 150 - 500 nm (Fig. 5.10, b). It should be noted that such a globular structure is due to the inclusion of refractory metals in the composition of the obtained coatings.

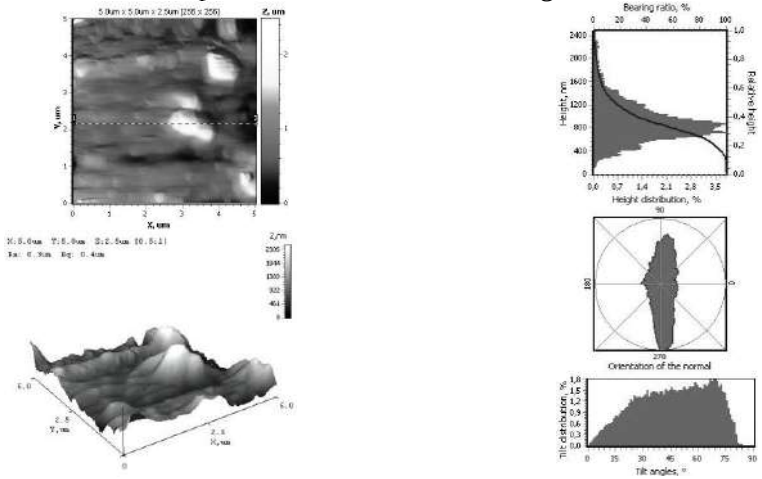

а

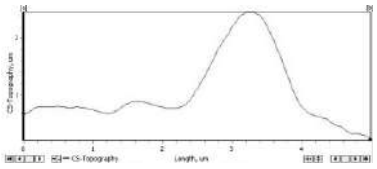

б *в*

Figure 5.10 - 2D-, 3D-map of the surface (a), the profile of the section between markers 1 and 2 (b) and the histogram of the distribution of heights, inclination angles of elementary surface sections and orientation angles (c) of the CEC based on Co91W7Zr_2. Scanning area 5 × 5 μm.

The histograms of heights' distribution, the orientation of the normal and distribution of normal slope to the surface make it possible to estimate the size and geometry of grains and agglomerates over the entire scanning field of the sample. The results of the analysis indicate that for coatings deposited by stationary electrolysis, sharp protrusions of various heights prevail, the distribution of grains over the surface is uniform, however, the histogram of the distribution of inclination angles of grains that have angles with a large slope are absent (Fig. 5.9, c; 5.10, c) indicates rather sharp differences between the heights.

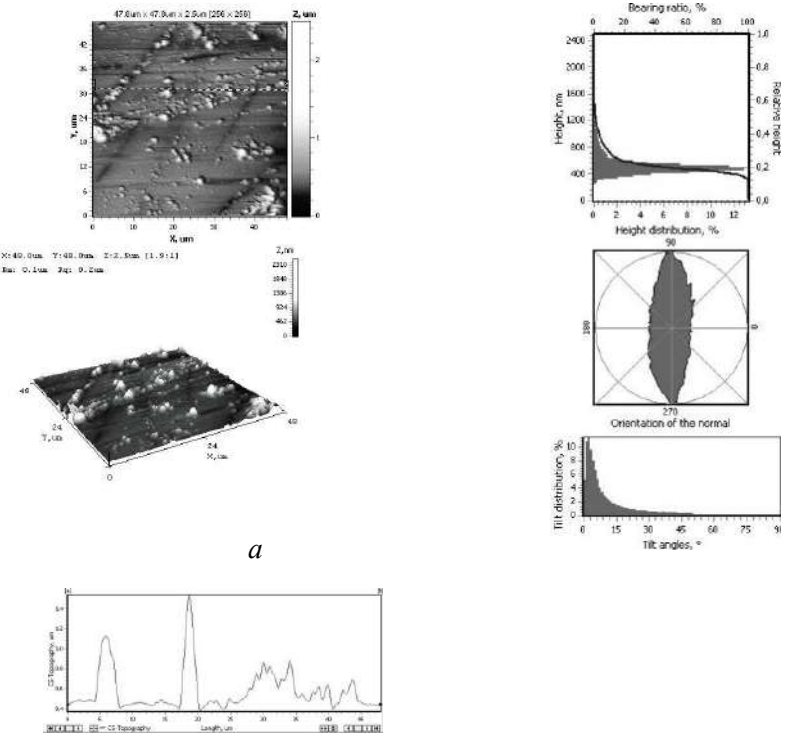

а

б *в*

Figure 5.11 - 2D-, 3D-map of the surface (a), the profile of the section between markers 1 and 2 (b) and the histogram of the distribution of heights, inclination angles of elementary surface sections and orientation angles (c) CEC based on Co8613Zr1. Scanning area 48 × 48 μm.

The use of a pulsed electrolysis mode contributes to the enrichment of the coatings with tungsten, however, the zirconium content is reduced to 0.5 mass% (Fig. 5.11). The transition to the nanorelief (scanning area 5 × 5 μm) makes it possible to analyze the surface of detached agglomerates, on which a small substructure is visualized, in shape and size similar to the grains of the main surface layer (Fig. 5.12). However, regardless of the scanned area, these indicators are higher compared to the substrate material, which indicates the development of the surface.

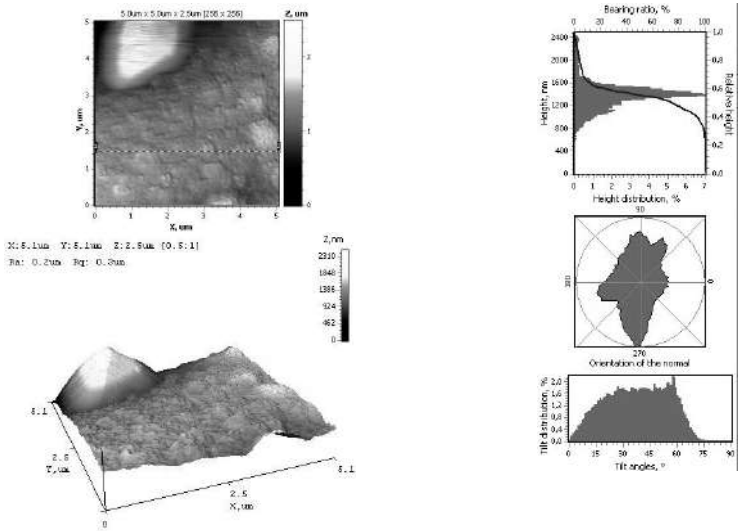

а

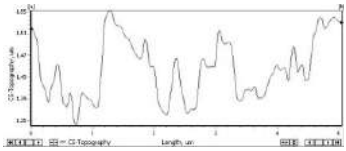

б *в*

Figure 5.12 - 2D-, 3D-map of the surface (a), the profile of the section between markers 1 and 2 (b) and the histogram of the distribution of heights, inclination angles of elementary surface sections and orientation angles (c) of the CEC based on Co86W13Zr1. Scanning area 5 × 5 μm.

The results obtained confirm the fact that the surface characteristics change with a change in the scanning scale, which was established as a result of studies of films and coatings' surface obtained under various conditions [190].

Surface roughness characteristics of composite coatings based on cobalt alloys, obtained using atomic force microscopy in accordance with GOST 2409-94, are presented in Table 5.1.

Table 5.1

Indicators of surface roughness of materials with various nature

Coating composition, mass. %	Roughness parameters					
	Scanning area, μm	*Ra*, μm	*Rq*, μm	R_{max}, μm	*Rsk*	*Rku*
Steel St3	48x48	155	228	240	0,8	7,0
	10x10	188	253	70	0,6	4,3
Co60Mo23W17	48x48	99	110	150	0,01	3,0
	5x5	8	9	30	0,13	2,9
Co62Mo33Zr5	48x48	164	268	2500	2,6	10,9
	5x5	369	479	1100	0,9	3,6
Co65Mo31Zr4	48x48	76	120	450	4,4	49,5
	5x5	39	57	170	1,3	5,5
Co91W7Zr2	48x48	170	254	600	1,8	9,4
	5x5	280	379	600	1,2	5,0
Co86W13Zr1	48x48	114	189	1500	3,3	20,5
	5x5	190	292	290	0,5	6,3

The results obtained show that an increase in the content of zirconium in the composition of alloys causes an increase in the surface roughness of coatings (Ra) by 1.4-2.1 times, which is associated with the inclusion of Zr oxides in the composition of the coating. An increase in the tungsten content in the CEC composition, on the contrary, contributes to a decrease in the arithmetic mean roughness. Thus, the surface relief is smoothed due to the embedding of tungsten and its oxides into the depressions of the surface layer of the coating. However, Co65Mo31Zr4 coatings have the most uniform surface. The use of pulsed electrolysis, along with an increase in the current density, reduces the surface roughness parameters of cobalt-based composite alloys.

The parameter (Rq) is more sensitive to extreme values of surface irregularities than (Ra), which makes it possible to define Co60Mo23W17 coatings as CEC with the most uniform structure, which is confirmed by the surface topography (Fig. 5.3b, 5.4b). The Rq parameter for most surfaces of the investigated CECs based on alloys exceeds the Ra index by 1.4-1.7 times, however, for Co60Mo23W17 coatings, this value does not exceed 1.1 for all scan areas.

The value of the Rsk parameter for Gaussian surfaces, which are Co-Mo-WOx alloy coatings, approaches 0, and the value itself describes the shape of the probability distribution function that the profile corresponds to the height Z. In profiles with a positive asymmetry coefficient, microroughnesses with clear high peaks dominate, which are different from the average. All other investigated coatings based on cobalt alloys have a value of Rsk ≥1.5, which indicates that the surface has a complex shape and usual parameters (Ra and Rq).

Another important characteristic of surface roughness is Rku, which is a measure of the height distribution over the surface. So the coatings Co-Mo-ZrO2, Co-W-ZrO2, as well as the lining St3 have Rku> 3, which indicates that the surface has a wide and low peak of the distribution function of irregularities. For Co-Mo-WOx coatings, the Rku index is ~ 3, which corresponds to a Gaussian surface; therefore, we can safely assert that the sample surface is leveling due to the formation of a coating.

Based on the studies of the features of the topography of the coating surfaces based on the KEP Co-Mo-WOx, Co-Mo-ZrO_2, and Co-W-ZrO_2 alloys, one can classify roughness as 9-11 class [191].

However, the topography and the degree of surface development of all the above coatings, as was shown earlier [192, 193], are favorable for catalytic processes that pass through the stage of adsorption and are also realized in a diffusion mode.

4.2 X-ray phase analysis of electrochemical systems

Along with the formation of a developed globular surface, the phase composition of coatings can be an important factor affecting their properties, in particular, catalytic activity, since it determines the distribution of active acCECtor centers over the surface.

It is known that electrolytic alloys in their physicochemical properties may differ from those obtained by the metallurgical method. In terms of phase structure, they do not correspond to the equilibrium diagrams of thermal alloys. The conditions of electrodeposition and the composition of electrolytes are the determining factors in the formation of a certain structure of electrolytic deposits [194].

To establish the phase composition, we compared the X-ray diffractograms of Co-Mo-WOx CECs deposited on a copper substrate by a pulse current with an amplitude of 8 A / dm2 at a ratio tp / tp = 2/10 ms (Fig. 5.13, 1) and a direct current with a density of 4 A / dm2 (Figure 5.13, 2).

In the diffraction spectra, the high intensity peaks at angles of 60º and 90º correspond to a copper substrate. In addition, replicas corresponding to the α-Co phase of intermetallic compounds Co7W6 and Co7Mo6 were revealed, and a rather wide halo of about 15º at 2θ angles of 43-58º (Fig. 5.13), which reflects the amorphous structure of the coatings. The most important fact is the appearance of reflections of metallic molybdenum and tungsten on the X-ray diffraction patterns of the CEC based on the Co-Mo-WOx alloy deposited by a pulsed current. Metallic Mo and W are formed in accordance with the mechanism proposed in [264] during the reduction of intermediate oxides of refractory metals by ad atoms of hydrogen upon interruption of the polarization current. The sizes of the coherent scattering zones of the amorphous part of the alloy are 2–8 nm [195].

X-ray diffractograms (Fig. 5.14) demonstrate the difference in the phase composition of electrolytic coatings Co-Mo-ZrO_2 obtained by pulsed current of various amplitudes of 6 A / dm^2 (Fig. 5.14, 1) and 4 A / dm2 (Fig. 5.14, 2).

The figure shows the α-Co lines, intense reflections at the angles of 52º, 60º and 90º correspond to the copper base. In addition, lines of intermetallic compounds Co3Mo, Co7Mo6 and a small halo 10 ° wide at angles 2θ 48-58 ° were found, which reflects the amorphous structure of the materials. The absence of lines corresponding to zirconium or its intermetallic compounds is explained by the low content of this metal. The most significant result should be considered the presence of metallic molybdenum in coatings

deposited with a pulsed current of 4 A / dm^2. In addition, the high intensity of the lines of intermetallic compounds of this sample is due to the enrichment of the alloy with a high-temperature component. The dimensions of the coherent scattering zones of the amorphous part of the alloy are 2–6 nm [196].

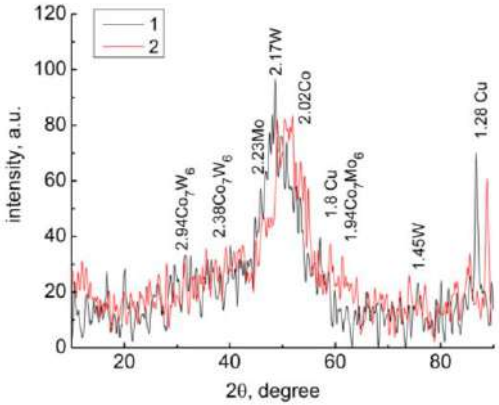

Figure 5.13 - X-ray diffractograms of the CEC Co-Mo-WOx: 1 - 8 A / dm^2; ti = 2 ms, tp = 10 ms, 2 - 4 A / dm^2.

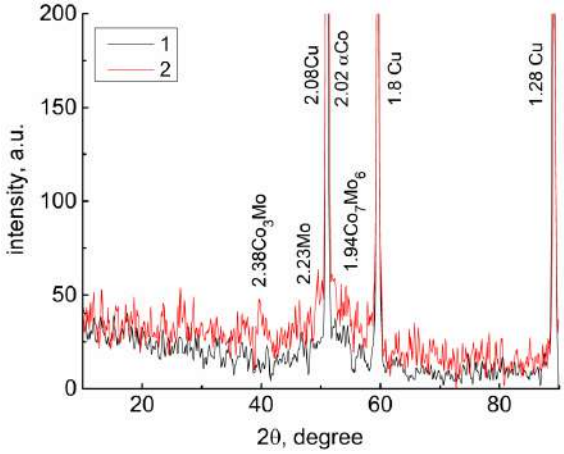

Figure 5.14 - X-ray diffractograms of the CEC Co-Mo-ZrO2: 1 - 6 A / dm2; 2 - 4 A / dm2 ti = 2 ms, tp = 10 ms.

X-ray diffraction patterns of Co-W-ZrO_2 CECs obtained by pulsed currents of various amplitudes differ from Co-Mo-WOx and Co-Mo-ZrO_2 by a high content of intermetallic compounds and the absence of metallic phases of tungsten or molybdenum (Fig. 5.15).

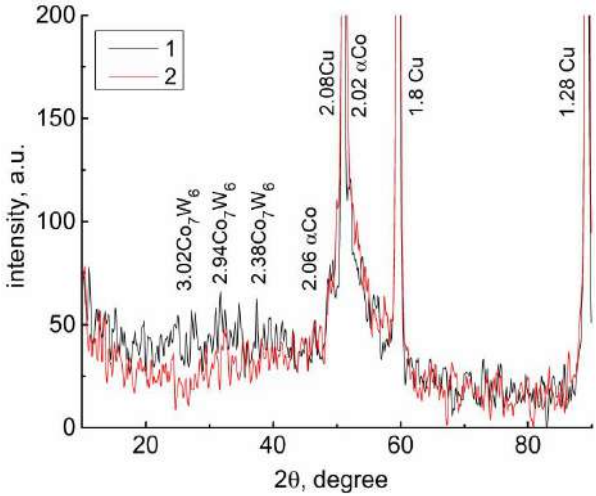

Figure 5.15 - X-ray diffractograms of the CEC Co-W-ZrO2:
1 - 6 A / dm2; 2 - 4 A / dm2 ti = 2 ms, tp = 10 ms.

The intensity of the lines of the Co7W6 intermetallic compounds increases with the tungsten content, and a rather wide halo at 2θ angles of 48-65º confirms the presence of an X-ray amorphous structure. The sizes of the coherent scattering zones of the amorphous part of the alloy are smaller in comparison with those considered above and amount to 2–5 nm.

Thus, the analysis of diffractograms of composite coatings based on Co-Mo-WOx alloys indicates an amorphous-crystalline structure, and for Co-W-ZrO_2 and Co-Mo-ZrO_2 - the presence of a sufficiently large amount of α-Co. The difference in the morphology and structure of the surface, as well as the phase composition of electrolytic alloys, affects their electrochemical behavior, namely, corrosion resistance and catalytic activity in electrode reactions.

4.3 Physical, mechanical and corrosive properties

It is known that the mechanical properties of thin-layer systems, as well as internal stresses in coatings, are determined, among other things, by the macrostructure of the latter. By varying the electrolysis conditions, it is possible to form materials with different degrees of structure dispersion and, consequently, properties. The crystal structure of galvanic systems depends on two processes: nucleation of crystallization centers at the cathode and subsequent crystal growth, as well as the ratio of the rates of these processes.

The microhardness of the studied materials Co-Mo-WOx, Co-Mo-ZrO_2 and Co-W-ZrO2, as well as the substrate material (st. 3) was determined by the method of indentation of a diamond pyramid on a PMT-3 hardness tester at a load of P = 0.02 - 0, 2 kg and a holding time of 10 s. The experiment was carried out after 24 hours aging of the obtained coatings at room temperature. The CEC thickness for analysis was no less than 30 μm. The measurements were carried out at least at 3 points with subsequent averaging of the data; the confidence interval was ± 10.

It was found that the content of refractory metals does not significantly affect the microhardness of cobalt coatings with such metals [197]; however, such a dependence on the conditions of electrodeposition was revealed [198]. The specific features of the formation of the structure of the coatings directly affect the morphology of the surface formed during deposition, with the most pronounced effect of the cathodic current density [199]. So with an increase in the current density, the rate of nucleation of crystallization centers increases faster than the rate of crystal growth, therefore, the grain size decreases, and the coatings become fine-grained (Fig. 4.6, 4.19, 4.31) or even acquire an amorphous structure.

The dependence of the microhardness Hv of the CEC Co-Mo-WOx, Co-Mo-ZrO2 and Co-W-ZrO2 on the cathode current density is extreme (Fig.5.16): in the range from 2 to 8 A / dm^2 Hv increases with increasing and reaches maximum Hv = 1100 kg / mm^2 for ECC Co-Mo-WOx, Hv = 490 kg / mm^2 for ECC Co-Mo-ZrO2 i Hv = 220 kg / mm2 for ECC Co-W-ZrO^2.

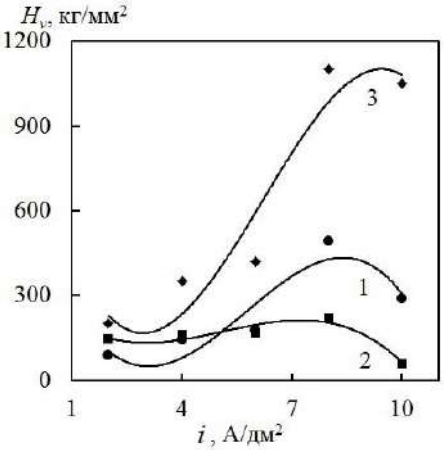

Figure 5.16 - Influence of current density on microhardness of CEC Co-Mo-ZrO_2 (1), Co-W-ZrO_2 (2) and Co-Mo-WO_x (3). Impulse electrolysis mode: t_i=5·10^{-3} s, $t_п$=1·10^{-2} s. pH=8

This is due to a decrease in the size of grains and conglomerates on the surface of the coatings. In addition, small values of the current density contribute to a more uniform distribution of the coating over the surface of the substrate due to the low crystallization rate. At i = 10 A / dm^2, the microhardness of the CEC based on cobalt alloys decreases, and for zirconium-containing coatings this dependence is sharper (Hv = 51 kg / mm^2) due to the formation of loose cracking layers on the surface, which clearly contain cobalt hydroxides. This assumption is confirmed by the results of micro-X-ray spectral analysis.

It is known from practice that the acidity of the electrolyte significantly affects the productivity of the electrodeposition process - the current efficiency, the quality of the coating, and, consequently, their physical and mechanical properties. Even a slight change in the pH of the electrolyte can lead to disruption of the electrolysis process and the deposition of poor-quality coatings.

For pyrophosphate-citrate electrolytes used in this study for the deposition of CEC Co-Mo-WOx, Co-Mo-ZrO2, Co-W-ZrO_2, it is characteristic that the degree of protonation of ligands (citrate and pyrophosphate) decreases with increasing pH. Accordingly, the complex compounds of cobalt in the electrolyte will be strengthened,

and the potential for its reduction shifts to the negative side and approaches the reduction potentials of tungstates (molybdates) and zirconium [199].

However, it is necessary to pay attention to the fact that with the transition to an alkaline medium, the danger of the formation of cobalt hydroxides in the electrolyte increases, which leads to their undesirable inclusion in the coating composition. In parallel with the metal reduction reaction, the hydrogen evolution reaction proceeds, which significantly affects the alloy formation process as a whole.

On the basis of the studies carried out, it was found that the optimal range for the formation of CEC with cobalt alloys is the pH range = 8-9 [200]. Moreover, at pH more than 9, the current efficiency of the CEC of cobalt-based alloys decreases sharply, and after reaching pH 10, an insoluble precipitate is formed in the electrolyte and the near-electrode layer. The result of this process is the formation of hydroxo salts and cobalt hydroxides, and, as a consequence, the quality of the coatings deteriorates, and, consequently, a decrease in their microhardness (Fig. 5.17).

The effect of temperature on the formation of electroplated coatings is not unambiguous. On the one hand, as the temperature rises, the diffusion of ions accelerates, which makes it possible to increase the current density at which the process of dendrite formation and the formation of spongy sediments has not yet begun. On the other hand, an increase in the electrolyte temperature leads to an increase in the crystal growth rate, which causes the formation of a coarse-grained structure.

At temperatures $T \leq 50$ ° C, the influence of the first of the factors considered prevails, as a result of which the quality of the coatings improves, and, accordingly, their microhardness increases, especially for Co-Mo-ZrO_2 and Co-W-ZrO_2 coatings (Fig. 5.18). It should be noted that the microhardness Hv of the Co-W-ZrO_2 CEC quite naturally depends on the tungsten content, which was noted in [200]. It is not advisable to establish the effect of temperature on the microhardness of the Co-Mo-WOx CEC, since high-quality coatings in the galvanostatic mode can be deposited only at elevated temperatures ($T \geq 40$ ° C).

Thus, for the formation of CEC Co-Mo-WOx, Co-Mo-ZrO2, Co-W-ZrO2 with high microhardness, it is necessary to carry out electrolysis at an elevated electrolyte temperature and current density of ~ 8 A / dm^2.

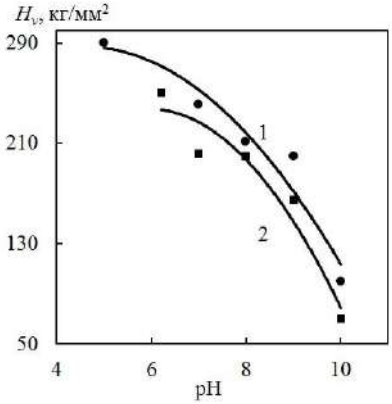

Figure 5.17 - Influence of the acidity of the electrolyte solution on the microhardness of the CEC Co-Mo-ZrO_2 (1) and Co-W-ZrO_2 (2). Pulse electrolysis mode: i = 8 A / dm^2, t_i = 5 ms, t_p = 10 ms. Temperature T = 25 ° C.

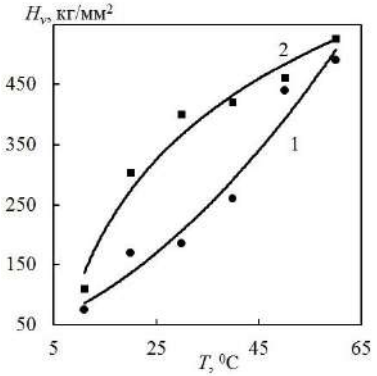

Figure 5.18 - Influence of temperature on microhardness (a) ECC of alloys Co-Mo-ZrO_2 (1) and Co-W-ZrO_2 (2). Pulse electrolysis mode: i = 8 A / dm^2, t_i=5·10^{-3} s, t_p=1·10^{-2} s. pH=7

Corrosion resistance of coatings

The determination of the corrosion resistance of the synthesized materials was carried out by the method of polarization resistance by recording anodic and cathodic voltammograms [200]. Corrosion current density Icor was determined by extrapolation at the point of intersection of linear sections of partial anodic and cathodic

polarization dependences near the corrosion potential Ecor (sections up to 50 mV) in Tafel coordinates lg$i$ – ΔE

From the known values of the corrosion current, the depth index of the corrosion rate k_h was calculated using the equation:

$$k_h = \frac{8{,}76 \cdot k_{\text{кп}} \cdot i_{\text{кор}}}{\rho_{\text{сп}}} \quad (2.29)$$

where k_{cc} - electrochemical equivalent of metal or composite coating, kg / C;

i_{cor} is the corrosion current density, A / m^2;

ρ_{cc} is the density of the composite coating, kg / m^3.

The results of corrosion tests were verified by electrode impedance spectroscopy (ESI) [201] in a 2% NaCl medium. SEI was recorded in a two-electrode cell on electrodes of the same composition with an area of 1 cm2, planar located at a distance of 1 cm from each other. For measurements, we used an Autolab-30 electrochemical module, model PGSTAT301N Metrohm Autolab, equipped with an FRA-2 (Frequency Response Analyzer) module in the frequency range 10^{-2} - 10^6 Hz. The module was controlled using the Autolab 4.9 program according to the standard procedure with subsequent processing of the data set in the ZView 2.0 package. Modeling of the structure and state of the phase boundary was carried out by the method of equivalent circuits. Parameters with an equivalent circuit modeling error of no more than 10% are acCECted for consideration. The measurements were carried out at a temperature of 18 ± 1 °C.

Along with the formation of a developed globular surface, the phase composition of coatings is an important factor affecting their properties and, in particular, corrosion resistance. A preliminary assessment of the influence of the chemical composition of the Co-Mo-WO_x, Co-Mo-ZrO_2, Co-W-ZrO_2 CECs on their corrosion behavior indicates that the stationary potential (corrosion potential) significantly depends on both the composition and morphology of the coating and the acidity of corrosive environment. It should be noted that the corrosion of all the investigated CECs based on cobalt alloys proceeds with oxygen depolarization, regardless of the acidity of the solution.

Corrosion behavior of Co-Mo-WOx, Co-Mo-ZrO2, Co-W-ZrO2 coatings with a wide range of alloy-forming metals in media of different acidity against the background of 1M sodium sulfate [202] was evaluated by recording and further analysis of cathodic and anodic polarization dependencies (fig. 5.19-5.21). The depth index of the corrosion rate k_h was calculated from the values of the polarization resistance.

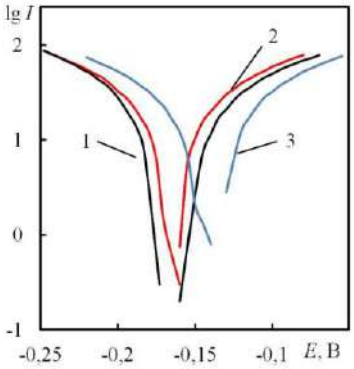

Figure 5.19 – Polarization dependences of CEC
Co-Mo-WO_x (1), Co-W-ZrO_2 (2), Co-Mo-ZrO_2 (3) in acidic medium (pH=3)

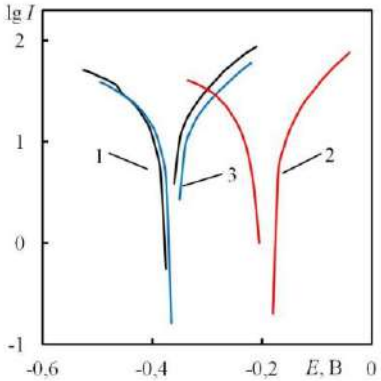

Figure 5.20 – Polarization dependences of CEC
Co-Mo-WO_x (1), Co-W-ZrO_2 (2), Co-Mo-ZrO_2 (3) in neutral medium (pH=6,5)

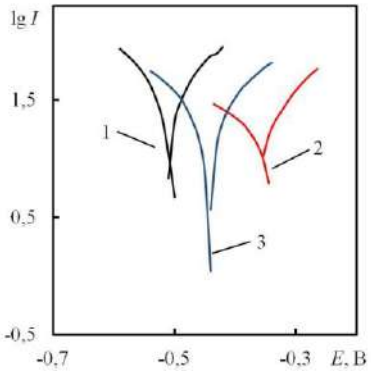

Figure 5.21 - Polarization dependences of CEC
Co-Mo-WO_x (1), Co-W-ZrO_2 (2), Co-Mo-ZrO_2 (3) in alkaline medium
(pH = 10.5)

Analysis of the results shows that a significant difference in stationary electrode potentials for each group of CECs is observed when the composition of the model medium changes. The dependence on the pH of solutions is especially pronounced, which additionally makes it possible to position the obtained materials as type II metal oxide electrodes. That is why it is impossible to compare the corrosion resistance of the metal components of the CEC by the values of the potentials, which were measured under different conditions.

It is expected that the most positive are the corrosion potentials (Table 5.2) of the studied CEC samples in media with a minimum pH, and the most negative — in an alkaline solution. This is due to the fact that, in terms of their chemical properties, tungsten and molybdenum are capable, in the presence of an oxidizing agent, of forming acidic oxides that are stable in acidic media.

In a neutral environment in the presence of chloride ions, a local corrosion process occurs, which is accompanied by alkalization of the surface layer of the electrolyte due to the conjugate reaction of oxygen reduction and destruction of the protective layer of refractory metal oxides. At the same time, in an alkaline environment, cobalt is able to passivate to form oxides or hydroxides, which are chemically stable at high pH values.

The values of corrosion resistance Rp of composite coatings based on cobalt alloys were calculated. The smallest Rp value, which is 590 Ohm, was obtained for Co83W16Zr1 coating in an acidic medium, while in neutral and alkaline media, Rp increases by 5-10 times, depending on the CEC composition. The highest corrosion resistance is inherent in the Co91W7Zr2 CEC in a neutral environment.

Table 5.2

Corrosion properties of CEC Co-Mo-WO_x, Co-Mo-ZrO_2, Co-W-ZrO_2

The composition of the covers, % масс.	pH 3		pH 6,5		pH 10,5	
	E_{cor}, В	k_h, мм/year	E_{cor}, В	k_h, мм/year	E_{cor}, В	k_h, мм/year
Steel	–0,34	$1{,}4\cdot10^{-2}$	-0,35	$9\cdot10^{-3}$	-0,32	$1{,}3\cdot10^{-2}$
Co71Mo20W9	–0,26	$3{,}05\cdot10^{-4}$	–0,36	$1{,}53\cdot10^{-4}$	–0,49	$3{,}2\cdot10^{-4}$
Co82Mo15W3	–0,33	$2{,}9\cdot10^{-4}$	–0,37	$2{,}1\cdot10^{-4}$	–0,39	$3{,}2\cdot10^{-4}$
Co83Mo14Zr3	–0,21	$2{,}7\cdot10^{-4}$	–0,29	$0{,}95\cdot10^{-4}$	–0,35	$1{,}5\cdot10^{-4}$
Co81Mo18Zr1	–0,13	$2{,}8\cdot10^{-4}$	–0,36	$1{,}65\cdot10^{-4}$	–0,44	$3{,}12\cdot10^{-4}$
Co64Mo33Zr3	–0,42	$1{,}3\cdot10^{-4}$	–0,36	$3{,}0\cdot10^{-3}$	–0,45	$1{,}6\cdot10^{-3}$
Co91W7Zr2	–0,27	$3{,}8\cdot10^{-4}$	–0,29	$0{,}15\cdot10^{-4}$	–0,44	$1{,}7\cdot10^{-4}$
Co83W16Zr1	–0,26	$6{,}1\cdot10^{-4}$	–0,33	$1{,}56\cdot10^{-4}$	–0,45	$1{,}8\cdot10^{-4}$
Co85W14Zr1	–0,18	$3{,}3\cdot10^{-4}$	–0,19	$1{,}69\cdot10^{-4}$	–0,35	$2{,}4\cdot10^{-4}$

The corrosion potential of samples with a composite coating Co-Mo-WOx in all model media shifts in the negative direction with an increase in the percentage of Mo from 10.4 to 29.5 wt.% And a constant total content of refractory components [203]. At the same time, the depth index of the corrosion rate decreases.

Analysis of the behavior of zirconium-containing CECs indicates that the content of zirconium practically does not affect the corrosion resistance of systems, which can be explained by its small amount. However, the corrosion resistance of samples with Co-Mo-ZrO_2 and Co-W-ZrO_2 coatings in alkaline and neutral media is higher than Co-Mo-WOx.

For the practice of corrosion protection, corrosion resistance under open circuit conditions is of particular interest. Long-term tests of CEC Co-Mo-WOx, Co-Mo-ZrO_2, Co-W-ZrO_2 deposited on steel substrates indicate that already on the 4th day there is a relative

stabilization of corrosion potentials in acidic, neutral and alkaline media (Fig.5.22 -5.24, a). The shift of the potential towards positive values can be explained by a gradual increase in porosity and destruction of the CEC (Figs. 5.22 -5.24, b) and the contribution of the substrate potential.

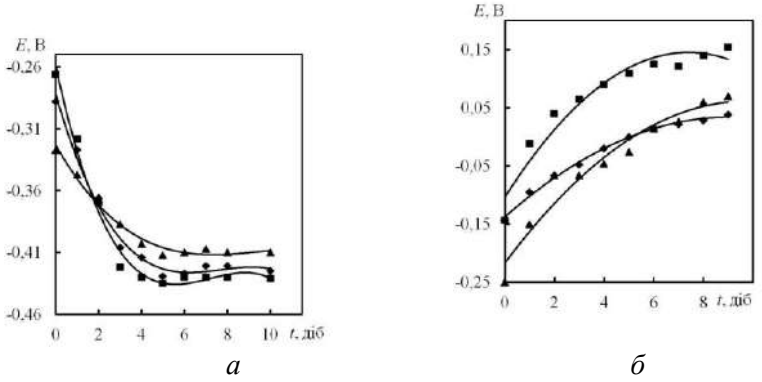

а *б*

Figure 5.22 - Chronopotentiograms of CEC Co-Mo-WO_x (♦), Co-Mo-ZrO_2 (■), Co-W-ZrO_2 (▲) on steel (a) and copper (b) at pH = 3

Comparative analysis of the corrosion resistance of Co-Mo-WOx, Co-Mo-ZrO_2, Co-W-ZrO_2, coatings deposited on various substrates of steel and copper indicates that their use as an anodic coating is impractical, since on the Co-Mo-WOx, Co-Mo-ZrO_2 microcracks are present (Fig. 5.21, 5.22), which accelerates corrosion processes.

The corrosive behavior of the studied CECs based on cobalt in an acidic medium is similar, which is explained by the rather high content of cobalt. In this case, one cannot neglect the contribution of refractory metals and their oxides to the inhibition of the corrosion process.

In a 3% NaCl solution, after 4 days, there is a slow decrease in the stationary potential (corrosion potential) (Fig.5.23), which is associated with the diffusion of chloride ions through protective films and accelerated corrosion, however, the Co-Mo-WOx CEC is characterized by the highest stability

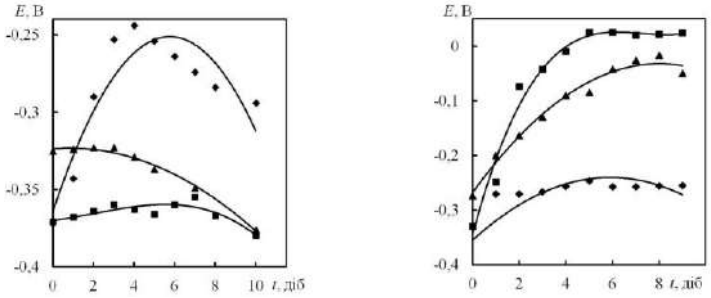

а *б*

Figure 5.23 - Chronopotentiograms of CEC Co-Mo-WO_x (♦), Co-Mo-ZrO_2 (■), Co-W-ZrO_2 (▲) on steel (a) and copper (b) at pH = 6.8

The corrosion behavior of CEC Co-Mo-WO_x, Co-Mo-ZrO_2, Co-W-ZrO_2 in an alkaline environment indicates that the coatings that contain ZrO_2 have a more positive corrosion potential compared to Co-Mo-WO_x (Fig. 5.24).

The corrosion behavior of CEC Co-Mo-WOx, Co-Mo-ZrO2, Co-W-ZrO2 in an alkaline environment indicates that coatings that contain ZrO2 have a more positive corrosion potential compared to Co-Mo-WOx (Fig. 5.24).

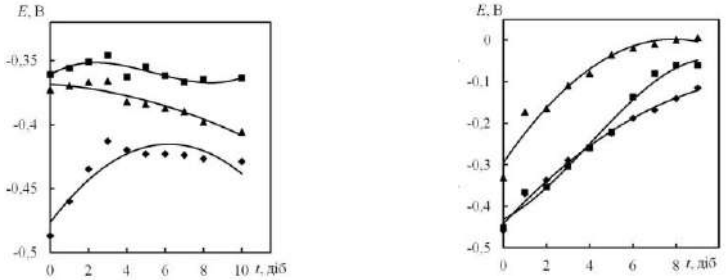

а *б*

Figure 5.24 - Chronopotentiograms of CEC Co-Mo-WO_x (♦), Co-Mo-ZrO_2 (■), Co-W-ZrO_2 (▲) on steel (a) and copper (b) at pH = 11

The electrode impedance (SEI) spectra of coated electrodes (Figs. 5.25, 5.26) in the Nyquist coordinates (Figs. 5.25 a, 5.26 a) and Bode (Figs. 5.25 b, 5.26 b) reflect the fact that the systems can be described by a modified equivalent Voight's scheme, which is characteristic of multiphase systems [275].

Such a circuit usually contains elements: R1 is the resistance of the electrolyte, L is the resistance of the inductor, CPE is the element of the constant phase (capacitance of the phase interface), Faraday resistance Rf. The CPE elements determine the fractality of the phases, and their inclusion in the antiphase indicates the limitation of the rate of charge transfer. The resistance of the L1 inductor is due to the occurrence of the galvanomagnetic Hall effect in the high-frequency region, which is characteristic of metals that form hydrated oxide films of variable valence on the surface. The occurrence of the galvanomagnetic effect is confirmed by the transition of the phase angle toward the positive values in the Bode diagrams.

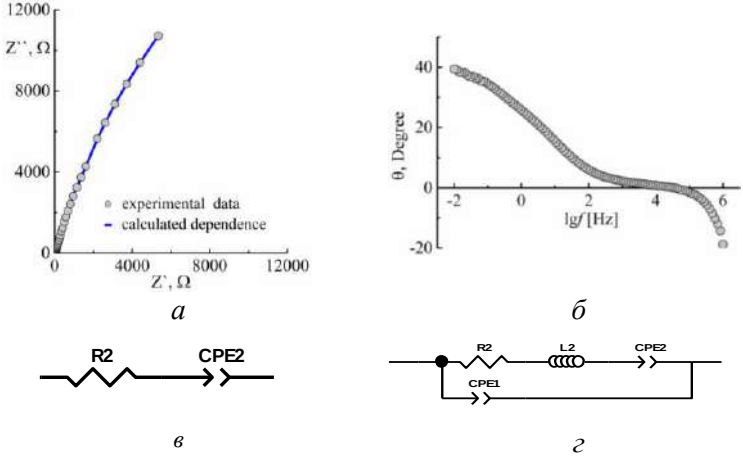

Figure 5.25 - Electrochemical impedance spectra in Nyquist (a) and Bode coordinates (b) and equivalent low (c) and high (d) frequency substitution scheme for the Co-Mo-WO_x electrode

At low frequencies of 10^{-2}-10^{2} Hz, the equivalent circuit of electrodes with Co-Mo-WOx coating includes two elements - the Faraday resistance R2 and the element of the constant phase CPE2 (Fig. 5.25, c), and the value of CPE2 is in the range of 0.46 ± 0.15, which corresponds to an average value of 0.5 and characterizes the diffusion in a thin layer. At medium and high frequencies of 102-106 Hz, additional elements appear: the inductance L2, which is associated with the presence of intrinsic magnetic properties of the sample and the second element CPE1, which characterizes the double layer at the electrolyte/coating interface (Fig. 5.25, d).

Thus, we can say that diffusion occurs in a thin surface layer, and the boundary between the film and the surface of the metal phase does not interfere with the flow of electric current, since the absolute values of the ohmic resistance vary in the range of 22–25 Ohms. At the same time, at the potential of free corrosion, the Faraday resistance of the system corresponds to a corrosion rate below 0.05 mm / year, which indicates the chemical resistance of the material.

The Co-Mo-ZrO_2 coated electrode is described by a more complex equivalent circuit (Fig. 5.26, c, d). In the low-frequency range, in addition to the resistance of the electrolyte R1 and the Faraday resistance R3, the circuit includes an open Warburg element W1 and an imperfect capacitor (Fig. 5.26, c), with CPE2 = 0.76 ± 0.7, which is characteristic of the capacitive behavior of the system diffusion. At high frequencies, the inductance L1 associated with the intrinsic magnetic properties of the material and the diffuse element of Warburg in the thin layer WS1 are included (Fig. 5.26, d).

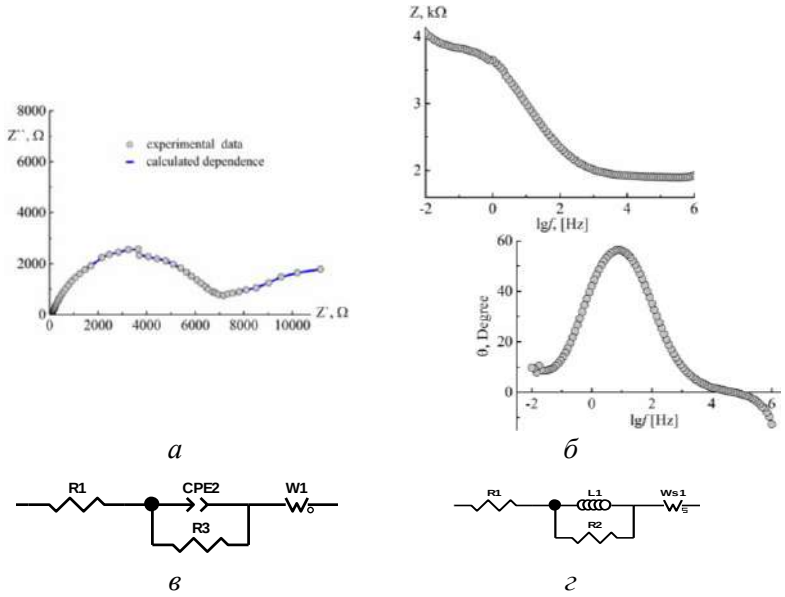

Figure 5.26 - Electrochemical impedance spectra in Nyquist (a) and Bode coordinates (b) and equivalent Co-Mo-ZrO_2 electrode circuit at low (c) and high (d) frequencies

Thus, at high frequencies, the imperfect capacitor exhibits its own self-induction, and diffusion is limited to a thin surface layer. The corrosion resistance of the electrode coated with Co-Mo-ZrO_2 is an order of magnitude higher than that of Co-Mo-WO_x, which provides a depth of less than 0.01 mm / year and allows to consider such a coating more stable in aggressive environments. Obviously, this is due to the inclusion of resistive and stoichiometric zirconium oxides in the composition of the surface layers.

The good coincidence of the experimental data (points on SEI Figs. 5.25, 5.26, a, b) and the calculated dependences (solid lines) testifies to the correctness of the approach to the assessment of the corrosion behavior of electrodes with CEC.

4.4 Catalytic properties of CEC

Catalytic properties of CEC in the electrochemical reaction of hydrogen evolution

The electrocatalytic properties of CECs and alloys of various compositions were evaluated according to the kinetic parameters of the model hydrogen evolution reaction, since these parameters are known for the most efficient catalysts (platinum) and individual metals [276]. The hydrogen exchange current density and the Tafel coefficients (a, b), which reflect the influence of the nature of the electrodes on the process kinetics, were determined on the basis of the analysis of polarization dependences (Figs. 5.27–5.29).

The hydrogen evolution reaction belongs to the number of multistage processes and depending on the conditions (medium, electrode material, temperature), can take place by various mechanisms. For example, at the mercury electrode the limiting stage is the discharge of hydroxonium ions with the formation of adsorbed hydrogen, which is further removed through a rapid stage of electrochemical desorption:

$$H_3O + + \bar{e} \leftrightarrow H_{ads} + H_2O, \quad (5.1)$$

$$H_3O + + H_{ads} + \bar{e} \leftrightarrow H_2 + H2O \quad (5.2)$$

In alkaline solutions, electrochemical desorption can occur with the participation of water molecules:

$$H_2O + \bar{e} \leftrightarrow H_{ads} + OH^- \quad (5.3)$$

$H_{ads} + H_2O + \bar{e} \leftrightarrow H_2 + OH^-$ (5.4)

Under certain conditions, the stage of electrochemical desorption may become slower than the stage of discharge and the release of hydrogen will occur by the mechanism of electrochemical desorption (Folmer-Geirowski mechanism). Possible mechanism of hydrogen evolution, in which the discharge stage is slow (5.1, 5.3) and the removal of adsorbed hydrogen occurs by recombination (Folmer-Tafel mechanism).

$2H_{ads} \leftrightarrow H_2$ (5.5)

In turn, when the conditions of hydrogen evolution change, the recombination stage (5.5) may act as a slow stage when the discharge stage (5.1) proceeds rapidly. For a certain range of electrode materials in some region of overvoltages, an adsorption-chemical mechanism is possible, the first stage of which is the adsorption of hydrogen molecules from solution on the electrode surface, followed by electrochemical desorption (5.2). In addition, the electrochemical stage can proceed with the simultaneous transfer of two electrons:

$H_3O^+_{(surf)} + 2\bar{e} \leftrightarrow H_{2(surf)} + OH^-$ (5.6)

or

$2H_3O^+_{(surf)} + 2\bar{e} \leftrightarrow H_{2(surf)} + 2H_2O$ (5.7)

Stage electron transfer is also possible in accordance with the scheme:

$H_3O^+_{(surf)} + \bar{e} \leftrightarrow H_3O_{(surf)}$ (5.8)

$H_3O_{(surf)} + \bar{e} \leftrightarrow H_{2(surf)} + OH^-$ (5.9)

One or another hydrogen evolution mechanism depends on the overvoltage region and on the binding energy of the adsorbed hydrogen atom with the metal surface. A conclusion about the true nature of the process of cathodic hydrogen evolution can be made on the basis of a comparison of the kinetic regularities arising from the mechanism and analysis of experimental data.

An analysis of the results of studying hydrogen evolution on samples with synthesized ECCs showed that, in the investigated potential range, the cathode polarization dependences are linearized in Tafel coordinates. The electrocatalytic properties of CEC based on Co-Mo-WOx and Co-Mo-ZrO_2 alloys (Fig. 5.27, 5.28) differ from CEC Co-W-ZrO_2 (Fig. 5.29), which is especially noticeable in an alkaline medium

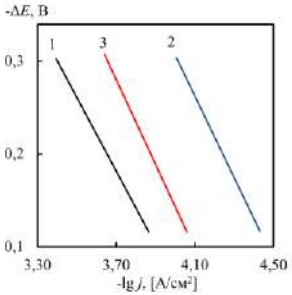

Figure 5.27 - Overvoltage of hydrogen evolution in acidic (1), neutral (2) and alkaline (3) media on a CEC of composition, mass %: Co71Mo20W9

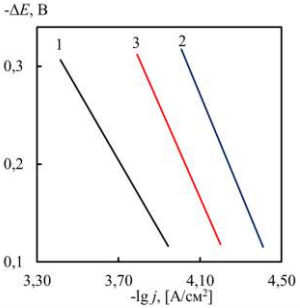

Figure 5.28 - Overvoltage of hydrogen evolution in acidic (1), neutral (2) and alkaline (3) media on a CEC of composition, mass %: Co80Mo19Zr1

Obviously, this behavior is explained by the more significant influence of molybdenum on the process of hydrogen evolution in an alkaline medium, since the content of molybdenum in the composition of these CEC is practically the same.

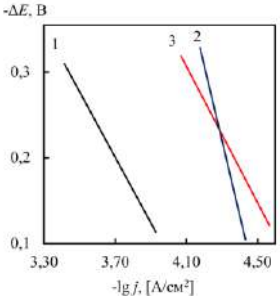

Figure 5.29 - Overvoltage of hydrogen evolution in acidic (1), neutral (2) and alkaline (3) media on a CEC composition, mass %: Co85W14Zr1

In addition, the composite coatings Co-Mo-WOx and Co-Mo-ZrO_2 have a more uniformly developed microglobular surface compared to the Co-W-ZrO_2 CEC.

The Tafel constant (bc), regardless of the acidity of the solution and the CEC composition, is 0.4-0.5 V (Table 5.3), which indicates a delayed stage of the discharge and removal of hydrogen atoms formed by recombination (Volmer-Tafel mechanism). This confirms the well-known fact that for metals of the iron subgroup, which have a high adsorption capacity with respect to hydrogen, the most likely to be the removal of hydrogen atoms by catalytic recombination.

The value of a varies within a wide range from 1.6 to 3.0, which is associated with the presence of metal oxides on the surface of the CEC and possibly, an insufficiently developed surface of the coatings.

Table 5.3

Electrocatalytic characteristics of various materials

Electrode material, metal content, mass %	Среда								
	acidic			neutral			alkaline		
	–a, В	*–b*, В	$\lg i_H^0$, [A/sm^2]	*–a*, В	*–b*, В	$\lg i_H^0$, [A/sm^2]	*–a*, В	*–b*, В	$\lg i_H^0$, [A/sm^2]
Pt100 [276]	0,1	0,03	–3,33	–	–	–	0,31	0,10	–3,10
Co100 [276]	0,62	0,14	–4,4	–	–	–	0,6	0,14	–4,3
Mo100 [276]	0,66	0,08	–8,2	–	–	–	0,67	0,14	–4,8
W100 [276]	0,43	0,1	–4,3	–	–	–	–	–	–
Co71Mo20W9	1,6	0,38	–4,0	1,9	0,46	–4,2	2,0	0,44	–4,1
Co85W14Zr1	1,6	0,39	–4,2	3,0	0,50	–4,5	1,9	0,39	–4,2
Co80Mo19Zr1	1,5	0,36	–4,2	2,3	0,50	–4,6	2,1	0,43	–4,2

Elementary Co, W and Mo are nanodispersed in nature and therefore interact more actively with adsorbed atomic hydrogen, which is continuously formed during electrolysis by the one-electron Volmer mechanism.

Atomic hydrogen, as follows from its standard electrode potential $E^0_{H^+/H}$ = –2,1065 V, has a high reactivity, which can lead to the formation of monohydrides CoH, WH and MoH by a chemical

mechanism, which causes a decrease in the overvoltage of hydrogen evolution on nickel and cobalt alloys [277].

For the entire pH range under study, the values of the hydrogen exchange current density for composite coatings Co-Mo-WOx, Co-Mo-ZrO_2 and Co-W-ZrO_2 are comparable and close to those of nanodispersed cobalt (Table 5.3). At the same time, CEC Co71Mo20W9 has the highest catalytic activity in an acidic environment, which exceeds the indices of alloy-forming metals.

The transfer coefficient (α) calculated from the results of experimental data for the reaction of hydrogen evolution at the CEC is in the range of 0.1-0.2, depending on the composition of the alloys and the acidity of the medium.

The reactions taking place on the CEC electrodes and cobalt alloys in acidic (5.10) and alkaline (5.11) media can be represented by the following schemes:

$Co_xM_yOx_z + sH_3O^+ + (n+m)\bar{e} \leftrightarrow Co_{x-n}M_{y-m}Ox_z + nCoH_{ads} + mMH_{ads} + (s-(n+m))H_2O,$ (5.10)

$Co_xM_yOx_z + sH_2O \leftrightarrow Co_{x-n}M_{y-m}Ox_z + nCoH_{ads} + mMH_{ads} + (s-(n+m))OH^-$ (5.11)

$Co_{x-n}M_{y-m}Ox_z + nCoH_{ads} + mMH_{ads} \leftrightarrow Co_xM_yOx_z + ((n+m)/2)\ H_2$ (5.12)

де M – Mo,W; Ox – tungsten or zirconium oxides.

An analysis of the experimental results shows that the hydrogen exchange current density on CEC and ternary cobalt alloys exceeds the indices of not only individual components, but also exceeds this parameter for binary alloys [278, 279]. This is due to the coprecipitation into the alloy of elements located on opposite sides of the trend line of the dependence of the hydrogen exchange current on the difference in the binding energy "metal - hydrogen" and "metal - oxygen", as well as the influence of the dimensional parameter and the nature of the surface relief of ternary alloys. In combination, this provides the formation of a synergistic system similar in properties to platinum and palladium.

Electro- and photocatalytic properties of CEC

The use of nanostructured thin-film materials based on catalytically active metals and oxides creates the prerequisites for an effective solution to the problems of water purification from organic

pollutants and infectious agents [204]. Redox reactions on the surface of the films contribute to the decomposition of pollutants to environmentally friendly components. Photocatalysis under the influence of visible and ultraviolet radiation acts as a stimulating factor in these processes [205]. Photocatalysis is usually described by the group model [206], in which two reactions occur simultaneously: oxidation with photogeneration of holes and reduction with photogeneration of electrons.

The increased activity of nanosized photocatalysts can be explained by the high degree of dispersion of materials, that is, the number of atoms on the surface or on the faces of crystals can be compared with the number of atoms located inside. In addition, as the particle size of semiconductor photocatalysts approaches to several nanometers, the electron wavelength becomes comparable to the crystal size. In this case, charge carriers are considered at the quantum-mechanical level, as particles in a box, the dimensions of which are determined by the dimensions of the crystal. Such nanosized particles of a solid in which quantum effects are manifested are called Q-particles.

The concentration of the azo dye methyl orange (MO) in the course of photocatalytic destruction was determined by measuring the optical density of a colored solution using a KFK-2 photoelectric colorimeter [207]. To convert polychromatic light into monochromatic, a blue light filter was used during measurements, which transmits light with a wavelength of $\lambda = 430 - 460$ nm and is maximally absorbed by the test solution. Optical density was determined in cells with a thickness of 5.060 mm [208].

Before testing the photocatalytic properties of composite coatings under the action of UV radiation, the dye solution in contact with the catalyst was kept in the dark for 30 min to establish adsorption equilibrium [209].

When the surface of the coatings is irradiated with ultraviolet light, the process of photoexcitation of the catalyst occurs due to the formation of electrons and holes, which either directly interact with dye molecules or initiate the formation of OH radicals with high reactivity. Thus, the process of destruction of MO occurs with intense decolorization of the solution.

It was found that composite coatings Co-Mo-WOx obtained by pulsed electrolysis from a citrate-pyrophosphate electrolyte have higher photoactivity compared to zirconium-containing composites obtained under the same conditions.

Based on the results of the study of photodegradation and MO (Fig.5.48, a), it was found that the efficiency of removing the azo dye methyl orange from the solution was 24%, 18% and 10% for 30 min of ultraviolet irradiation on the

Co-Mo-WO_x, Co-Mo-ZrO_2 CEC and Co-W-ZrO_2, respectively. To study the kinetics of MF photodegradation under the action of light in the presence of the obtained photocatalysts, the dependences $\ln(C/C_0) = f(t)$ were plotted. The slope of the linearized dependence (Figure 5.48, b) determines the rate constant k, which was $1{,}06 \cdot 10^{-2}$ min^{-1}, $0{,}80 \cdot 10^{-2}$ min^{-1} i $0{,}47 \cdot 10^{-2}$ min^{-1} for Co-Mo-WO_x, Co-Mo-ZrO_2 i Co-W-ZrO_2, respectively.

The higher photoactivity of the Co-Mo-WOx CEC can be explained by the presence of two non-stoichiometric oxides of molybdenum and tungsten, capable of forming mobile radical oxygen-containing particles under the influence of ultraviolet irradiation and a developed micro-globular surface.

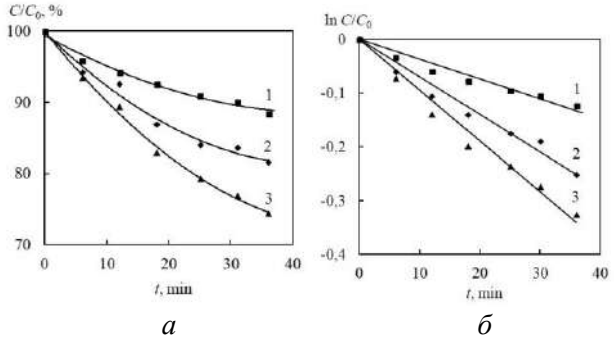

а *б*

Figure 5.48 - Chronograms of the concentration of the azo dye methyl orange from the time of exposure on the photocatalyst:
Co-W-ZrO_2 (1); Co-Mo-ZrO_2 (2); Co-Mo-WO_x (3)

CONCLUSIONS

Thus, it was established that the surface of the Co60Mo23W17 coatings consists of spherical grains and is characterized by a sufficiently high density, homogeneity and uniformity of the structure with a small number of high peaks up to 870 nm. With an increase in the current density on the surface of the coatings, a network of cracks is formed through an internal stress associated with a high deposition rate and a difference in the type and parameters of the crystal lattice of alloy-forming metals.

The results of studies of the surface topography of the Co-W-ZrO_2 CEC deposited using a stationary mode and a pulsed current show that the surface of coatings formed by a unipolar pulsed current is more uniformly developed as compared to those deposited at a constant current. The surface relief of the Co-W-ZrO_2 coatings deposited in the galvanostatic mode differs from the substrate and, regardless of the scanning area, is more ordered and uniform. On the surface, stand-alone cone-shaped agglomerates of 1 - 4 μm are visualized, formed by a number of small and sharp grains with an average size of 150 - 500 nm.

It was found that the electrodeposition current density and temperature affect the microhardness of the obtained cobalt-based systems. Systems containing both molybdenum and tungsten Co-Mo-WO_x exhibit high microhardness up to 1100 kg / mm2 in comparison with zirconium-containing Co-Mo-ZrO_2 and Co-W-ZrO_2, for which this indicator does not exceed 550 kg / mm^2.

A study of the corrosion resistance of samples with Co-Mo-WOx, Co-Mo-ZrO_2, Co-W-ZrO_2 coatings proved that the presence of molybdenum or tungsten increases the chemical resistance in comparison with the substrate material in all corrosive environments. According to the value of the depth index of corrosion, they can be assigned on a ten-point scale to be very stable.

The regularities of the cathodic hydrogen evolution on the CEC Co-Mo-WOx, Co-Mo-ZrO_2 and Co-W-ZrO_2 have been established. Based on the analysis of kinetic regularities, a mechanism of hydrogen evolution is proposed. The values of the exchange current

of the electrochemical reaction of hydrogen evolution from solutions of different acidity on the materials under study correlate with those for metals of the platinum family and exhibit high electrocatalytic activity in comparison with individual metals.

It was found that the coatings Co-Mo-WOx, Co-Mo-ZrO_2 and Co-W-ZrO_2 exhibit photocatalytic activity in the reaction of destruction of the azo dye under the action of UV irradiation. In this case, the Co-Mo-WOx systems have a higher catalytic activity in comparison with the Co-Mo-ZrO_2 and Co-W-ZrO_2 CEC, and can be compared with the conversion coatings of titanium oxides. The results obtained indicate the possibility of creating photocatalytic converters using mixed composite materials formed on metal carriers for purifying wastewater from organic aromatic compounds.

REFERENCES

1. Padgurskas J., Snitka V., Jankauskas V., Andriušis A. Ultrasonic actuators for nanometre positioning // Wear. – 2006. Vol. 17, № 7 - P. 260 - 652.
2. Ilie F. Tribotechnical materials science and tribotechnology // Tribology. – 2006. Vol. 6 - 39, 774 p.
3. Белая книга по нанотехнологиям / под ред. З.А. Мансурова, М.Т. Габдуллина, М.М. Муратова, М. Нажипкызы // Алматы: Қазақ университеті, 2021. - 338 с.
4. Vickerman J. C., Gilmore I. S. Surface Analysis: The Principal Techniques / Wiley, Chichester, 2009. - P. 423-428.
5. Мансуров З.А., Шабанова Т.А., Мофа Н.Н. Синтез и технологии наноструктурированных материалов. Алматы: Қазақ университеті, 2012 - 316 с.
6. Brunett D.M. Titanium in medicine : Material Science, Surface Science, Engineering, Biological Responces and Medical Applications (Engineering Materials) / D.M. Brunett, P. Tengvall, M. Textor, P. Thomsen. – Berlin; Heidelberg; New York: Springer – Verlag, 2001. – pp. 673 – 948.
7. Kasuga T. Apatite formation on TiO_2 in simulated body fluid / T. Kasuga, H. Kondo, M. Nodami // J. Cryst. Growth. – 2002. – Vol. 235. – pp. 235 – 240.
8. Белая книга по нанотехнологиям / под ред. З.А. Мансурова, М.Т. Габдуллина, М.М. Муратова, М. Нажипкызы // Алматы: Қазақ университеті, 2018. - 340 с.
9. Сарсенбинов Ш.Ш., Яр-Мухамедов Ш. Х., Яр-Мухамедова Г. Ш. Физические основы формирования структуры композиционных материалов с заданными свойствами Монография. Казахский национальный государственный университет им аль-Фараби, 2007.- 404 с.
10. Подчерняева И.А. Микроструктура излома лазерно-искрового покрытия на титане после абразивного изнашивания / И.А. Подчерняева, В.М. Панашенко, В.М. Верещака, Г.С. Олейник // Фізико-хімічна механіка матеріалів. – Львів : ФМІ. – 2009. – № 5. – С. 107 – 112.
11. Мансуров З.А., Дмитриев Т.П., Алиев Е.Т., Даулбаев Ч.Б. Аддитивные технологии (3D принтинг): моногр. Қазақ университеті. — ISBN: 978-601-04-3092-1. — 2017. — 192 с.
12. Суздалев, И.П. Нанотехнология. Физико-химия нанокластеров, наноструктур и наноматериалов: Учебное пособие для вузов / под ред. И.П. Суздалев. – Изд. 2-е, перер. и доп. - М.: КД Либроком, 2014. - 489 с.
13. Цао, Гочжун Наноструктуры и наноматериалы. Синтез, свойства и применение / Цао Гочжун, Ин Ван; Пер. с англ. А.И. Ефимова, С.И. Каргов , англ. - М.: Научный мир, 2012. - 520 с.
14. Нарівський О. Е. Корозійно-електрохімічна поведінка конструкційних матеріалів для пластинчастих теплообмінників у модельних оборотних водах: дис. … канд. техн. наук: 05.17.14 / Нарівський Олексій Едуардович. – Львів, 2009. – 209 с.

15. Narivs'kyi O.E. Micromechanism of corrosion fracture of the plates of heat exchangers // Materials Science. - 2007. – Vol. 43. № 1, – P. 124-132.

16. Narivs'kyi O.E. Corrosion fracture of platelike heat exchangers // Materials Science. – 2005. - Vol. 41. № 1, – P. 122-128.

17. Нарівський О. Е. Закономірності і механізми локальної корозії корозійнотривких сталей і сплаву аустенітного класу для ємнісної та теплообмінної апаратури : автореф. дис. ... д-ра техн. наук : 05.17.14 / О. Е. Нарівський; НАН України, Фіз.-мех. ін-т ім. Г.В. Карпенка. - Львів, 2015. - 42 с. - укр.

18. Pistorius P. C. Growth of corrosion pits on stainless steel in chloride solution containing dilute sulphate // Corrosion Science. – 1992. – Vol. 33. № 12, – P. 1885-1897.

19. Pistorius P. C. Aspects of the effects of electrolyte composition on the occurrence of metastable pitting on stainless steel // Corrosion Science. – 1992. – Vol. 36. № 3, – P. 525-538

20. Антонова О.С. Биомиметрическое нанесение наноструктурированных фосфатно-кальциевых покрытий на титан / О.С. Антонова, В.В. Смирнов, Л.И. Шворнева и др. // Перспективные материалы. – М. : ООО "Интерконтакт Наука" – 2007. – № 6. – С. 44 – 48.

21. Шевырев А.А. Нанесение сверхпроводящих ниобиевых покрытий на титан из расплава солей / А.А. Шевырев, В.Н. Колосов // Неорганические материалы. – М. : Наука. – 2011. – Т. 47, № 1. – С. 34 – 40.

22. Пат. 2251589 Российская федерация, МПК[7] C23C18/08, C23C28/02, C25D3/12, C25D5/14. Способ нанесения двухслойного износостойкого покрытия на титан и его сплавы / Каблов Е.Н., Жирнов А.Д., Ильин В.А. и др.; заявитель и патентообладатель ФГУП "ВНИИАМ". – 2003130783/02; заявл. 21.10.2003; опубл. 10.05.2005.

23. Пат. 2291918 Российская федерация, МПК C25D11/26, A61F2/02. Кальций-фосфатное покрытие на титане и титановых сплавах и способ его нанесения / Шашкина Г.А., Шаркеев Ю.П., Колобов Ю.Р., Карлов А.В.; заявитель и патентообладатель ИФПМ СО РАН. – 2005116663/02; заявл. 31.05.2005; опубл. 20.01.2007.

24. Sul Y. T. The electrochemical oxide growth behavior on titanium in acid and alkaline electrolytes / Y.T. Sul, C.B. Johansson, Y. Jeong, T. Albrektsson // Medical Engineering & Physics. – York : Elsevier. – 2001. – Vol. 23, no. 5. – pp. 329 – 346.

25. Ашуркевич К.В. Формирование и свойства фотокаталитически толстых пленок с диоксидом титана / К.В. Ашуркевич, И.А. Николаенко, В.Е. Борисенко // Доклады БГУИР.– Минск: БГУИР.– 2012.– № 6 (68). – С.1–6.

26. Справочник по анодированию / [под ред. Е.Е. Аверьянова]. – М.: Машиностроение, 1988. – 224 с.

27. Petukhov D.I. Formation mechanism and packing options in tubular anodic titania films / D.I. Petukhov, A.A. Eliseev, I.V. Kolesnik et al. // Microporous and Mesoporous Materials. – 2008. – № 114. – pp. 440 – 447.

28. Суминов И.В. Плазменно-электролитическое модифицирование поверхности металлов и сплавов / Суминов И.В., Белкин П.Н., Эпельфельд А.В. и др. – М. : Техносфера, 2011. – 464 с.

29. Казанцев И.А. Технология получения композиционных материалов микродуговым оксидированием: монография / Казанцев И.А., Кривенков А.О. – Пенза : Информационно-издательский центр ПГУ, 2007.– 240 с.

30. Клапків М. Фазовий склад плазмоелектрохімічних оксидокерамічних покривів / М. Клапків, В. Посувайло, Б. Стельмахович та ін. // Фізико-хімічна механіка матеріалів. – Львів : ФМІ. – 2006. – № 5. – С. 750 – 755.

31. Гордиенко П.С. Образование покрытий на аноднополяризованных электродах в водных электролитах при потенциалах искрения и пробоя / П.С. Гордиенко, 1996. – Владивосток : Дальнаука. – 216 с.

32. Слугинов Н.П. Электролитическое свечение / Н.П. Слугинов. – С.-Пб. : Типорафия Демакова. – 1884. – 66 с.

33. Гюнтершульце А. Электролитические конденсаторы / А. Гюнтершульце, Г. Бетц. – М. : Оборонгиз. – 1938. – 200 с.

34. Тихоненко В.В. Упрочняющие технологии формирования износостойких поверхностных слоев / В.В. Тихоненко, А.М. Шкилько // Фізична інженерія поверхні. – 2011. – Т. 9, № 3. – С. 237 – 243.

35. Бехштедт Ф. Поверхности и границы раздела полупроводников / Бехштедт Ф., Эндерлайн Р.М. – Баку: Мир, 1990. – 390 с.

36. Terleeva O.P. Comparison Analysis of Formation and Some Characteristics of Microplasma Coatings on Aluminum and Titanium Alloys / O.P. Terleeva, V.I. Belevantsev, A.I. Slonova et al. // Protection of Metals. – 2006. – Vol. 42, № 3. – P. 272 – 278.

37. Жуков С.В. Исследование физико-механических свойств, структуры и фазового состава покрытий, полученных методом микродугового оксидирования / Жуков С.В., Кантаева О.А., Желтухин Р.В. и др. // Приборы. – М. МНТО ПМ. – 2008. – №4. – С. 28 – 32.

38. Mc Neil W. Anodic film growth by anion deposition in aluminate, tungstate and phosphate solutions / W. Mc Neil, L.L. Gruss // Journal of The Electrochemical Society. – 1963. – Vol. 110.– no 8 – pp. 853 – 855.

39. Gruss L.L. Anodic Spark Reaction Products in Aluminate, Tungstate and Silicate Solutions / L.L. Gruss, W. Mc Neil // Electrochem. Technol. – 1963. – Vol. 1.– no 9–10. – p.283–287.

40. Щукин Г.Л. Некоторые особенности электрохимической обработки алюминия и его сплавов. Теория и практика анодного окисления алюминия: справочник // Г.Л. Щукин, А.Л. Беланович, В.Б. Коледа. – Казань, 1990. – 235 с.

41. Федоров В.А. Формирование упрочненных поверхностных слоев методом микродугового оксидирования в различных электролитах и при изменении токовых режимов / В.А. Федоров, В.В. Белозеров, Н.Д. Великосельская // Физика и химия обработки материалов. – 1991. – № 1. – С. 87 – 93.

42. Tompson G.E. Porous anodic alumina: fabrication, characterization and applications / G.E. Tompson // Thin Solid Films. – 1997. – V. 297. – P. 192 – 201.

43. Адамсон А. Физическая химия поверхностей / Адамсон А. – М.: Мир, 1997. – 320 с.

44. Хенли В.Ф. Анодное оксидирование алюминия и его сплавов / Хенли В.Ф. – М. : Металлургия, 1986. – 152 с.

45. Гордиенко П.С. Электрохимическое формирование покрытий на алюминии и его сплавах при потенциалах искрения и пробоя / П.С. Гордиенко, В.С. Руднев – Владивосток: Дальнаука, 1999. – 233 с.

46. Баковец В.В. Плазменно-электролитическая анодная обработка металлов / В.В.Баковец, О.В.Поляков, И.П. Долговесова. – Новосибирск: Наука, 1991. – 168 с.

47. Одынец Л.Л. Физика окисных пленок / Л.Л. Одынец, Е.Я. Ханина Петрозаводск: Изд-во ПГУ, 1981. – 74 с.

48. Руднев В.С. Исследование кинетики формирования ПЭО-покрытий на сплавах алюминия в гальваностатическом режиме / В.С. Руднев, П.С. Гордиенко, А.Г. Курносова, Т.И. Орлова // Электрохимия. – 1990. – Т. 26, № 7. – С. 839 – 846.

49. Гордиенко П.С. Плазменно-электролитическое оксидирование титана и его сплавов / П.С. Гордиенко, С.В.Гнеденков. – Владивосток: Дальнаука, 1997. – 344 с.

50. Черненко В.И. Получение покрытий анодно-искровым электролизом / В.И.Черненко, Л.А.Снежко, И.И.Папанова.– Л.: Химия, 1991. – 208 с.

51. Черненко В.И. Теория и технология анодных процессов при высоких напряжениях / В.И.Черненко, Л.А.Снежко, И.И.Папанова, К.И. Литовченко. – К.: Наукова думка, 1995. – 198 с.

52. Klein N. Electrical breakdown mechanisms in thin insulators / N. Klein // Thin Solid Films. – 1978. – V. 50. – P. 223 – 232.

53. Суминов И.В. Плазменно-электролитическое оксидирование (теория, технология, оборудование) / И.В.Суминов, А.В.Эпельфельд, В.Б. Людин и др. – М. : ЭКОМЕТ, 2005. – 368 с.

54. Малышев В.Н. Особенности формирования покрытий методом анодно-катодного микродугового оксидирования / В.Н. Малышев // Защита металлов. – 1996. – Т. 32, № 6. – С. 662 – 667.

55. Тырина Л.М. Получение, состав и каталитическая активность модифицированных платиной плазменно-электролитических оксидных структур на алюминии / Л.М. Тырина, В.С. Руднев, П.М. Недозоров и др. // Журнал неорганической химии.– 2011. – Т. 56, № 9. – С. 1503 – 1509.

56. Кусков В.Н. Особенности роста покрытия при микродуговом оксидировании алюминиевого сплава / В.Н. Кусков, Ю.Н. Кусков, И.М. Ковенский, Н.И. Матвеев // Физика и химия обработки материалов. – 1990. – №6. – С. 101–103.

57. Марков Г.А. Плазменно-электролитическое оксидирование / Г.А. Марков, В.И. Белеванцев, О.П. Терлеева и др. // Вестн. МГТУ. Сер. Машиностр. –1992. – № 1. – С. 34 – 56.

58. Yerokhin A.L. Plasma electrolysis for surface engineering. Review / A.L.Yerokhin, X.Nie, A.Leyland, et al. // Surface and Coating Technol. – 1999. – V. 122. – P. 73 – 93.

59. Юнг Л. Анодные оксидные пленки / Л. Юнг – Л. : Энергия, 1967. – 232 с.

60. Гюнтершульце А. Электролитические конденсаторы / А. Гюнтершульце, Г. Бетц. – М. – Оборонгиз. –1938. – 200 с.

61. Verwey E.J.W. The structure of the electrolytic oxide layer on aluminum / E.J.W. Verwey // z. Kristallograf. – 1935. – B.94 – № 3–4. – S. 317 – 322.

62. Cabrera N. Theory of the oxidation of metals / N. Cabrera, N. Mott // Rep. Prog. Phys. – 1949. – Vol. 12. – no 3. – pp. 163 – 167. doi:10.1088/0034-4885/12/1/308

63. Dewald J.F. A theory of the kinetics of formation of anodic films at high fields / J.F. Dewald // J. Electrochem. Soc. – 1955. – V.102. – no 1. – pp. 1 – 6.

64. Fromhold A.T. Kinetics of oxide film growth on metal crystals: thermal electron emission and ionic diffusion / A.T. Fromhold, E.L. Cook // Phys. rev. – 1967. – V.163. – no 3. – pp.650–664.

65. Dignam M.J. Mechanism of ion transfer through oxide films / M. Dignam // In: Oxides and oxide films. – N.Y. : Marsel Dekker Inc., 1972. – V. 1. – pp. – 80 – 286.

66. Богоявленский А.Ф. Анодирование металлов: межвузовский сборник / А.Ф. Богоявленский, Я.И. Александров. – Казань : КАИ им. А.Н. Туполева. – 1984. – 65 с.

67. Богоявленский А.Ф. О механизме образования анодно-окисных покрытий на алюминии / А.Ф. Богоявленский // Журнал прикладной химии. 1972. – Т. 45. – № 3. – С. 682 – 685.

68. Boguta D.L. On Composition of Anodic-Spark Coatings Formed on Aluminum Alloys in Electrolytes with Polyphosphate Complexes of Metals / D.L. Boguta, V.S. Rudnev, T.P. Yarovaya et al // Russian Journal of Applied Chemistry. – 2002. – V. 75, № 10. – P. 1605 – 1608.

69. Krishtal M.M. Oxide Layer Formation by Micro-Arc Oxidation on Structurally Modified Al-Si Alloys and Applications for Large-Sized Articles Manufacturing / M.M. Krishtal // Advanced Materials Research, 2009. – Vol. 59. – pp. 204 – 208.

70. Шандров Б.В. Основы технологии микродугового оксидирования / Б.В. Шандров, Е.М. Морозов, А.В. Жуковский – М. : Альянс, 2008. – 80 с.

71. Rudnev V.S. Properties of Coatings Formed on Titanium by Plasma Electrolytic Oxidation in a Phosphate-Borate Electrolyte / V.S. Rudnev, T.P. Yarovaya, V.S. Egorkin et al // Russian Journal of Applied Chemistry. – 2010. – V. 83, № 4. – P. 664 – 670.

72. Тырина Л.М. Формирование на титане и алюминии анодных слоев с марганцем, магнием и фосфором / Л.М. Тырина, В.С. Руднев, Е.А. Бозина и др. // Защита металлов. – 2001. – Т. 37, № 4. – С. 366 – 369.

73. Rudnev V.S. Anodic Spark Coatings on Titanium and AMцM Alloy from Baths Containing Aluminum Polyphosphate Complexes / V.S. Rudnev, T.P. Yarovaya, V.V. Kon'shin et al // Protection of Metals. – 2003. – V. 39, № 2. – P. 182 – 187.

74. Пат. 1788793 Российская федерация, МПК6 C25D11/26. Электролит для микродугового оксидирования титана и его сплавов / Гордиенко П.С., Хрисанфова О.А., Коркош С.В.; заявитель и патентообладатель Институт химии ДО АН СССР. – 4632560/26, заявл. 15.12.1988; опубл. 27.05.1996.

75. Гордиенко П.С. Формирование износостойких покрытий на титане / П.С. Гордиенко, С.В. Гнеденков, О.А. Хрисанфова и др. // Электронная обработка материалов.– 1990.– Т. 155, № 5.– С.32 – 35.

76. Пат. 2046156 Российская федерация, МПК6 C25D11/04. Электролит для формирования покрытий на вентильных металлах / Гордиенко П.С., Гнеденков С.В., Хрисанфова О.А. и др.; заявитель и патентообладатель Институт химии ДО РАН. – 5043332/26; заявл. 21.05.1992; опубл. 20.10.1995.

77. Корягин С.И. Способы обработки материалов / С.И. Корягин, И.В. Пименов, В.К. Худяков. – Калининград : Калининградский университет, 2000. – 448 с.

78. Пат. 2238352 Российская федерация, МПК[7] C25D11/02. Способ получения покрытий / Казанцев И.А., Скачков В.С., Розен А.Е., Кривенков А.О.; заявитель и патентообладатель ПГУ. – 2003126876/02; заявл. 02.09.2003; опубл. 20.10.2004.

79. Якименко Л.М. Электродные материалы в прикладной электрохимии / Л.М. Якименко. – М. : "Химия", 1977. – 264 с.

80. Gong D. Titanium oxide nanotube arrays prepared by anodic oxidation / D. Gong, C.A. Grimes, O.K. Varghese et al.// J. Mater. Res. – 2001. – V. 12. – P. 3331 – 3334.

81. Derby B. Characterisation of Interfaces Between Liquid Tin and Alumina in the Presence of Titanium Alloy Additions / B. Derby, S. Holt // Interface Science. – 2004. – V. 12 – P. 29 – 37

82. Пат. 2363775 Российская федерация, МПК[7] C25D11/26. Способ получения покрытий на изделии, выполненных их титана и его сплавов / Ковалева М.Г., Колобов Ю.Р., Сирота В.В. и др.; заявитель и патентообладатель "БГУ". – заявл. 10.07.2008; опубл. 10.08.2009.

83. Пат. 2238351 Российская федерация, МПК[7] C25D11/02. Способ получения покрытий / Атрощенко Э.С., Скачков В.С., Казанцев И.А.; заявитель и патентообладатель ПГУ. – заявл. 02.09.2003; опубл. 20.10.2004.

84. Семенова Т.Л. Новый класс сенсоров электронно-ионного типа на основе оксидных структур анодных пленок / Т.Л. Семенова, П.С. Гордиенко, А.В. Ефименко // Электронный журнал "Исследовано в России".

85. Kim J.-Y. Frequency-dependent pulsed direct current magnetron sputtering of titanium oxide films / J.-Y. Kim, E. Barnat, E. J. Rymaszewski, and T.-M. Lu // J. Vac. Sci. Technol. A – 2001. – V. 19, № 2. – P. 429 – 434.

86. Rudnev V.S. Magnetoactive Oxide Layers Formed on Titanium by Plasma Electrolytic Technique / V.S. Rudnev, A.Yu. Ustinov, I.V. Lukiyanchuk et al // Protection of Metals and Physical Chemistry of Surfaces. – 2010. – V. 46, № 5. – P. 566 – 572.

87. Фишгойт Л.А. Коррозионно-электрохимические свойства интерметаллидов системы титан-алюминий / Л.А. Фишгойт, Л.Л. Мешков // Вестн. Моск. ун-та. Сер. 2. Химия. – 1999. – Т. 40, № 6. – С. 369 – 372.

88. Логачева В.А. Формирование тонких пленок оксидов в установке с автоматическим эллипсометром / В.А. Логачева, О.В. Новикова, М.В. Марчуков, А.А. Чуриков // Конденсированные среды и межфазные границы. – 2007. – Т. 9, № 4. – С. 405 – 410.

89. Талимов А.В. Формирование термостойких анодных окисных пленок и их использование для изготовления фотодиодов на InSb / А.В. Талимов, В.Ю. Филиновский, А.Г. Титов // Прикладная физика. – 2002. – № 4. – С. 134 – 142.

90. Невский О.И. Электрохимическая размерная обработка металлов и сплавов. Проблемы теории и практики: Монография / О.И. Невский, В.М. Бурков, Е.П. Гришина и др. – Иваново : ГОУ ВПО Иван. гос. хим-технол. ун-т. – 2006. – 282 с.

91. Ланин В.Л. Формирование токопроводящих контактных соединений в изделиях электроники / Ланин В.Л., Достанко А.П., Телеш Е.В. – Минск : Изд. центр БГУ, 2007. – 574 с.

92. Шандров Б.В. Технологическое оборудование для микродугового оксидирования : научное издание / Б.В. Шандров, В.М. Смелянский, Е.М. Морозов, А.В. Жуковский // Автомобильная промышленность.– 2005. – № 10. – С. 28 – 31.

93. Пат. 2152255 Российская федерация, МПК[7] B01J37/34, B01J21/00, B01J21/04, B01J23/16, B01J23/70 Способ получения оксидных каталитически активных слоев и каталитически активный материал, полученный данным способом / Мамаев А.И., Бутягин П.И.; заявитель и патентообладатель Мамаев А.И. – 98113500/04; заявл. 14.07.1998; опубл. 10.07.2000.

94. Евдокимов В.Д. Технология упрочнения машиностроительных материалов / В.Д. Евдокимов, Л.П. Клименко, А.Н. Евдокимова. – К.: Профессионал, 2006. – 352 с.

95. Меркулов В.И. Основы конденсаторостроения / Меркулов В.И. – Томск : Изд. ТПУ, 2001. – 121 с.

96. А. с. 1339818 СССР. Устройство для преобразования переменного напряжения в асимметрическое переменное / Марков Г.А., Шулепко Е.К., Терлеева О.П. и др. – Опубл. в БИ, 1987, №35. (НО2М 5/257).

97. Aroutiounian V.M. Metal oxide photoelectrodes for hydrogen generation using solar radiation-driven water splitting / V.M. Aroutiounian, V.M. Arakelyan, G.E. Shahnazaryan // Solar Energy. – 2005. – V. 78. – P. 581 – 592.

98. Loebl P. Nucleation and growth in TiO_2 films prepared by sputtering and evaporation / P.Loebl, M. Huppertz, D. Mergel // Thin Solid Films. – 1994.– Vol. 251 – P. 72 – 79.

99. Атрощенко Э.С. Технология и свойства композиционных материалов на основе алюминия и титана, полученных методом микродугрового оксидирования / Э.С. Атрощенко, А.Е. Розен, Н.В. Голованова и др. // Известия высших учебных заведений. Черная металлургия. – 1999. – №10. – С. 36 – 39.

100. Малышев В.Н. Самоорганизующиеся процессы при формировании покрытий методом микродугового оксидирования / В.Н. Малышев // Перспективные материалы. – 1998. – №1. – С. 16 – 21.

101. Суминов И.В. Синтез керамикоподобных покрытий при плазменно-электролитической обработке вентильных металлов / И.В. Суминов, А.В. Эпельфельд, А.М. Борисов и др. // Известия АН. Серия Физическая. – 2000. – Т. 64. – № 4. – С. 763 – 766.

102. Ростовщикова Т.Н. Катализ реакций хлоролефинов аллильного строения наноразмерными оксидами железа / Т.Н. Ростовщикова, О.И. Киселева, Г.Ю. Юрков и др. // Вестн. Моск. ун-та. Сер. 2. Химия. – 2001. – Т. 42. – № 5. – С. 318 – 324.

103. Пат. 2385740 Российская Федерация, МПК[7] A61L27/54, A61F2/02, A61C8/00 Биоактивное покрытие на имплантате из титана и способ его получения / Легостаева Е.В., Шаркеев Ю.П., Толкачева Т.В. и др.; заявитель и патентообладатель ИФПМ СО РАН. – заявл. 17.09.2008; опубл. 10.04.2010.

104. Пат. 2361622 Российская Федерация, МПК[7] A61L27/06/ A61K6/04. Способ получения биопокрытия на имплантатах из титана и его сплавов/ Родионов И.В., Серянов Ю.В., Бутовский К.Г.; заявитель и патентообладатель СГТУ. – заявл. 09.04.2008; опубл. 20.07.2009.

105. Пат. 2394601 Российская Федерация, МПК7 A61L27/06, A61L27/32 Способ модифицирования поверхности имплантатов из титана и его сплавов / М.Б. Иванов, Ю.Р. Колобов, М.А. Трубицын и др.; заявитель и патентообладатель Федеральное агентство по науке и инновациям, БГУ. – заявл. 09.10.2008; опубл. 20.07.2010.

106. Пат. 2397735 Российская Федерация, МПК[7] A61F2/02, A61F2/30, A61F2/36. – Способ изготовления медицинского имплантата из бета-титанового-молибденового сплава и соответствующий имплантат / Баликтай С., Келлер А.; заявитель и патентообладатель ВАЛЬДЕМАР ЛИНК ГМБХ унд КО. КГ. – 2007135069/14; заявл. 27.02.2006; опубл.27.08.2010.

107. Rudnev V.S. Anodic spark deposition of P, Me(II) or Me(III) containing coating on aluminium and titanium alloys in electrolytes with polyphosphate complexes / V.S. Rudnev, T.P. Yarovaya, D.L. Boguta et al // J. Electroanal. Chem. – 2001. – V. 497. – № 1–2. – P. 150 – 158.

108. Кондриков Н.Б. Влияние предварительной обработки титана на морфологию поверхности и электрохимические свойства селективных электродов на основе оксидов рутения и титана / Н.Б. Кондриков, Е.В. Щитовская, М.С. Васильева и др. // Электронный журнал "Исследовано в России". – 2002. – С. 1005 – 1008.

109. Rudnev V.S. Oxide Zirconium Containing Films on Titanium / V.S. Rudnev, K.N. Kilin, T.P. Yarovaya et al // Protection of Metals. – 2008. – V. 44. – № 1. – P. 62 – 64.

110. Гнеденков С.В. Антифрикционные свойства покрытий, полученных методом микродугового оксидирования на титане / С.В. Гнеденков, С.Л. Синебрюхов, О.А. Хрисанфова и др. // Электронный журнал "Исследовано в России". – 2002. – С. 376 – 387.

111. Руднев В.С. Анодно-искровое осаждение P- и W- или Mo-содержащих покрытий на сплавы алюминия и титана / В.С. Руднев, И.В. Лукиянчук, В.В. Коньшин, П.С. Гордиенко // Журнал прикладной химии. – 2002. – Т. 75. – № 7. – С. 1099 – 1103.

112. Пат. 2152255 Российская Федерация, МПК[7] B01J37/34, B01J21/00, B01J21/04, B01J23/16, B01J23/70. Способ получения оксидных и каталитически активных слоев и каталитически активный материал,

полученных данным способом / Мамаев А.И.; заявитель и патентообладатель Мамаев А.И. – заявл. 14.07.1998; опубл. 10.07.2000.

113. Руднев В.С. Каталитически активные структуры на металлах / В.С. Руднев, Н.Б. Кондриков, Л.М. Тырина и др. // Серия. Критические технологии. Мембраны. – 2005. – № 4 (28). – С. 63 – 67.

114. Rudnev V.S. Comparative Analysis of the Composition, Structure, and Catalytic Activity of the NiO–CuO–TiO_2 on Titanium and NiO–CuO–Al_2O_3 on Aluminum Composites / V.S. Rudnev, L.M. Tyrina, A.Yu. Ustinov et al // Kinetics and Catalysis. – 2010. – V. 51. – № 2. – P. 266 – 272.

115. Rudnev V.S. Iron- and Nickel-Containing Oxide–Phosphate Layers on Aluminum and Titanium / V.S. Rudnev, V.P. Morozova, T.A. Kaidalova et al // Russian Journal of Inorganic Chemistry. – 2007. – V. 52. – № 9. – P. 1350 – 1354.

116. Васильева М.С. Формирование и состав содержащих Mn, Co, Pb, Fe анодных слоев на титане / М.С. Васильева, В.С. Руднев, Л.М. Тырина и др. // Известия высших учебных заведений. Химия и химическая технология. – 2003. – Т. 46 (5). – С. 164 – 165.

117. Fathollahzade N., Raeissi K. A tribocorrosion study of cobalt–tungsten electrodeposited coating with a mixed amorphous/nanocrystalline structure // The Intern J of Surf. Eng. and Coatings. V. 94, 2016 - Issue 6.- Pp. 328-335.

118. Tsyntsaru N., Dikusar A., Cesiulis H. et.al. Tribological and corrosive characteristics of electrochemical coatings based on cobalt and iron superalloys // Powder Metallurgy and Metal Ceramics 48 (7), 419-428.

119. Казанцев И.А. Износостойкость композиционных материалов на основе титана, полученных микродуговым оксидированием / И.А. Казанцев, А.О. Кривенков, А.Е. Розен, С.Н. Чугунов // Технические науки. Машиностроение и машиноведение. – 2008. – № 1. – С. 159 – 164.

120. Пат. 2420615 Российская Федерация, МПК C25D11/08, C25D11/26 Изделие производства и способ анодного нанесения покрытия из оксидной керамики на алюминий и/или титан / Долан Шон Э.; заявитель и патентообладатель Хенкель АГ УНД КО КГаА (DE). – 2007119381/02; заявл. 25.10.2005; опубл. 27.11.2008.

121. Предпатент РК № 2038. Способ получения композиционных покрытий из боридов никеля // Ш.Х.Яр-Мухамедов, Е.А.Джамбусинов, Г.Щ.Яр-Мухамедова.- Опубл. 14.07.1992.

122. Andersen T. The Manganese Dioxide Electrodes in Aqueous Solution / T. Andersen // Modern Aspects of Electrochemistry.– 2002.– V.30.– P.313–413.

123. Уэллс К. Структурная неорганическая химия / Уэллс К. – М.: Мир, 1988. – 537с.

124. Сокольский Г.В. Структура и свойства образцов диоксида марганца различного происхождения / Г.В. Сокольский, Н.Д. Иванова, Е.И. Болдырев // Укр. хим. журн. – 1998. – Т.64, 2. – С.118 – 121.

125. Тырина Л.М. Термическое поведение анодно-искровых покрытий с марганцем и фосфором на титане / Л.М. Тырина, В.С. Руднев, С.Б. Буланова и др. // Защита металлов.– 2003.– Т.39. – № 4. – С. 371 – 375.

126. Теоретические основы химии редких и рассеянных элементов / Н.Д.Сахненко, М.В.Ведь, В.В.Штефан, М.М.Волобуєв; под ред. Н.Д.Сахненко. – Харьков : НТУ «ХПИ», 2011. – 424 с.

127. Ермоленко И.Ю., Ведь М.В. , Сахненко Н.Д. Электрохимический рециклинг псевдосплавов вольфрама : монография. – Харьков : НТУ «ХПИ», 2014 . – 162 с.

128. M.Ved, M.Glushkova, N.Sakhnenko Catalitic properties of binary and ternary alloys based on silver // Functional Materials, 2013. – Vol. 20, №1.- P.87-91.

129. Ведь М.В., Глушкова М.А., Сахненко Н.Д., Фомина Л.П., Корний С.А. Особенности электроосаждения сплавов Ag-Co в импульсном режиме // Гальванотехника и обработка поверхности, 2013.- № 1.- С.25-30

130. Sakhnenko M., Ved M., Bairachna T., Shepelenko O., Zubanova S. Redox flow batteries – perspective means of electrochemical energy storage // Технологический аудит и резервы производства, 2013.- № 4(2). – С.22-24

131. Сахненко М.Д. Анодна поведінка алюмінію у водних розчинах дифосфату / М.Д. Сахненко, М.В. Ведь, Т.П. Ярошок та ін. // Вісник НТУ "ХПІ". – Х.: НТУ "ХПІ", 2007. – № 32. – С. 16 – 19.

132. Сахненко М.Д. Электрохимия наноламинатов: оксидные покрытия / Н.Д. Сахненко, М.В. Ведь // Вісник НТУ "ХПІ". – Харків: НТУ "ХПІ". – 2010. – №47. – С.81–90.

133. M. Ved, D. Alami, M. Slavkova. Bases of Inorganic and Organic Chemistry : textbook. – Kharkov : NTU “KhPI”, 2016. – 260 p.

134. Yar-Mukhamedova G., Ved M., Sakhnenko N., Karakurkchi A., Yermolenko I. Iron binary and ternary coatings with molybdenum and tungsten /Applied Surface Science. V. 383, № 15, 2016, - P. 346–352.

135. Ведь М.В., Сахненко Н.Д., Богоявленская Е.В. Моделирование процесса формирования покрытий смешанными оксидами на алюминии // Коррозия: материалы, защита.- 2011.- № 8.- С.42-47.

136. M. O. Glushkova, M. V. Ved’, M. D. Sakhnenko. Corrosion Properties of Cobalt–Silver Alloy Electroplates // Materials Science , 2013. – Vol. 49, № 3. – P. 292-297.

137. Ведь М.В., Сахненко Н.Д., Глушкова М.А., Гапон Ю.К., Козяр М.А. Влияние режимов электролиза на состав и морфологію тернарных сплавов Co-Mo-W(Zr, Ag) // Вопросы химии и химической технологии, 2013.- Вып. 4.- С.140-144.

138. Сахненко Н.Д., Ведь М.В., Каракуркчи А.В. Электроосаждение покрытий сплавом железо-молибден // Вопросы химии и химической технологии, 2013.- Вып. 4.- С.178-182.

139. Ved’ M.V., Sakhnenko N.D., Karakurchi A.V., and Zyubanova S.I. Electrodeposition of Iron–Molybdenum Coatings from Citrate Electrolyte // Russian Journal of Applied Chemistry, 2014, Vol. 87, No. 3, pp. 276−282

140. Сахненко Н.Д., Ведь М.В., Быканова В.В. Фотокатализаторы на основе оксида циркония для очистки органосодержащих сточных вод // Химическая промышленность Украины, 2014. – № 2(121). – С. 58-63

141. Андрощук Д.С., Майба М.В., Сахненко Н.Д. Особенности оксидирования сплава АЛ-25 в микродуговом режиме / Актуальные проблемы теории и практики электрохимических процессов **:** Сборник статей молодых ученых. В 2 т. – Саратов : СГТУ им.Ю.А.Гагарина, 2014. – Т.1. – С248-251.

142. Ведь М.В. Оцінка імовірності деградації матеріалів під впливом фарадеївських реакцій / М.В. Ведь, М.Д. Сахненко, Желавський С.Г. та ін. // Фізико-хімічна механіка матеріалів. – Львів : ФМІ НАН України, 2000. – № 1. – Т. 2. – С. 617 – 622.

143. Сахненко Н.Д., Ведь М.В., Майба М.В., Ярошок Т.П. Формирование покрытий оксидами редких металлов на сплавах титана в микродуговом режиме // Коррозия: материалы, защита.- 2013.- №8.- С.34-37

144. Ведь М.В., Сахненко Н.Д., Ермоленко И.Ю., Корний С.А. Моделирование и оптимизация процесса электрохимического рециклинга псевдосплавов вольфрама // Энерготехнологии и ресурсосбережение, 2013. – № 4. – С.41-46.

145. Ведь М.В., Сахненко Н.Д., Богоявленская Е. В. Организация рабочего процесса в камере сгорания ДВС в присутствии каталитических материалов // Двигатели внутреннего сгорания, 2013.- № 2.- С.109-111

146. Майба М. Функциональные покрытия на сплавах титана / М. Майба, М. Ведь, Н. Сахненко. – Saarbrücken : LAP Lambert Academic Publishing, 2013. – 168 с.

147. Лунарска Е. Oxide film formed on Ti by the microark anodic method / Е. Лунарска, О. Черняева, М. Ведь, М. Сахненко // Ochrona przed Korozja. – 2007. – № 11А. – Р. 265 – 269.

148. Михеев А.Е. Технологические возможности микродугового оксидирования алюминиевых сплавов / А.Е. Михеев // Вестник машиностроения. – 2003. – № 2. – С. 56 – 63.

149. Ведь М.В. Каталітичні та захисні покриття сплавами і складними оксидами: електрохімічний синтез, прогнозування властивостей / М.В.Ведь, М.Д. Сахненко. – Х.: НТУ "ХПІ", 2010. – 272 с.

150. Ведь М. Поверхнева обробка сплавів титану та алюмінію / М. Ведь, М. Сахненко, О. Богоявленська та ін. // Фізико-хімічна механіка матеріалів. – Львів : ФМІ ім. Г. В. Карпенка НАН України. – 2010. – Спецвипуск № 8. – С. 392 – 396.

151. Nie X. Deposition of layered bioceramic hydroxyapatite/TiO2 coatings on titanium alloys using a hybrid technique of micro-arc oxidation and electrophoresis / X. Nie, A. Leyland, A. Matthews // Surface & Coatings Technology. – 2000. – V. 125, № 1 – 3. – P. 407 – 414.

152.

153. Williams D.E. Explanation for initiation of pitting corrosion of stainless steel at sulfide inclusions // Journal of Electrochemical Society. – 2000. – № 147. – P. 1763-1766.

154. Pardo A. Pitting corrosion behaviour of austenitic stainless steel-combining effects of Mn and Mo additions // Corrosion Science. – 2008. – № 50. – P. 1796-1806.

155. Narivskyi A.E. Determination of pitting resistance steel AISI304 became in chloride-containing environment which are in work of type heat excahngers // Physicochemical mechanics of materials. – 2006. - 50 – P. 136-140.

156. Narivs'kyi O.E. Influence of the heterogeneity AISI321 on its pitting in chloride-containing media // Materials Science. – 2007. – Vol. 43, Issue 2. – P. 256-264.

157. A Dikusar, H Cesiulis,Pastore M., Cabrini S., Lorenzi T., Manfredi D., Biamino S. Corrosion resistance of direct metal laser sintering (DMLS) AlSiMg alloys //EUROCORR 2014 -Improving materials durability: from cultural heritage to industrial applications. 2014. 458 p.

158. Gutierrrez de Sainz-Solabarria S. Estudio de la susceptibilidad de un acero inoxidable austenitico estabilizado con niobio al danado por tensocorrosion en midioH2S (SSC) y corrosion intergranular en otros medios agresivos // Deformación metálica. – 1996. – Vol. 226. № 6, P. 77–83.

159. Davis J.R.; Surface Engineering for Corrosion and Wear Resistance; ASM International, 2005; pp. 1-159.

160. Schlesinger M., Paunovic M., Modern Electroplating, 5th edition, John Wiley & Sons, Inc., 2010.

161. N., A. Dikusar, H. Cesiulis et al. Powder Metall Met Ceram (2009) 48: 419.

162. Gamburg Y.D., E.N. Zakharov, G.E. Goryunov. Electrodeposition Russ J Electrochem (2001) 37: 670

163. Ved' M.V., N.D. Sakhnenko, A.V. Karakurkchi, I.Yu. Yermolenko, Issues of Chemistry and Chemical Technology (2015) 5-6(98): 53.

164. Kublanovsky V., O. Bersirova, A. Dikusar, et al. Phys. Chem. Mech. Mater. (2008) 7: 308.

165. Porto M., de Lima Bellia V., de Morais Nepel T. et al. J Mater res technol. (2019) 8(5): 4547.

166. V. Vasauskas, J. Padgurskas, R. Rukuiža et al. Mechanika (2008) 4(72): 21.

167. Ved M., Sakhnenko M., Glushkova M., Bairachna T. Electrodeposited Cobalt Alloys as Materials for Energy Technology // MRS Proceeding , 2013.- Vol.1491.- 6 P.

168. Yar-Mukhamedov Y., Atchibayev R. Baisholanova K., Myrzakul S. «Computer simulation of composition coatings with set properties» / 19th International Sc. GeoConf. SGEM 2019. Vol. 19 (6.1). 2019.- P. 125-130.

169. Jargelius-Pettersson R.F. Electrochemical investigation of the influence of nitrogen alloying on pitting corrosion of austenitic stainless steels // Corrosion Science. – 1999. – Vol. 41. № 8, – P. 1639-1664.

170. Schmuki P. The composition of the boundary region of MnS inclusions in stainless steel and its relevance in triggering pitting corrosion // Corrosion Science. – 2005. – № 47. – P. 1239-1250.

171. Web E. G. Pit initiation at single sulfide inclusions in stainless steel. II. Detection of local pH, sulfide and thiosulfide // Journal of Electrochemical Society. – 2002. – № 149. – P. 280-285.

172. Narivskiy A., Yar-Mukhamedov Y., Mukashev K., Muradov A Investigation of electrochemical properties in chloride-containing commercial waters / 18th International Sc. GeoConf. SGEM 2018. Vol. 18 (6.1). 2018.- P. 267-275.

173. Sakhnenko, N., Yermolenko, I., Yar-Mukhamedova, G. Atchibayev R. A nano-coatings protective properties in aminum environments / 18th International Sc. GeoConf. SGEM 2018. Vol. 18 (6.1). 2018.- P. 297-303.

174. Dutta R. S. The sensitization and stress corrosion cracking of nitrogen-containing stainless steels // Corrosion Science. – 1993. - Vol. 34, № 1, –P. 51-60.

175. Gehrke J. Qualification of stress and test methods for use in combined fatigue algorithms for riveted joints //EUROCORR 2014 - Improving materials durability: from cultural heritage to industrial applications. – 2014. – P. 135-140.

176. Sakhnenko M. Modification of electrode materials by alloys and oxide systems / M. Sakhnenko, M. Ved, O. Bogoyavlenska et al / International conference "Ion transport in organic and inorganic membranes" : Conference Proceedings. – Krasnodar, 2011. – P. 177.

177. Сахненко М.Д. Закономірності електрохімічного формування покриттів складними оксидами на поверхні сплавів алюмінію та титану / М.Д. Сахненко, М.В. Ведь, Т.П. Ярошок та ін. // Вісник НТУ "ХПІ".–Харків: НТУ "ХПІ". – 2008. – №15. – С.88 – 94.

178. Glushkova M. A. Functional coatings electrochemical synthesis / M. A. Glushkova, M. V. Ved, N. D. Sakhnenko et al / Book of Abstracts of 6-th International Conference on Chemistry and Chemical Education "Sviridov Readings 2012" / edit. E. I. Vasilevskaya. – Minsk : Publ. Center of BSU, 2012. – P. 57.

179. Сахненко Н. Наноструктурные защитные и каталитические покрытия / Н. Сахненко, М. Ведь, Ю. Александров и др. / VI Міжнародний салон винаходів і нових технологій "Новий Час". – Севастополь, 2010. – С. 56 – 57.

180. Lunarska E. Structure and properties of the oxide layers formed on al alloy by the microarc-anodic treatment / E. Lunarska, M. Ved, N. Sakhnenko, O. Chernayeva // Фізико-хім. механіка матеріалів, Спецвипуск № 7. – Львів: ФМІ НАН України. – 2008. – Т.1. – С.380 – 384.

181. Ведь М.В., Сахненко Н.Д., Глушкова М.А., Майба М.В., Дементий А.В. Каталитическая активность покрытий на основе переходных металлов // Энерготехнологии и ресурсосбережение.- Киев: Ин-т газа, 2012. - № 3. – С.38-43.

182. Нарівський О.Е. Особливості селективного розчинення металів у пітингах на поверхні сталі AISI304 // Фізико-хімічна механіка матеріалів. – 2016. – № 11 Спеціальний випуск "Проблеми корозії та протикорозійного захисту конструкційних матеріалів". – С. 50–55.

183. Gutierrrez de Sainz-Solabarria S. Estudio de la susceptibilidad de un acero inoxidable austenitico estabilizado con niobio al danado por tensocorrosion en midioH2S (SSC) y corrosion intergranular en otros medios agresivos // Deformación metálica. – 1996. – Vol. 226. № 6, P. 77–83.

184. Olefjord I. The influence of nitrogen on the passivation of stainless steels /I. Olefjord, L. Wegrelius // Corrosion Science. – 1996. – Vol. 38, № 7, P. 1203-1220.

185. Ved', M., Sakhnenko, N., Yermolenko, I., Yar-Mukhamedova, G., Atchibayev R / Composition and corrosion behavior of iron-cobalt-tungsten/ Eurasian Chemico-Technological Journal Issue 20 (2), 2018, P. 145-152.

186. Kuznetsov V.V., Golyanin K.E., Pshenichkina T.V. Russian Journal of Electrochemistry (2012) 48: 1107.

187. E. Vernickaite, O. Bersirova, H. Cesiulis, N. Tsyntsaru, Coatings (2019) 9: 85.

188. N. Elezović , B.N. Grgur, N.V. Krstajić, V.D. Jović, Journal of the Serbian Chemical Society (2019) 70(6): 879.

189. M. Zacarin, M. de Brito, E. Barbano et al. Journal of Alloys and Compounds (2018) 750: 577.

190. Tseluikin V.N., Protection of Metals and Physical Chemistry of Surfaces (2009) 45: 287.

191. Low C.T.J., Wills R.G.A., Walsh F.C., Surface & Coatings Technology (2006) 201: 371.

192. Protsenko V.S., Vasil'eva E.A., Smenova I.V. et al. Surface Engineering and Applied Electrochemistry (2015) 51: 65.

193. Nicolenco A., Mulone A., Imaz N., et al. Front Chem. (2019) 7:241.

194. Ved' M.V., Sakhnenko N.D., Karakurchi A.V., Zyubanova S.I., Russ. J Appl. Chem. (2014) 87: 276.

195. Karakurkchi A.V., Ved' M.V., Ermolenko I.Yu., Sakhnenko N.D., Surface Engineering and Applied Electrochemistry (2016) 52: 43.

196. Ved M., Glushkova M., Sakhnenko N., Functional Materials (2013) 20: 87.

197. Yar-Mukhamedova G.Sh., Sakhnenko N.D., Ved' M.V. et al. IOP Conference Series: Materials Science and Engineering (2017) 213: 012019

198. Ved M.V., Sakhnenko N.D., Tkachenko T.M., Bairachnaya M.V., Functional Materials (2008) 15: 613.

199. Ved' M.V., Sakhnenko M.D., Karakurkchi H.V. et al. Materials Science (2016) 51: 701.

200. Karakurkchi A.V., Ved' M.V., Sakhnenko N.D. et al. Functional Materials (2015) 22: 181.

201. Sakhnenko N., Koziar M., Applied Surface Science (2017) 421 PA: 68.

202. Ved' M., Sakhnenko N., Nenastina T., Applied Surface Science (2018) 445: 298.

203. Yar-Mukhamedova G.Sh., Ved' M.V. Sakhnenko N.D., et al. Composition Electrolytic Coatings with Given Functional Properties. Chapter in an IntechOpen Book Applied Surface Science. London, UK (2019) 93-110. DOI: 10.5772/intechopen.84519.

204. Ved' M., Sakhnenko N., Yermolenko I., Yar-Mukhamedova G., Eurasian Chemico-Technol. J. 20 (2018) 145-154.

205. Sachanova, Y.I., Ermolenko, I.Y., Ved', M.V. Materials Science. 54 (4) (2019). 556–566. DOI: 10.1007/s11003-019-00218-x

206. Yar-Mukhamedova G. Sh. Darisheva A. M. Yar-Mukhamedov E. Sh. Materials Science, 54(6), (2019). 907-912. DOI 10.1007/s11003-019-00279-y

207. Ved', M., Sakhnenko, N., Yermolenko, I., Yar-Mukhamedova, G. Atchibayev R. Nano composition Ti-Co (Mn) coatings investigation / 18th International Sc. GeoConf. SGEM 2018. Vol. 19 (6.1). 2018.- P.307-315.

208. Atchibayev R., Mukashev K., Muradov A., Kyzyrova A., Aitbayev Z. Anti–corrosion properties of nanocomposite coatings in amine environments/18th International Sc. GeoConf. SGEM 2018. Vol. 19 (6.1). 2018.- P.39-47.

209. Яр-Мухамедова Г.Ш., Мукашев К. М., Мурадов А. Д., Атчибаев Р. А. Разработка рекомендаций по применению коррозионностойких нано-КЭП для защиты насосов воды ТЭЦ / International conference «Problems of corrosion protection of materials». Lvov, Ukraine. 2018. - P. 249-252.

Scientific publication

Yar-Mukhamedova Gulmira Shariphovna
Nenastina Tat'yana Aleksandrovna
Ved' Maryna Vital'yevna
Sakhnenko Nikolay Dmitrovich
Karakurkchi Anna Vladimirovna

NANOCOMPOSITE ELECTROLYTIC COATINGS BASED ON COBALT ALLOYS WITH REFRACTORY METALS: OBTAINING, PROPERTIES, APPLICATION

Monograph

IB №14822
Signed for publishing 16.06.2021. Format 60x84 1/16. Offset paper.
Digital printing. Volume 11,87 printer's sheet. 50 copies.
Publishing house «Qazaq university»
Al-Farabi Kazakh National University
KazNU, 71 Al-Farabi, 050040, Almaty

Printed in the printing house of the IP "Center for Operational Printing"